

# CLINICAL STUDIES IN SCANNING LASER POLARIMETRY

*Klinische studies met scanning laser polarimetrie*

## **Proefschrift**

ter verkrijging van de graad van doctor aan de Erasmus Universiteit Rotterdam  
op gezag van de Rector Magnificus Prof.dr.ir. J.H. van Bommel  
en volgens besluit van het College voor Promoties.

De openbare verdediging zal plaatsvinden op donderdag 3 april 2003 om 16:00 uur

## **door**

Thomas Peter Colen

geboren te Halle-Westfalen, Duitsland

---

## **Promotiecommissie**

### **Promotor**

Prof.dr. G. van Rij

### **Overige leden**

Prof.dr. H. Collewyn

Prof.dr. L. Feenstra

Prof.drs. C.C. Sterk

### **Copromotor**

Dr. H.G. Lemij

*voor mijn ouders*

Het drukken van dit proefschrift werd mede mogelijk gemaakt dankzij een financiële bijdrage van de Stichting Wetenschappelijk Onderzoek Het Oogziekenhuis Prof.dr. HJ Flieringa, de Stichting voor Ooglijders, Visio, Ergra Low Vision, Allergan, Bournonville Pharma, DORC Nederland BV, MSD Nederland, Pharmacia & Upjohn en Tramedico.

druk: Febodruk, Enschede  
ontwerp: Esther de Bruijn, Arnhem  
ISBN 90-9016760-9

# CONTENTS

CHAPTER 1	<i>General introduction</i>	7
CHAPTER 2	<i>Motion artifacts in scanning laser polarimetry</i> Ophthalmol 2002;109(8):1568-1572	17
CHAPTER 3	<i>Reproducibility of measurements with the Nerve Fiber Analyzer</i> J Glaucoma 2000; 9(5):363-370	27
CHAPTER 4	<i>Prevalence of split nerve fiber layer bundles in healthy eyes</i> Ophthalmology 2001;108(1):151-156	41
CHAPTER 5	<i>Retinal NFL thickness in human strabismic amblyopia</i> Bin Vis Strab Q 2000;15(2):141-146	49
CHAPTER 6	<i>Axonal loss in a patient with anterior ischemic optic neuropathy as measured with scanning laser polarimetry</i> Am J Ophthalmol 2000;130(6):847-850	57
CHAPTER 7	<i>Sensitivity and specificity of new GDx parameters</i> Submitted for publication	61
CHAPTER 8	<i>Sensitivity and specificity of the GDx; clinical judgement of standard printouts vs. the Number</i> J Glaucoma; in press	73
CHAPTER 9	<i>General discussion</i>	83
CHAPTER 10	<i>Summary &amp; Samenvatting</i>	93
	<i>Dankwoord</i>	99
	<i>List of publications</i>	101
	<i>Curriculum vitae</i>	112
	<i>Figures</i>	102
	<i>Appendix</i> The Rotterdam GDx course (CD-ROM)	112



## CHAPTER 1

### *General introduction*

## General

### Introduction

#### 1. Glaucoma

The number of people with glaucoma has been estimated at 66.8 million, with 6.7 million suffering from bilateral blindness.<sup>1</sup> This makes glaucoma the second leading cause of irreversible blindness worldwide. Glaucoma is a progressive optic neuropathy characterized by loss of retinal ganglion cells. It has a multifactorial origin with an elevated intraocular pressure (IOP) as the most important risk factor.<sup>2</sup> The hallmark of the disease is the typical excavation of the optic nerve head as seen on ophthalmic examination.<sup>3</sup> When left untreated, glaucoma results in visual field loss and eventually blindness. The course of events that leads to death of the retinal ganglion cell (RGC) is not exactly known. Roughly, there are two theories that explain how the RGC is affected in glaucoma: direct mechanical damage by elevated intraocular pressure and/or indirect damage by disturbances in ocular blood flow.<sup>4</sup> In considering the diagnosis of glaucoma, the physician will evaluate the IOP, the optic nerve head and the visual field. This seems to be a straightforward diagnostic process but, unfortunately, all three signs have their shortcomings as diagnostic criteria.

#### 2. Intraocular pressure (IOP)

Epidemiological data show that glaucoma is a multifactorial disease with elevated IOP as the most important risk factor.<sup>2</sup> Other risk factors include age, black ethnic origin, positive family history, myopia, diabetes, migraine and cardiovascular disease.<sup>2</sup> Glaucoma patients tend to have an elevated IOP, but not all patients have this sign. Conversely, not all people with an elevated IOP also develop glaucoma. This is illustrated by reports in which an abnormal IOP was defined as  $> 21$  mm Hg. The sensitivity for detecting glaucoma was 44% to 59%, at specificity levels between 92% to 95%.<sup>5-7</sup> The condition of elevated IOP without evidence of glaucoma is called ocular hypertension. Thus, although the IOP adds to an individual's risk profile for glaucoma, its sensitivity is too low to serve as a diagnostic criterion. In addition, the IOP is typically measured once during an ophthalmic visit, whereas large (undetected) fluctuations of the IOP during the day and also during the night may exist.<sup>8</sup> Finally, the IOP measurement may vary with corneal thickness.<sup>9</sup>

#### 3. Morphology of the optic disc

Glaucomatous cupping of the optic disc is the hallmark of the disease: with increasing loss of retinal ganglion cells, the optic disc becomes more and more excavated (or cupped). Traditional ophthalmoscopic judgement of the optic disc is subject to moderate inter- and intra-observer reproducibility,<sup>10,11</sup> and lacks a quantitative nature. Better reproducibility of judgement is obtained with stereophotographs of the optic disc,<sup>12,13</sup> but the results in terms of sensitivity and specificity for detecting glaucoma still vary widely between investigators. This may be, in part, due to practical problems with image acquisition. For a true stereographic (rather than a pseudo-stereographic) image, one needs to take two simultaneous images with a fixed parallax. Even more important is the need for fully dilated pupils and clear media in the patient. As a result of this, a part of the patient population is unsuited for imaging. In a recent report, 13% of the test population could not be successfully imaged.<sup>14</sup> All in all, stereophotographs have never become widespread in glaucoma diagnosis.



As glaucoma progresses, it is accompanied by progressive visual field loss in the patient. The assessment of the (damaged) visual field of the patient is called perimetry. It is an indispensable diagnostic test because of all tests, it most closely relates to the visual (dys)function of the patient. The Humphrey Field Analyzer (HFA, Zeiss Humphrey Systems, Dublin, CA, USA) is a widely used perimeter, both clinically and scientifically. Despite its value for glaucoma diagnosis, it has a number of drawbacks that preclude its use as a criterion for glaucoma. A considerable part of the test population fails to produce a reliable<sup>15</sup> test result. In one study, the sensitivity and specificity of the Glaucoma Hemifield Test (a much examined test parameter) was 94% and 90%, respectively.<sup>16</sup> However, these good results were obtained after exclusion of 31.5% of that part of the test population that had failed to produce a reliable test result. This may be explained by fatigue (as a result of the long test duration) or inability to understand the instructions during testing. Also, when subjects are performing perimetry for the first time, a learning effect has to be considered.<sup>17</sup> In many trials where long term perimetric data is analyzed, such as the recent Ocular Hypertension Treatment Study (OHTS), a perimetric baseline is routinely repeated.<sup>18</sup> Even when the subject is familiar with perimetry, the reproducibility of measurements may be poor. At some point in the OHTS, subjects whose visual field had become abnormal were re-tested. On the repeated test the abnormality was reproduced in only 14.1%.<sup>19</sup> Also, there is no consensus on the exact definition of the glaucomatous visual field, nor on its perimetric progression, despite the many efforts towards standardization.<sup>20-22</sup> Finally, histopathologic evidence suggests that 25-50% of all RGCs have to be damaged before visual field defects become apparent.<sup>23,24</sup>

#### **4. Visual field loss**

Of all the risk factors that play a role in glaucoma, the IOP is presently the only one that can be altered therapeutically. This can be done pharmaceutically (eye drops or oral medication) or surgically (laser surgery, filtering surgery or implant surgery). For a long time, unequivocal reports in the literature existed on the benefit of treating patients with ocular hypertension.<sup>25-32</sup> More recently, the Ocular Hypertensive Treatment Study (OHTS) set out to provide a definite answer to the dilemma.<sup>33</sup> It documented a delay or prevention of onset of glaucoma in the group that received topical hypotensive treatment as compared to the control group.

#### **5. Treatment of glaucoma**

There is good evidence that, once glaucoma has been established, IOP lowering treatment slows down progression of the disease. This has been shown for pharmaceutical treatment,<sup>34-36</sup> and for surgical treatment (Advanced Glaucoma Intervention Study).<sup>37</sup> Since glaucomatous damage is irreversible, patients will benefit from early detection and early initiation of treatment. This is important for patients who already have glaucoma (to slow down progression) and for subjects with a high risk profile for glaucoma (to prevent or delay the onset of glaucoma).

With no generally agreed upon criteria, diagnosing glaucoma can be quite a challenge, even to the experienced glaucoma specialist. Today, there is still no measure that relates to the nature of the disease (the retinal ganglion cell), that is quantitative, objective, well reproducible, fast and patient friendly to obtain, and, above all,

#### **6. Glaucoma as a clinical challenge**

highly sensitive and specific for glaucoma. This explains why a lot of research of the last decade has focussed on finding such a measure. One field of this research is called imaging.

## 7. Imaging

Along with the fast rise in laser technology and quality of optical components, various instruments were developed to assess structures that contain RGCs. Well-known imaging techniques include Scanning Laser Topography, commercially available as the Heidelberg Retina Tomograph<sup>38-41</sup> and the Topographic Scanning System.<sup>42,43</sup> This technique provides quantitative, three-dimensional information on the morphology of the optic disc. Retinal Thickness Analysis<sup>44</sup> provides quantitative data on the thickness of the retina and is not primarily a tool for glaucoma diagnosis. Optical Coherence Tomography<sup>45-47</sup> and Scanning Laser Polarimetry provide quantitative data on the thickness of the peripapillary retinal nerve fiber layer. The latter technology is studied in this thesis.

## 8. Scanning Laser Polarimetry (SLP)

The first scanning laser polarimeter (Laser Diagnostic Technologies, San Diego, CA, USA)<sup>48-50</sup> came to the market in 1993 as the Nerve Fiber Analyzer. Extensive hardware revisions lead to the Nerve Fiber Analyzer II, which was later upgraded to the Nerve Fiber Analyzer/GDx (in short: GDx). The GDx features statistical software that compares an individual's data to a normative database.

The GDx is a confocal scanning laser ophthalmoscope that assesses retinal nerve fiber layer (NFL) thickness in the peripapillary retina. The NFL is made up of axons from the RGCs. The working principle of polarimetry is based on the retinal NFL being the most form-birefringent structure in the retina. A polarized 780-nm laser beam is aimed at the peripapillary retina. As the laser light passes through the NFL, a phase shift in the state of polarization occurs. This phase shift is called retardation and is thought to arise at the level of the axonal microtubules.<sup>51</sup> The polarization is relatively unaltered by the remaining structures in the retina. After reflection by the retinal pigment epithelium, the light passes through the retina again, and is captured by the detector in the instrument where the amount of retardation is measured. The highest retardation values are found around the 12 o'clock and 6 o'clock position, and correspond to known locations of the superior and inferior NFL bundle.<sup>52-54</sup> It was found in a monkey model that the retardation linearly correlated with NFL thickness.<sup>54,55</sup> One degree of retardation corresponded to 7.4 microns of NFL thickness with a 514-nm laser.<sup>55</sup> Instead of a 514-nm laser, the current instrument uses a 780-nm laser source. Correcting for the wavelength, the manufacturers have chosen a conversion factor of 3 microns for every degree of retardation (Zhou Q, Laser Diagnostic Technologies, written communication). Unfortunately, this correlation has never been histopathologically validated in humans.

In about 0.7 seconds, the peripapillary retina is scanned at 65,536 locations, and a retardation image of 256x256 pixels is constructed. This image is color-coded: a continuous scale from yellow to red to blue represents areas from high to low retardation. A retardation image of a healthy eye (fig 1-1, p. 102) has red and yellow colors at the 12 and 6 o'clock position, corresponding to the superior and inferior arcuate

bundle. The image is typically blue in the nasal and temporal area. On the printout (fig 1-2) there is also a reflectance image that is constructed from the intensity of the backscattered light. Since it is an image constructed from monochromatic information, it lacks the usual detail of conventional optic disc photographs and clinicians should resist the urge to judge the optic disc from it. On the GDx printout, the reflectance image holds value as a reference image for the retardation data. In this image, the operator will typically position a circle or ellipse on the margin of the optic nerve head. A second one with 1.75 times the diameter of the first is displayed automatically. It allows the calculation of the parameters from those pixels that sit peripherally to it. The second circle is also the inner circle of a 10-pixel wide band, displayed on the retardation image. The retardation values under the band are displayed in the so-called double hump graph. This curve represents a cross section of the two arcuate bundles with the nasal and temporal areas in between.

For a quantitative approach to the retardation image, several automated parameters are available to the user. First, areas of blood vessels are automatically eliminated from analysis since they are a source of noise.<sup>56,57</sup> Next, the retardation image is divided into 4 sectors: a 120 deg superior sector, a 50 deg nasal sector, a 120 deg inferior sector and a 70 deg temporal sector. Finally, 14 parameters are calculated automatically. For example, the superior maximum parameter is the average of the 1500 thickest pixels in the 120 deg superior sector, and reflects the thickness of the superior nerve fiber bundle. All parameters that are calculated by the software are used to calculate a summary parameter called ‘the Number’. The Number ranges from 1-99. The higher the Number, the higher the probability of glaucoma. The Number is calculated by a proprietary algorithm that was developed with the help of a neural network.

After having used the GDx for some time, we found that images in some patients reproduced poorly. This turned out to be caused by eye movements during imaging, resulting in what we called “motion artifacts”. In *chapter 2* we have determined the effect of motion artifacts on the retardation values and have illustrated how motion artifacts can be recognized. Also, this has led to the definition of 4 criteria for image quality.

## 9. Clinical studies in SLP

In *chapter 3*, the reproducibility of measurements of high quality images was assessed. Weinreb *et al.*<sup>56</sup> had already reported a coefficient of variation of 4.5% for measurements with the NFA I. We argued that a coefficient of variation is of limited clinical value. We wanted to know how much a GDx output parameter from two consecutive measurements was allowed to change before it became statistically significant. The limits of agreement, first described by Bland and Altman,<sup>58</sup> is such a measure. We calculated the limits of agreement for all available GDx parameters, and for normal subjects and glaucoma patients separately.

In the normal eye, the NFL is thickest around the 12 and 6 o’clock position: the superior and inferior nerve fiber bundle. This was also found with the GDx.<sup>54</sup> Some patients, however, had an abnormal NFL pattern. These subjects were otherwise without abnormalities on ophthalmic examination, especially without evidence for

glaucoma. We called this variability in NFL orientation a “split bundle”. In *chapter 4*, a definition for split bundles is proposed, and the prevalence is determined in a large number of healthy eyes.

In *chapter 5*, we assessed NFL thickness in eyes with strabismic amblyopia. Although the amblyopic eyes had a poor visual acuity, we found no differences in NFL thickness when compared to the fellow, healthy eye. Clinically, this means that the standard normative database can also be used for amblyopic eyes under evaluation for glaucoma.

The NFL is also subject to other diseases than glaucoma. One such a disease is an anterior ischemic optic neuropathy (AION) where decreased perfusion of the anterior part of the optic nerve results in ischemic damage and visual loss. *Chapter 6* describes images of an eye that suffered from an AION. We found that the NFL had considerably decreased in thickness 3-4 weeks after the onset of the insult.

In *chapter 7*, four new GDx parameters have been examined. In addition to the parameters that are available on the GDx printout, several authors had developed new parameters, to better discriminate between normal subjects and glaucoma patients. The Ellipse Standard Deviation, developed by Choplin *et al.*,<sup>59</sup> is the standard deviation around the mean of the values contained in the measuring ellipse. The Normalized Superior Area developed by Xu *et al.*,<sup>60</sup> is the area under a 90 deg sector of the double hump graph with the highest retardation in the superior region. The Normalized Inferior Area is defined likewise, only for the inferior region. The fourth parameter is called the Discriminant Analysis, which is identical to the Linear Discriminant Function developed by Weinreb *et al.*<sup>61</sup> It is calculated by an algorithm that uses three existing parameters: average thickness, ellipse modulation and ellipse average. The new parameters had not been previously validated on a population other than the one from which they were derived. We imaged 263 normal subjects and 241 glaucoma patients and determined sensitivity and specificity values for detecting glaucoma of the four new parameters. Sensitivity values were calculated again for early, moderate and advanced glaucoma separately.

While working with the GDx, we found that printouts generally contained more useful information than was reflected by the parameters. We gradually developed a standardized interpretation protocol for GDx printouts. We found that other ophthalmologists found this protocol useful as well, and that initiated a series of instruction courses known as The Rotterdam GDx Course. In *chapter 8*, we evaluated the application of this interpretation protocol. We tested it against the Number, which was the current best parameter, and found that the sensitivity and specificity of subjective judgement was considerably better.

In *Chapter 9*, the general discussion of this thesis is presented. *Chapter 10* contains the summary of the main findings. The CD-ROM version of the Rotterdam GDx course can be found in the appendix.

1. Quigley HA. Number of people with glaucoma worldwide. *Br J Ophthalmol* 1996;80:389-93.
2. Wilson MR, Martone JF. In: Ritch R, Shields MB, Krupin T, editors. *The glaucomas*. 2nd ed. St. Louis MI: Mosby; 1996:758-61.
3. Jonas JB, Budde WM, Panda-Jonas S. Ophthalmoscopic evaluation of the optic nerve head. *Surv Ophthalmol* 1999;43:293-320.
4. Sommer A. Doyné Lecture. Glaucoma: facts and fancies. *Eye* 1996;10:295-301.
5. Sommer A, Tielsch JM, Katz J, et al. Relationship between intraocular pressure and primary open angle glaucoma among white and black Americans. The Baltimore Eye Survey. *Archives of Ophthalmology* 1991;109:1090-5.
6. Leske C, Connell A, Schachat A. The Barbados eye study. *Arch. Ophthalmol.* 1994;112:821-9.
7. Tielsch JM, Katz J, Singh K, et al. A population-based evaluation of glaucoma screening: the Baltimore Eye Survey. *Am J Epidemiol* 1991;134:1102-10.
8. Zeimer RC. In: Ritch R, Shields MB, Krupin T, *The Glaucomas*. 2nd ed. St. Louis MI: Mosby; 1996:429-45.
9. Bhan A, Browning AC, Shah S, et al. Effect of corneal thickness on intraocular pressure measurements with the pneumotonometer, Goldmann applanation tonometer, and Tono-Pen. *Invest Ophthalmol Vis Sci* 2002;43:1389-92.
10. Kahn HA, Leibowitz H, Ganley JP, et al. Randomized controlled clinical trial. National Eye Institute workshop for ophthalmologists. Standardizing diagnostic procedures. *Am J Ophthalmol* 1975;79:768-75.
11. Lichter PR. Variability of expert observers in evaluating the optic disc. *Trans Am Ophthalmol Soc* 1976;74:532-72.
12. Tielsch JM, Katz J, Quigley HA, et al. Intraobserver and interobserver agreement in measurement of optic disc characteristics. *Ophthalmology* 1988;95:350-6.
13. Feuer WJ, Parrish RK 2nd, Schiffman JC, et al. The Ocular Hypertension Treatment Study: reproducibility of cup/disk ratio measurements over time at an optic disc reading center. *Am J Ophthalmol* 2002;133:19-28.
14. Vitale S, Smith TD, Quigley T, et al. Screening performance of functional and structural measurements of neural damage in open-angle glaucoma: a case-control study from the Baltimore Eye Survey. *J Glaucoma* 2000;9:346-56.
15. Anderson DR, Patella VM. *Automated Static Perimetry*. 2nd ed. St. Louis: Mosby; 1999:104.
16. Katz J, Sommer A, Gaasterland DE, Anderson DR. Comparison of analytic algorithms for detecting glaucomatous visual field loss. *Archives of Ophthalmology* 1991;109:1684-9.
17. Cyrilin MN. In: Ritch R, Shields MB, Krupin T, *The Glaucomas*. 2nd ed. St. Louis MI: Mosby; 1996:574.
18. Johnson CA, Keltner JL, Cello KE, et al. Baseline visual field characteristics in the ocular hypertension treatment study. *Ophthalmology* 2002;109:432-7. Notes: CORPORATE NAME: Ocular Hypertension Study Group.
19. Keltner JL, Johnson CA, Quigg JM, et al. Confirmation of visual field abnormalities in the Ocular Hypertension Treatment Study. Ocular Hypertension Treatment Study Group. *Arch Ophthalmol* 2000;118:1187-94.
20. Advanced Glaucoma Intervention Study. 2. Visual field test scoring and reliability. *Ophthalmol* 1994;101:1445-55.
21. Spry PG, Johnson CA. Identification of progressive glaucomatous visual field loss. *Surv Ophthalmol* 2002;47:158-73.
22. Johnson CA, Sample PA, Cioffi GA, et al. Structure and function evaluation (SAFE): I. criteria for glaucomatous visual field loss using standard automated perimetry (SAP) and short wave-length automated perimetry (SWAP). *Am J Ophthalmol* 2002;134:177-85.

23. Quigley HA, Dunkelberger GR, Green WR. Retinal ganglion cell atrophy correlated with automated perimetry in human eyes with glaucoma. *American Journal of Ophthalmology* 1989;107:453-64.
24. Kerrigan-Baumrind LA, Quigley HA, Pease ME, et al. Number of ganglion cells in glaucoma eyes compared with threshold visual field tests in the same persons. *Invest Ophthalmol Vis Sci* 2000;41:741-8.
25. Shin DH, Kolker AE, Kass MA, et al. Long-term epinephrine therapy of ocular hypertension. *Arch Ophthalmol* 1976;94:2059-60.
26. David R, Livingston DG, Luntz MH. Ocular hypertension—a long-term follow-up of treated and untreated patients. *Br J Ophthalmol* 1977;61:668-74.
27. Kitazawa Y. Prophylactic therapy of ocular hypertension. A prospective study. *Trans Ophthalmol Soc N Z* 1981;33:30-2.
28. Epstein DL, Krug JHJr, Hertzmark E, et al. A long-term clinical trial of timolol therapy versus no treatment in the management of glaucoma suspects. *Ophthalmology* 1989;96:1460-7.
29. Kass MA, Gordon MO, Hoff MR, et al. Topical timolol administration reduces the incidence of glaucomatous damage in ocular hypertensive individuals. A randomized, double-masked, long-term clinical trial. *Archives of Ophthalmology* 1989;107:1590-8.
30. Schulzer M, Drance SM, Douglas GR. A comparison of treated and untreated glaucoma suspects. *Ophthalmology* 1991;98:301-7.
31. Heijl A, Bengtsson B. Long-term effects of timolol therapy in ocular hypertension: a double-masked, randomised trial. *Graefes Arch Clin Exp Ophthalmol* 2000;238:877-83.
32. Rossetti L, Marchetti I, Orzalesi N, et al. Randomized clinical trials on medical treatment of glaucoma. Are they appropriate to guide clinical practice? *Arch Ophthalmol* 1993;111:96-103.
33. Kass, M. A., Heuer, D. K., Higginbotham, E. J., Johnson, C. A., Keltner, J. L., Miller, J. P., Parrish, R. K. 2nd, Wilson, M. R., and Gordon, M. O. The Ocular Hypertension Treatment Study: a randomized trial determines that topical ocular hypotensive medication delays or prevents the onset of primary open-angle glaucoma. *Arch Ophthalmol* 120(6), 701-13; discussion 829-30. 2002.
34. Mao LK, Stewart WC, Shields MB. Correlation between intraocular pressure control and progressive glaucomatous damage in primary open-angle glaucoma. *Am J Ophthalmol* 1991;111:51-5.
35. The effectiveness of intraocular pressure reduction in the treatment of normal-tension glaucoma. Collaborative Normal-Tension Glaucoma Study Group. *Am J Ophthalmol* 1998;126:498-505.
36. Bergea B, Bodin L, Svedbergh B. Impact of intraocular pressure regulation on visual fields in open-angle glaucoma. *Ophthalmology* 1999;106:997-1004; discussion 1004-5.
37. The advanced glaucoma intervention study (AGIS): 7. The relationship between control of intraocular pressure and visual field deterioration. The AGIS Investigators. *Am J Ophthalmol* 2000;130:429-40.
38. Dreher AW, Weinreb RN. Accuracy of topographic measurements in a model eye with the laser tomographic scanner. *Investigative Ophthalmology & Visual Science* 1991;32:2992-6.
39. Bathija R, Zangwill L, Berry CC, et al. Detection of early glaucomatous structural damage with confocal scanning laser tomography. *J Glaucoma* 1998;7:121-7.
40. Kesen MR, Spaeth GL, Henderer JD, et al. The Heidelberg Retina Tomograph vs clinical impression in the diagnosis of glaucoma. *Am J Ophthalmol* 2002;133:613-6.
41. Miglior S, Casula M, Guareschi M, et al. Clinical ability of Heidelberg retinal tomograph examination to detect glaucomatous visual field changes. *Ophthalmology* 2001;108:1621-7.
42. Geyer O, Michaeli-Cohen A, Silver DM, et al. Reproducibility of topographic measures of the glaucomatous optic nerve head. *Br J Ophthalmol* 1998;82:14-7.

43. Cullinane AB, Waldock A, Diamond JP, Sparrow JM. Optic disc cup slope and visual field indices in normal, ocular hypertensive and early glaucomatous eyes. *Br J Ophthalmol* 2002;86:555-9.
44. Zeimer R, Shahidi M, Mori M, et al. A new method for rapid mapping of the retinal thickness at the posterior pole. *Invest Ophthalmol Vis Sci* 1996;37:1994-2001.
45. Pons ME, Ishikawa H, Gurses-Ozden R, et al. Assessment of retinal nerve fiber layer internal reflectivity in eyes with and without glaucoma using optical coherence tomography. *Arch Ophthalmol* 2000;118:1044-7.
46. Mistlberger A, Liebmann JM, Greenfield DS, et al. Heidelberg retina tomography and optical coherence tomography in normal, ocular-hypertensive, and glaucomatous eyes. *Ophthalmology* 1999;106:2027-32.
47. Zangwill LM, Bowd C, Berry CC, et al. Discriminating between normal and glaucomatous eyes using the Heidelberg Retina Tomograph, GDx Nerve Fiber Analyzer, and Optical Coherence Tomograph. *Arch Ophthalmol* 2001;119:985-93.
48. Dreher AW, Reiter K. Scanning laser polarimetry of the retinal nerve fiber layer. *Proc SPIE Int Soc Opt Eng* 1992;1746:34-8.
49. Dreher AW, Reiter K. Retinal laser ellipsometry: a new method for measuring the retinal nerve fiber layer thickness distribution. *Clin Vis Sci* 1992;7:481-8.
50. Dreher AW, Reiter K, Weinreb RN. Spatially resolved birefringence of the retinal nerve fiber layer assessed with a retinal laser ellipsometer. *Appl Opt* 1992;31:3730-5.
51. Hemenger RP. Birefringence of a medium of tenous parallel cylinders. *Appl Opt* 1989;28:4030
52. Jonas JB, Nguyen NX, Naumann GO. The retinal nerve fiber layer in normal eyes. *Ophthalmology* 1989;96:627-32.
53. Varma R, Skaf M, Barron E. Retinal nerve fiber layer thickness in normal human eyes. *Ophthalmology* 1996;103:2114-9.
54. Morgan JE, Waldock A. Scanning laser polarimetry of the normal human retinal nerve fiber layer: a quantitative analysis. *Am J Ophthalmol* 2000;129:76-82.
55. Weinreb RN, Dreher AW, Coleman A, et al. Histopathologic validation of Fourier-ellipsometry measurements of retinal nerve fiber layer thickness. *Arch Ophthalmol* 1990;108:557-60.
56. Weinreb RN, Shakiba S, Zangwill L. Scanning laser polarimetry to measure the nerve fiber layer of normal and glaucomatous eyes. *Am J Ophthalmol* 1995;119:627-36.
57. Tjon-Fo-Sang MJ, van Strik R, de Vries J, Lemij HG. Improved reproducibility of measurements with the nerve fiber analyzer. *J Glaucoma* 1997;6:203-11.
58. Bland JM, Altman DG. Statistical methods for assessing agreement between two methods of clinical measurement. *Lancet* 1986;307-10.
59. Choplin NT, Lundy DC, Dreher AW. Differentiating patients with glaucoma from glaucoma suspects and normal subjects by nerve fiber layer assessment with scanning laser polarimetry. *Ophthalmology* 1998;105:2068-76.
60. Xu L, Chen PP, Chen YY, et al. Quantitative nerve fiber layer measurements using scanning laser polarimetry and modulation parameters in the detection of glaucoma. *J Glaucoma* 1998;7:270-7.
61. Weinreb RN, Zangwill L, Berry CC, et al. Detection of glaucoma with scanning laser polarimetry. *Arch Ophthalmol* 1998;116:1583-9.





## CHAPTER 2

### *Motion artifacts in scanning laser polarimetry*

Colen TP and Lemij HG  
Ophthalmology 2002;109(8):1568-1572

## Abstract

**Purpose** The GDx (Laser Diagnostic Technologies, San Diego, CA) is a scanning laser polarimeter that measures retardation to assess retinal nerve fiber layer thickness *in vivo*. Eye movements during image acquisition may result in motion artifacts in the GDx image. The aim of this study was to investigate the effect of motion artifacts on the retardation values, and to illustrate how motion artifacts can be identified.

**Design** Observational case series.

**Participants** Thirty-two normal subjects and 28 glaucoma patients participated.

**Methods** We imaged all 60 subjects with the GDx. Images with identified motion artifacts were compared with images without motion artifacts from the same eye and the same session. In 25 cases, the artifact was identified in the superior segment only, and the effect on the superior maximum parameter was calculated. In 26 cases, the artifact was observed in the inferior segment only, and the effect on the inferior maximum parameter was calculated. In 9 cases, the artifact was observed superiorly and inferiorly, and the effect on both parameters was calculated. In all 60 cases, the effect on the Number (a summary parameter) was calculated. We also analyzed the groups of glaucoma patients and normal subjects separately.

**Main outcome measures** Superior maximum parameter, inferior maximum parameter, the Number parameter.

**Results** In general, the identified motion artifacts led to an increase in retardation, reflected by an increase in the superior maximum and inferior maximum parameter by  $5.9\mu$  and  $3.4\mu$  respectively ( $P < 0.001$ ). The Number decreased by 3.4 with motion artifacts ( $P = 0.001$ ). The variability of this effect was large. In one case, the motion artifact increased retardation by as much as  $28.6\mu$ . The effect of motion artifacts was higher in glaucoma patients than in normal subjects.

**Conclusions** The identified motion artifacts generally increase retardation values. This increase, however, is highly variable. Therefore, images with such motion artifacts should be viewed with caution, or excluded from analysis.

## Introduction

The GDx (Laser Diagnostic Technologies, San Diego, CA) is a scanning laser polarimeter that measures retardation originating from the retina, attributed to the birefringent properties of the nerve fiber layer (NFL). Retardation values are linearly correlated with NFL thickness, as has been shown in a monkey model.<sup>1</sup> The retardation map produced by the instrument therefore provides a measure of retinal NFL thickness. The GDx also calculates 14 parameters that may be used to dis-

criminate normal subjects from glaucoma patients.<sup>2-4</sup> A more detailed description of the GDx can be found elsewhere.<sup>5-7</sup>

In our experience, motion artifacts are commonly seen in a GDx image when the eye moved during image acquisition. They can affect the amount of measured retardation, and thus make the GDx data less reliable, or sometimes useless. Although the GDx software routinely checks the image quality, it does not detect motion artifacts. It was the aim of this study to examine the effect of motion artifacts on the retardation values in normal subjects and glaucoma patients, to demonstrate the importance of recognizing them, and to illustrate how they can be identified.

**Subjects and measurement procedures** Participating in a long-term follow-up trial, 350 subjects made their six-monthly visit, to be imaged with the GDx by one of three experienced operators. The subjects were imaged until at least three images per eye met all of the following four quality criteria: optic nerve head well-centered, just image illumination, good focus and no motion artifacts throughout the image. Just image illumination entails that the image is evenly illuminated and neither too bright, nor too dark. Patients became eligible for the current study, if their images also contained at least one image with a motion artifact. The image should otherwise be of high quality. Such an image with motion artifacts would have normally been deleted, but was now kept and compared with the first of the high-quality images. Only one image with motion artifacts was used per subject. When the arbitrarily determined sample size of 60 subjects was reached, the inclusion for this study was terminated.

## Methods

Of the 60 subjects, 32 were healthy volunteers (mean age 56.5 years) who had met their original inclusion criteria of Caucasian ethnic origin, age between 20-80 years, intraocular pressure  $\leq 21$  mm Hg, a normal appearance of the optic nerve head and normal visual fields (Humphrey Field Analyzer 24-2 full threshold program). They did not have diabetes, hypertension requiring medical treatment, any significant ocular history, a vertical cup/disc ratio of 0.6 or higher, nor an asymmetry of greater than 0.2 vertical cup/disc ratio between the two eyes. The other 28 subjects were glaucoma patients (mean age 66.9 years) who had met their original inclusion criteria of: Caucasian ethnic origin, age between 20-80 and a diagnosis of glaucoma (on the basis of reliable and repeated glaucomatous visual field abnormalities with matching optic disc abnormalities) established by one of our three glaucoma specialists. Exclusion criteria were diabetes, systemic hypertension requiring medical treatment, any ocular history or any ocular surgery. Refractive error was not among the selection criteria as long as it didn't compromise focussing.

The operators who selected the subjects for this trial were unaware of the outcome of the NFL thickness parameters. During all measurements, we saw to it that patients had their heads as upright as possible. Pupils were undilated and ambient lights were left on. IRB/Ethics Committee approval was obtained for this study and written informed consent was obtained from all participants at enrolment in the follow-up trial.

**Parameters** The GDx software calculates several parameters from the retardation image. The superior maximum (smax) parameter is the average value of the 1500 pixels with the highest retardation in the superior segment. The inferior maximum (imax) parameter is defined likewise for the inferior segment. Retardation values in degrees are converted to microns by multiplying them by 7.4, as one degree of retardation has been shown to correspond to 7.4 $\mu$  of nerve fiber layer thickness in a monkey model.<sup>1</sup> The Number is a summary parameter ranging from 0-100 that is calculated from existing parameters by a proprietary algorithm. A high value indicates a high probability of glaucoma, but not necessarily an advanced stage of the disease. For clarity, we limited our quantitative analysis of the effects of motion artifacts to only these three parameters.

**Motion artifacts & description of examples** Motion artifacts occur when the eye of the patient moves during image acquisition. The eye movements can be optionally seen on the GDx monitor when the individual scans (approx. 20) are displayed in quick succession (the so-called “movie”). The hallmark of motion artifacts is sharp, colored lines along the blood vessels in the retardation image. The lines are not present on images when the eye was kept still during scanning. When the blood vessels are located in an area that appears red on the retardation image, motion artifacts usually appear as bright yellow lines. When the blood vessels are located on a blue background, the motion artifacts usually appear as red lines. In addition, the overall retardation in the area of the motion artifacts tends to be higher as compared to an image without motion artifacts. Figure 2-1 (p.103) shows four examples of images with motion artifacts. The eyes in example #1 and #2 are healthy; the eyes in example #3 and #4 are glaucomatous. Going from left to right, we have presented the reflectance image, the retardation image containing motion artifacts, and the retardation image of the same eye without motion artifacts. The reflectance image of the scan without motion artifacts is not shown to save space. Several motion artifacts have been marked with an arrow.

In example #1, there are a few motion artifacts in the superior segment. Note the yellow lines along the blood vessels in the middle image, and their absence in the right image. The smax parameter was 82 $\mu$  in the image with motion artifacts, and 74 $\mu$  in the image without motion artifacts.

In example #2, quite a large motion artifact can be seen superiorly (note the bright yellow line) in addition to a smaller motion artifact more to the right. The smax parameter was 100 $\mu$  in the image with motion artifacts and 93 $\mu$  in the image without motion artifacts. Also, two motion artifacts may be identified inferiorly. The imax was 98 $\mu$  in the image with the identified motion artifacts and 87 $\mu$  in the image without motion artifacts. Note that with the motion artifacts the retardation in the entire superior segment has increased visibly in the image.

Example #3 shows large motion artifacts inferiorly, and some small motion artifacts superiorly. The imax is 97 $\mu$  in the image with motion artifacts and 89 $\mu$  in the image without motion artifacts. By contrast, the smax is lower in the image with motion artifacts than in the image without motion artifacts (70 $\mu$  and 73 $\mu$  respectively). In our experience, this is a rare finding.

Example #4 shows how large the effect of motion artifacts can be. In the image with motion artifacts, the  $s_{max}$  was  $79\mu$  and the  $i_{max}$  was  $70\mu$ . In the image without motion artifacts the  $s_{max}$  was  $50\mu$  and the  $i_{max}$  was  $57\mu$ . Due to all the red color, which is probably entirely caused by artifact, the image with motion artifacts may not seem very abnormal to the inexperienced user. However, the image without artifacts shows an eye with retardation levels that are clearly subnormal, indicating advanced glaucoma. This is also illustrated by the visual field of this eye in fig 2-2 (p.104).

Finally, in images with motion artifacts, a black rectangle may be observed at the edge of the image. This can be observed at the left side of example #2 and #3, and on the right side of example #4. During scanning, approximately 20 separate scans are acquired at different angles of polarization. All 20 scans are required to construct the displayed retardation image. Obviously, all 20 scans need to be aligned. Only those pixels that overlap in all 20 scans, are finally displayed; all missing pixels will be presented in black. With eye movements, missing pixels are most likely to occur at the edges.

**Statistical methods** Since all patients served as their own controls, a relatively low sample size of 60 subjects was thought to be sufficient at the start of the trial. A special version of the GDx 2.0.09 software enabled us to automatically translate all parameters into a statistical software package (SPSS version 9.0, SPSS Inc., Chicago, IL). A paired Student's t-test, with the level of statistical significance set at  $\alpha = 0.05$  was used to compare all images with motion artifacts to those without.

First, data of all 60 images were pooled and analyzed together. If a motion artifact was identified superiorly, the  $s_{max}$  parameter was calculated. In case of an inferior motion artifact, we calculated the  $i_{max}$  parameter. If a motion artifact was identified superiorly and inferiorly, both parameters were calculated. Irrespective of where the motion artifact was, the Number was calculated. We now compared the parameters of images with motion artifacts to those in images without motion artifacts. Then, the same calculations were applied to the normal eyes and the glaucomatous eyes separately.

Finally, we counted the number of healthy subjects and the number of glaucoma patients in which the  $s_{max}$  parameter had been affected beyond the limits of agreement as calculated in a separate study population.<sup>8</sup> The limits of agreement for the  $s_{max}$  was found to be  $7.2\mu$  for normals and  $8.7\mu$  for glaucoma patients.<sup>9</sup> The limits of agreement indicate how much a particular parameter would have to change to fall outside the ranges of variability of a repeated measurement, and thus become clinically significant. Motion artifacts that affect a parameter beyond these limits could potentially interfere with a clinical decision.

In general, motion artifacts significantly increased the retardation. This was clearly reflected by the  $s_{max}$  and  $i_{max}$  parameter, but also by the Number (table 2-1). In all subjects, motion artifacts increased the superior maximum ( $s_{max}$ ) parameter by, on average,  $5.9\mu$  ( $p < 0.001$ ), corresponding to 7.4%. For the inferior maximum ( $i_{max}$ ) parameter this increase was  $3.4\mu$  ( $p < 0.001$ ; 3.9%). These differences showed a large

## Results

variability. For example, the range of the mean difference in the  $s_{\max}$  parameter was from  $-6.0\mu$  to  $+28.6\mu$ , with a standard deviation of  $7.1\mu$ . In three cases, the retardation in images with motion artifacts was lower than in images without motion artifacts. On the other hand, the difference in the  $s_{\max}$  parameter could be as high as  $28.6\mu$ , which corresponded to 58%.

The increase in retardation caused by motion artifacts was higher in glaucoma patients than in normals. For example, the mean difference in the  $s_{\max}$  parameter was  $7.7\mu$  in glaucoma patients and  $4.4\mu$  in normals. The effect of motion artifacts was again highly variable, as illustrated by the high standard deviation values.

In normals, the change in The Number caused by motion artifacts was small and statistically not significant ( $p=0.31$ ). In glaucoma, the Number generally decreased with motion artifacts by, on average, 6.4 ( $p=0.001$ ). This decrease, however, could be as high as 33.

To understand the results in terms of limits of agreement, we calculated the number of subjects who had an increase in the  $s_{\max}$  beyond the limits of agreement. These limits are  $7.2\mu$  for healthy subjects, and  $8.7\mu$  for glaucoma patients. This was true for 5 out of 32 (i.e. 15.6%) healthy subjects, and for 5 out of 28 (i.e. 17.9%) glaucoma patients.

## Discussion

This is the first study that addresses motion artifacts in GDx scans. We have demonstrated that they generally increase retardation values, especially in glaucoma patients. Also, the artifactual retardation may vary considerably, thereby unpredictably affecting the measurements. We therefore think that scans with identified motion artifacts should be disregarded for further analysis. Looking for motion artifacts should therefore occur with the patient still by the GDx, to allow for rescanning the eye, if required.

As a result of the artifactual increase in retardation, glaucomatous eyes may be falsely classified as normal. This will likely impair the sensitivity of this technology for detecting glaucoma. Also, the follow-up of individual eyes will be less sensitive for detecting real change over time because artifactually high retardation measurements may mask true progression. In addition, baseline images with motion artifacts may, at a later stage, be the cause of a false positive appearance of progressive NFL thinning. We have demonstrated that, due to motion artifacts, 15.6% of normals and 17.9% of glaucoma patients showed an increase in retardation beyond its limits of agreement.

We have demonstrated how to identify motion artifacts, which is, in most cases, fairly easy. Only occasionally can some doubt remain whether yellow lines along blood vessels reflect a thicker part of the NFL, or whether they are artifactual. In these situations, the software can play back a movie of the optic nerve head that was recorded during the 0.7 seconds of image acquisition, showing whether the eye was kept still during imaging or not. Also, making several scans in a row can be of help, since the difference between motion artifacts and no motion artifacts can easily be seen in subsequent images. Since the GDx image quality check software does not detect motion artifacts, a 'passed' overall image quality score does not mean the image is free of motion artifacts. A software utility that can detect motion artifacts would be very useful, especially for the beginning user.

In conclusion, motion artifacts may cause spuriously higher retardation in scanning laser polarimetry. As a result the sensitivity for detecting glaucoma is likely to be adversely affected. In addition, follow-up will probably be less useful if images with motion artifacts are not identified and disregarded, especially at base line imaging. Fortunately, motion artifacts are usually easily identified and should prove no limitation to the experienced clinician working with the GDx.

*Acknowledgments:* The authors thank Irene C. Notting, MD, for selecting, judging and coding the GDx printouts.

Table 2-1.

The effect of motion artifacts on three different GDx parameters.

Parameters	n	with MA	without MA	mean difference	SD of difference	range of difference	95% CI of difference	p-value
<b>All subjects 60</b>								
Smax ( $\mu$ )	34	85.4	79.5	5.9 (7.4%)	7.1	-6.0 ; +28.6	+3.4 ; +8.3	< 0.001
Imax ( $\mu$ )	35	91.5	88.1	3.4 (3.9%)	3.4	-1.6 ; +12.4	+2.3 ; +4.7	< 0.001
The Number	60	30.2	33.6	-3.4 (10.1%)	7.4	-33 ; +11	-5.3 ; -1.5	0.001
<b>Normals 32</b>								
Smax ( $\mu$ )	19	93.1	88.7	4.4 (5.0%)	7.3	-6.0 ; +23.2	+0.8 ; +7.9	0.018
Imax ( $\mu$ )	20	97.1	94.3	2.8 (3.0%)	3.3	-1.6 ; +10.6	+1.2 ; +4.3	0.001
The Number	32	15.0	15.7	-0.7 (4.5%)	3.7	-11 ; +11	-2.0 ; +0.7	0.31
<b>Glaucoma 28</b>								
Smax ( $\mu$ )	15	75.7	67.9	7.7 (11.3%)	6.6	+1.2 ; +28.6	+ 4.1 ; +11.4	< 0.001
Imax ( $\mu$ )	15	84.1	79.7	4.4 (5.5%)	3.6	-0.7 ; +12.4	+ 2.4 ; +6.4	< 0.001
The Number	28	47.6	54.1	-6.4 (11.8%)	9.1	-33 ; +2	-10.0 ; -2.9	0.001

Data of all subjects were pooled and mean values of three different parameters are given with motion artifacts (MA) and without motion artifacts. The mean difference between the two is expressed in microns and as a percentage of the value without motion artifacts. For this difference the standard deviation (SD), the range, the 95% confidence interval (CI) and the p-values are given. Also, all values are presented again for the group of glaucoma patients and the group of normal subjects separately.



1. Weinreb RN, Dreher AW, Coleman A, et al. Histopathologic validation of Fourier-ellipsometry measurements of retinal nerve fiber layer thickness. *Arch Ophthalmol* 1990;108:557-60.
2. Tjon-Fo-Sang MJ, Lemij HG. The sensitivity and specificity of nerve fiber layer measurements in glaucoma as determined with scanning laser polarimetry. *Am J Ophthalmol* 1997;123:62-9.
3. Weinreb RN, Zangwill L, Berry CC, et al. Detection of glaucoma with scanning laser polarimetry. *Arch Ophthalmol* 1998;116:1583-9.
4. Choplin NT, Lundy DC, Dreher AW. Differentiating patients with glaucoma from glaucoma suspects and normal subjects by nerve fiber layer assessment with scanning laser polarimetry. *Ophthalmology* 1998;105:2068-76.
5. Dreher AW, Reiter K. Retinal laser ellipsometry: a new method for measuring the retinal nerve fiber layer thickness distribution. *Clin Vis Sci* 1992;7:481-8.
6. Tjon-Fo-Sang MJ, de Vries J, Lemij HG. Measurement by nerve fiber analyzer of retinal nerve fiber layer thickness in normal subjects and patients with ocular hypertension. *Am J Ophthalmol* 1996;122:220-7.
7. Weinreb RN, Shakiba S, Zangwill L. Scanning laser polarimetry to measure the nerve fiber layer of normal and glaucomatous eyes. *Am J Ophthalmol* 1995;119:627-36.
8. Bland JM, Altman DG. Statistical methods for assessing agreement between two methods of clinical measurement. *Lancet* 1986;307-10.
9. Colen TP, Tjon-Fo-sang MJ, Mulder PG, Lemij HG. Reproducibility of measurements with the nerve fiber analyzer (NFA/GDx). *J Glaucoma* 2000;9:363-70.

## References



## CHAPTER 3

### *Reproducibility of measurements with the Nerve Fiber Analyzer*

Colen TP and Lemij HG  
Journal of Glaucoma 2000;9(5):363-370

## Abstract

**Purpose** To determine the reproducibility of measurements with the Nerve Fiber Analyzer (NFA), a scanning laser polarimeter designed for quantifying glaucoma, in both normal and glaucomatous subjects. We also assessed the variance of measurements between instruments.

**Methods** Measurements were made with the third generation NFA, the GDx. The study consisted of three parts. In the first part, we measured right eyes of 10 healthy volunteers on 5 consecutive days. In the second part, 45 glaucoma patients underwent NFA measurements of one randomly selected eye on two separate days within a 5-week period. For all 14 available parameters, reproducibility of measurements was expressed in terms of 95% limits of agreement, and as the intraclass correlation coefficient. The NFA software has an option of creating a mean image from a selection of single images; for both parts of the study, the reproducibility of measurements was calculated for a 'single image', and a 'mean of 3' image. In the third part of the study, 17 volunteers underwent repeated NFA measurement sessions on each of 3 different instruments. Using MANOVA, we determined the variance of measurements between instruments.

**Results** The reproducibility of measurements varied considerably across parameters. Limits of agreement in mean images for superior maximum and inferior maximum were  $7.2\mu$  and  $7.7\mu$ , respectively in our healthy subjects, and  $8.7\mu$  and  $7.9\mu$ , respectively in our glaucoma patients. For normal subjects, the intraclass correlation coefficient was  $>90\%$  in 10 out of 14 parameters. In glaucomatous subjects the intraclass correlation coefficient was  $>90\%$  in 13 out of 14 parameters. Some parameters reproduced better in a mean than in a single image; these differences, however, were small, and in general not statistically significant. The between instruments component also varied across parameters, being highest in ratio-based parameters.

**Conclusions** 1. The reproducibility of measurements varied across parameters. 2. In general, the reproducibility of measurements with the NFA was high. 3. The reproducibility of measurements was similar between normal and glaucomatous subjects. 4. Any measured change in nerve fiber layer thickness would be statistically significant if it exceeded about  $7\text{--}8\mu$  in the superior maximum or inferior maximum parameter in normal subjects. 5. Reproducibility of measurements hardly differed between single images and mean images. 6. The reproducibility of measurements between the 3 instruments we used was highest for straight parameters.

## Introduction

The Nerve Fiber Analyzer (NFA; Laser Diagnostic Technologies, San Diego, CA) is a scanning laser polarimeter, designed for the detection and follow-up of glaucoma. It uses a 780-nm diode laser to scan the retina, and to assess the retinal nerve fiber layer (NFL) thickness in the peripapillary region, by measuring changes in polarization (i.e., retardation) of the scanning laser beam. Results from previous studies with the NFA<sup>1,2</sup> have shown a high sensitivity and specificity in discriminating between a normal and glaucomatous NFL.

Knowing the reproducibility of measurements of a method provides an insight into its precision, which is crucial to a meaningful assessment of changes over time. Many studies into the reproducibility of measurements of the NFA have been published. Some results were obtained with the NFA I<sup>3-7</sup> and later studies were carried out with the NFA II.<sup>8-10</sup> No results obtained with the latest NFA version (the GDx), have yet been reported. The GDx has identical hardware as the NFA II, but yields a different set of parameters (only 6 of the 14 parameters available on the GDx were available on the NFA II).

In some studies, the ‘within-pixel’ reproducibility was calculated, rather than the reproducibility within a parameter. In the within-pixel procedure, several retardation images were aligned, and for every pixel, a standard deviation was calculated. The standard deviations of all 65536 pixels (or only of those outside the peripapillary circle) were averaged. This approach gives the clinician an overall impression of the reproducibility of the measurements in a particular patient. In addition, within pixel reproducibility of measurements can be used for determining statistically significant, localized, change over time. To that end, the software can digitally subtract consecutive images, highlighting pixels where a statistically significant change has occurred, all based on the location specific within pixel reproducibility of a given eye. It is yet unclear how sensitive, specific, and meaningful this approach is.

The reported overall within-pixel reproducibility in the literature usually looks extremely good, being around 3-5 $\mu$ . Although it demonstrates the high precision of the instrument, it probably has little intuitive clinical meaning. The GDx provides 14 parameters that may be used clinically for the diagnosis and follow-up of patients. Clinicians might therefore be more interested in how well these parameters reproduce.

The intraclass correlation coefficient (ICC) and the coefficient of variation (CV) are common ways to express the reproducibility of measurements per parameter. We think, however, that these measures are not very intuitive to the clinician. We therefore looked for a method that expresses the reproducibility of measurements per parameter, that is intuitive and has direct clinical meaning. The ‘limits of agreement’, as described by Bland and Altman in the Lancet in 1986<sup>11</sup> is such a method. It is based on the difference between two consecutive measurements, and the 95% range of this difference. It has the same unit of measure as the parameter itself and provides the amount of change of a parameter that is needed for it to be statistically significant. Limits of agreement may be useful to the clinician to assess the significance of any measured change over time.

This study consisted of three parts. In the first part, we determined the reproducibility of measurements in healthy subjects. In the second part, it was assessed in glaucoma patients. These two parts addressed the variance of measurements within a single instrument. In the third part of this study, we assessed this variance across instruments.

**The Nerve Fiber Analyzer** A detailed description of the NFA has been published elsewhere.<sup>3,12,13</sup> In short, a 780 nm diode laser scans the peripapillary retina with a scanning angle of 15x15 degs. The laserlight is polarized and as it passes through the re-

## Methods

tinal nerve fiber layer (NFL), a phase shift called retardation occurs, attributed to the parallel orientation of the microtubules inside the retinal axons. This phase shifting property of the NFL is called birefringence. In the backscattered light, the amount of retardation is thought to linearly reflect the retinal NFL thickness, as has been shown in a monkey model.<sup>14</sup> The retinal NFL thickness is then displayed in a color-coded 256x256 pixels image.

In this image, the operator will typically position a circle or ellipse on the margin of the optic nerve head. A second one with 1.75 times the diameter of the first is displayed automatically, allowing the analysis of only those pixels that sit peripherally to it. Areas of blood vessels are a source of noise<sup>6</sup> and are therefore automatically excluded for analysis by the software. The entire image is divided into 4 segments centered on the optic disc: superior 120°, inferior 120°, nasal 50° and temporal 70°. For a quantitative approach, several parameters are available.

The GDx is a third generation NFA, with a built-in normative database. For all 14 parameters that are available to the user, the percentile in the normal range is computed. When it is below 10% or over 90%, the percentile is displayed on the printout.

**Measurement procedures** In our study, a measurement session (for brevity a ‘measurement’) for one eye always consisted of obtaining a minimum of 3 single images of high quality each (i.e. well focussed, the optic disc well centered in the image, equal and total illumination in all segments and no detectable eye movement during image acquisition). Typically, this required about 6 tries. The software of the instrument allows the operator to select any amount of images that may then be aligned and converted into one ‘mean image’. In the first two parts of our study, we assessed the reproducibility of measurements for single images (always the first of our 3 images of high quality) and for a ‘mean of 3’ image. In the third part of the study, only the ‘mean of 3’ image was considered. In selecting the 3 images of high quality, the operator was masked to the results of the previous measurements. During all measurements, we saw to it that patients had their heads as upright as possible. All three GDx instruments were located in similar, adjacent rooms with ambient lights left on. The software and hardware configuration of all three instruments was identical. All measurements were carried out by the same operator who also manually positioned the ellipse in all images.

**Subjects** In the first part of the study, measurements were taken on 5 consecutive days of right eyes of 10 healthy volunteers. Their ages ranged from 22 to 61 years (mean: 36 years). None of them had any ocular history; all had an IOP below 21 mm Hg, normal looking optic discs and normal visual fields (GHT within normal limits) on the Humphrey Field Analyzer (24-2 full threshold program). The refractive error of all subjects was between +7 and -7 D.

In the second part, we measured one eye of 45 glaucoma patients on two separate days within 5 weeks. The age of the patients was on average 63 years (range from 39 to 77 years); the mean defect (MD) of the patients was on average -10.7dB (stan-

dard deviation = 7.04). If a patient had glaucoma in one eye only, that eye was considered. If a patient had glaucoma in both eyes, one eye was selected randomly. Patients were recruited from the Glaucoma Service of our hospital, and all had glaucomatous visual field defects with glaucomatous appearing optic discs. Patients with any coexisting ocular disease, including pseudophakia, or systemic diseases with possible ocular involvement, such as diabetes, were excluded from the study.

In the third part of the study, 17 volunteers (4 glaucoma patients and 13 healthy subjects without any ocular history, aged between 27 and 62 years) had their right eye measured twice on each of 3 different instruments. Again, a measurement consisted of a mean of 3 single images of high quality.

Informed consent was obtained from all participating subjects after the nature of the procedure had been fully explained

**Statistical Analysis** For all statistical tests, the level of statistical significance was set at  $\alpha=0.05$ . There was no suspicion of non-normality for the within-patient variability of all parameters in both the normal subjects and glaucoma patients.

In the first two parts of the study, the reproducibility of measurements was expressed as 95% limits of agreement (LA) and in terms of the intraclass correlation coefficient (ICC). Calculations were performed for all 14 parameters available to the user. The definitions of all 14 parameters have been presented in the appendix. Some parameters (what we call straight parameters) relate to direct measurements, whereas others are obtained more indirectly by division of direct measures (these are so called ratio-parameters marked by (r) in Tables 1-3) or by a neural network analysis (The Number). LA relate to the agreement of measurements on two consecutive days within the same subject, and are defined, in this article, as 1.96 times the square root of two times the within-subject variance." LA are also called 'reproducibility' and represent a critical value that will not be exceeded with 95% probability by the absolute difference of two single measurements within the same subject on two consecutive days under the same conditions, assuming a normally distributed within-subject variability with the same variance across all subjects. In the methods described by Bland and Altman, the LA are calculated from two repeated measurements. If one has more than two repeated measurements, the within-subject variance can also be estimated, with greater precision than with only two repeated measurements. This was done in our normal group, where we used a series of 5 repeated measurements per subject.

In addition to the traditional LA, we also expressed the LA of a parameter as a percentage of the mean of the between-subjects distribution of that variable (LA%). This ad-hoc expression equals  $1.96 * \sqrt{2}$  times the coefficient of variation, and is only presented here in order to facilitate the mutual comparison of the LA of different variables. In addition, means and total standard deviations have been presented per parameter (Tables 3-1 and 3-2).

Our second measure to express the reproducibility of measurements was the ICC; we estimated the within-subject and between-subject variances, again assuming that the within-subject variance was the same across the volunteers. The ICC was

obtained by expressing the between-subject variance as a percentage of the total (within- plus between subject) variance. The ICC represents the power by which subjects can be distinguished from each other by their measurement outcome. It is generally accepted that reproducibility of measurements is high when the ICC is >90%.

In the normal subjects, differences in within-subject standard deviation between measurements based on single images and mean images were compared within the same subject with a Wilcoxon matched pairs signed ranks test after logarithmic (ln) transformation of the standard deviation. In the glaucoma group, a sign test was used because of too many zero within-subject standard deviations. We have presented p-values related to the statistical significance of differences in LA between single images and mean images (Table 3-1 and 3-2).

For the third part of the study, a random effects model with subject and instrument as random factors, was used to estimate three variance components: between-subject variance, between instrument variance, and error (or within-instrument) variance. Because of imbalance in the data of this experiment a maximum likelihood method was used ('PROC MIXED' in the SAS statistical package).

## Results

**Reproducibility of measurements in normal subjects** For all available parameters, the mean value across subjects, the standard deviation (SD), the 95% Limits of Agreement (LA), the 95% Limits of Agreement as a percentage of the mean value (LA%), and the Intraclass correlation coefficients (ICC) for normal subjects have been summarized in Table 3-1. The reproducibility of measurements varied considerably between parameters. In general, the straight parameters were more robust than the ratio-parameters. For example, in mean images, superior maximum had LA(%) of 8.5% of the mean values, whereas the LA(%) was 29.2% for maximum modulation. In mean images in healthy subjects, the parameters with LA of 10% and lower were: superior maximum, inferior maximum, symmetry, average thickness, superior average, inferior average and ellipse average. The superior/nasal parameter reproduced better than the superior ratio (which is a superior/temporal ratio).

In mean images, the LA of the superior maximum and inferior maximum parameter were  $7.2\mu$  and  $7.7\mu$ , respectively. In some parameters, the LA were lower in mean images than in single images. In others, it was vice versa. However, these differences were small, and only one out of 14 p-values that reflected the statistical significance of this difference, was  $<0.05$  (superior maximum;  $p=0.007$ ).

The differences in ICC between single images and mean images were small, and probably insignificant. In mean images, the intraclass correlation coefficient (ICC) was over 90% except for superior ratio, inferior ratio, maximum modulation and ellipse modulation.

**Reproducibility of measurements in glaucoma patients** As for normal subjects, some parameters had higher LA than others (table 3-2). Reproducibility of measurements was not consistently better or worse in glaucoma patients as compared to normals. In single images, LA were lower for 7 parameters in glaucoma patients as com-



pared to healthy subjects. In the remaining 7 parameters, the LA were higher. For mean images, the same was observed.

All parameters, except the number, had lower LA in mean images than in single images. However, in only one of the 14 parameters was this difference statistically significant (superior integral;  $p=0.021$ ).

The differences in ICC between single images and mean images were also small, and probably insignificant. The ICC for mean images was over 90% in all parameters except for maximum modulation.

**Variability between instruments** The results of the analysis of variance have been presented in Table 3-3. All components that contribute to the variance of a repeated measurement have been expressed in percentages of the total variance of 100%.

The reproducibility of measurements varied across parameters. The *between patients* component was by far the largest one. In general, the straight parameters showed much less variation than the ratio parameters. Of the straight parameters the between instrument variation was on the same order of magnitude as the *within instrument* variation (typically 2-5% of the total variation). Of the ratio parameters, both the *between instrument* and the *within instrument* (or error) component could be as high as 31.1%.

We have shown that the reproducibility of measurements of the GDx varies considerably across parameters. For example, 95% limits of agreement (LA) in normal subjects varied from 7.1% for ellipse average to 29.2% for maximum modulation. We therefore think it is more meaningful to speak of ‘the reproducibility of a parameter’, rather than of ‘the reproducibility of a technology’.

## Discussion

The 3 parameters similar to those that have shown a high sensitivity and specificity for detecting glaucoma with the NFA I,<sup>1</sup> (superior maximum, inferior maximum and symmetry) were among the most robust parameters (LA of each approximately 9% and the ICC well over 90%). These three parameters, however, did not discriminate very well between normal and glaucoma in the study by Weinreb et al.<sup>2</sup> Three parameters that discriminated well in their study, and reproduced well in our study, were ellipse average, inferior average and average thickness.

It is generally accepted that the reproducibility of measurements is high when the ICC is over 90%. This was true for most of the parameters that we have investigated, both in glaucoma patients and normals. We therefore conclude that the reproducibility of measurements with the GDx, in general, is high.

We have also found that the LA are not consistently better or worse in glaucoma patients than in normal subjects. Also, the ICC in normal subjects was over 90% in 10 out of 14 parameters; in glaucoma patients the ICC was over 90% in 13 out of 14 parameters. These conclusions are in agreement with those of Holló *et al.*,<sup>9</sup> who reported coefficients of variation that were similar for glaucoma patients and control subjects with the NFA II.

We have presented LA for all available GDx parameters. The tenet of these LA is that they are a clinically meaningful and intuitive parameter: as soon as a change in a certain parameter exceeds these limits, it reflects a statistically significant change. Any change within these limits is, with 95% probability, a coincidence. All parameters have their own characteristic LA. We believe that LA provide, in principle, clinically useful information to assess the significance of any change measured over time. How meaningful this approach is, has yet to be shown in long-term studies. The Number is unlikely to be useful for detecting change over time, since it reflects the likelihood of glaucoma, and not the severity of the disease.

Our results show that some parameters tend to be slightly more robust in mean images than in single images, especially in glaucoma patients. However, the present differences were small and statistically significant for only one in 14 parameters (both in the group of normals and in the glaucoma group). This one p-value, however, probably has little meaning in a series of multiple comparisons. One might expect that, in case of no differences between 20 given test variables, one in every 20 p-values will be below 0.05. We therefore conclude that LA are generally slightly lower in mean images than in single images, but that these differences do not reach statistical significance. In general, one would expect a mean image to have a better reproducibility than a single image, since one is averaging over more pixels of information, thus reducing the effect of random noise. Fortunately, this difference was not statistically significant. In a previous study with the NFA II we did find a statistical significance between a mean of three and a single image. (Colen et al., IOVS 1998;89(suppl):S-3223) It is unclear why we found no such statistical significance with the GDx.

One might conclude from our study that a single image is just as good as a mean image since the LA of single images does not differ statistically significantly from that of mean images. However, using only one image is not the same as taking only one image. We always take a minimum of 6 images per eye. This makes it easier for us to select those images of highest quality (fewest motion artifacts, best illumination etc.)

Finally, we have demonstrated that reproducibility of measurements across three different instruments is highest for straight parameters. Ratios are less robust, obviously because both the numerator and the denominator will have their variability. Notably if the denominator is relatively small to its variability, the variability of the ratio will be large. Not surprisingly, symmetry was more robust than the other ratio parameters in normal subjects (relatively large denominator), but not as robust in glaucoma patients, where small denominators were to be expected in individual cases.

In conclusion, we have explored the reproducibility of measurements with the Nerve Fiber Analyzer/GDx. Some parameters are promisingly robust to serve in follow-up of patients, and we are currently investigating the significance of the more robust parameters in long-term follow-up studies.

The reproducibility of measurements varied across parameters. In mean images in healthy subjects the parameters with LA of 10% and lower were: superior maximum, inferior maximum, symmetry, average thickness, superior average, inferior average and ellipse average. The ICC indicated that the reproducibility of measurements with the NFA in general is high. The LA in normal and glaucomatous subjects were similar. The tenet of the LA is that, for example, in normals, any measured change in nerve fiber layer thickness is statistically significant when it exceeds about 7-8 $\mu$  in the superior maximum or inferior maximum parameter. Differences between single and mean images were small and not statistically significant. Finally, reproducibility of measurements across three different instruments was highest for straight parameters.

## Conclusions

*Acknowledgement: We thank Laser Vision for courteously lending us a GDx for the third part of our study.*

## Appendix

GDx Parameters	<p><b>Superior Maximum:</b> This is the average of the 1500 thickest pixels in the superior quadrant.</p> <p><b>Inferior Maximum:</b> This is the average of the 1500 thickest pixels in the inferior quadrant.</p> <p><b>Symmetry:</b> This is the ratio of the average of the 1500 thickest pixels in the superior quadrant over the average of the 1500 thickest pixels in the inferior quadrant.</p> <p><b>Superior Ratio:</b> This is the ratio of the average of the 1500 thickest pixels in the superior quadrant over the average of the 1500 median pixels in the temporal quadrant.</p> <p><b>Inferior Ratio:</b> This is the ratio of the average of the 1500 thickest pixels in the inferior quadrant over the average of the 1500 median pixels in the temporal quadrant.</p> <p><b>Superior/Nasal:</b> This is the ratio of the average of the 1500 thickest pixels in the superior quadrant over the average of the 1500 median pixels in the nasal quadrant.</p> <p><b>“The Number”:</b> This is an experimental number currently under evaluation. A neural network has been trained to look at all values obtained when an image is acquired. The neural network then assigns a number between 0 and 100 to each patient according to the following scale: 0 = totally normal, 100 = glaucoma. Early evaluation of the number indicates that patients who score between 0-30 are normal; patients scoring over 70 are glaucomatous; and those scoring between 30-70 are glaucoma suspects. Patients in this last category may prove to be “borderline” or “outside normal limits” on some GDx parameters but not exhibit any visual field loss or other indications of glaucoma.</p> <p><b>Max Modulation:</b> Provides an indication of the difference between the thickest parts of the nerve fiber layer and the thinnest parts. First, the average is calculated for 1) the 1500 thickest points in the superior quadrant, 2) the 1500 thickest points in the inferior quadrant, 3) the 1500 median points in the nasal quadrant and 4) the 1500 median points in the temporal quadrant. Once an average number is derived for each quadrant, the lowest number is subtracted from the highest number. The resulting number is then divided by the lowest number.</p> <p><b>Average Thickness:</b> The average thickness of all pixels in the image; evaluates all 65,536 points used to create an image. The Average is calculated by adding up all of the values of the usable pixels outside of the optic nerve head (as designated by the operator) and dividing by the number of pixels used.</p> <p><b>Ellipse Modulation:</b> Like “Max Modulation”, Ellipse Modulation is an indication of the difference between the thickest parts of the nerve fiber layer and the thinnest parts. The difference is that, rather than using all of the points in the image, Ellipse Modulation uses the points in the ellipse surrounding the optic nerve. Ellipse Modulation is calculated by taking the thickest pixel along the ellipse, subtracting the thinnest pixel along the ellipse, and dividing the total by the value of the thinnest pixel.</p> <p><b>Ellipse Average</b> (measurement is in microns): The average thickness of the nerve fiber layer around the ellipse surrounding the optic nerve.</p> <p><b>Superior Average</b> (measurement is in microns): The average thickness of the nerve fiber layer along the portion of the ellipse surrounding the optic nerve in the superior quadrant.</p> <p><b>Inferior Average</b> (measurement is in microns): The average thickness of the nerve fiber layer along the portion of the ellipse surrounding the optic nerve in the inferior quadrant.</p> <p><b>Superior Integral</b> (measurement is in millimeters squared): The total area under the curve (or total volume) of the nerve fiber layer along the superior portion of the ellipse surrounding the optic nerve.</p>
----------------	--

SINGLE IMAGE							MEAN OF 3					
	unit	mean	SD	LA	LA (%)	ICC (%)	mean	SD	LA	LA (%)	ICC (%)	p-value
superior maximum	μ	85.0	14.45	9.4	11.0	94.6	84.6	14.7	7.2	8.5	96.9	.007
inferior maximum	μ	90.5	15.45	9.0	10.0	95.6	89.3	15.6	7.7	8.6	96.8	.139
symmetry (r)		0.95	0.12	0.11	11.9	89.4	0.96	0.13	0.09	9.3	94.3	.799
superior ratio (r)		2.29	0.45	0.43	18.8	88.1	2.34	0.50	0.47	20.0	88.8	.333
inferior ratio (r)		2.41	0.33	0.51	21.1	69.1	2.43	0.35	0.50	20.3	73.6	.285
superior/nasal (r)		2.12	0.35	0.26	12.2	93.2	2.13	0.38	0.32	15.1	90.8	.721
the number		18.5	13.2	11.7	63.2	89.8	18.7	13.1	10.4	55.6	91.9	.327
maximum modulation (r)		1.60	0.34	0.42	26.0	80.4	1.64	0.39	0.48	29.2	80.0	.114
average thickness	μ	62.0	7.8	4.7	7.6	95.1	60.8	7.7	4.8	8.0	94.9	.678
ellipse modulation (r)		2.62	0.33	0.55	21.1	64.5	2.75	0.37	0.60	21.7	65.7	.646
ellipse average	μ	65.4	7.7	5.1	7.8	94.3	64.3	7.6	4.6	7.1	95.3	.260
superior average	μ	75.7	11.1	8.1	10.7	93.1	74.2	10.9	7.8	10.5	93.4	.515
inferior average	μ	77.0	11.3	7.1	9.2	94.9	76.0	10.4	6.7	8.9	94.6	.799
superior integral	mm2	0.19	0.035	0.025	12.7	93.4	0.19	0.034	0.026	13.7	92.4	.333

Reproducibility of all 14 available parameters has been calculated for single images and 'mean of 3' images. Parameters marked with an (r) are ratio-based parameters. The unit of measurement has been given; some parameters are without dimension. The mean value across subjects (and the standard deviation SD) has been given for every parameter. Limits of Agreement (LA) have been presented in the same dimension as the parameter itself. To compare between parameters, LA have also been expressed as a percentage of their mean value (LA%). In addition, the Intraclass Correlation Coefficient (ICC) has been given for every parameter. The final column represents p-values for statistical significance of differences in LA between single images and mean images.

**Table 3-1.**  
Reproducibility  
of measure-  
ments in healthy  
subjects

**Table 3-2.**  
Reproducibility  
of measure-  
ments in glau-  
coma patients

		MEAN OF 3					
		mean	SD	LA	LA (%)	ICC (%)	p-value
superior maximum	μ	65.7	17.3	8.7	13.3	96.7	.449
inferior maximum	μ	72.8	18.9	7.9	10.9	97.7	.720
symmetry (r)		0.92	0.17	0.12	12.6	94.1	.432
superior ratio (r)		1.61	0.41	0.28	17.6	93.6	.613
inferior ratio (r)		1.76	0.36	0.28	15.8	91.9	.442
superior/nasal (r)		1.51	0.29	0.17	11.1	95.7	.142
the number		59.4	24.4	17.7	29.8	93.0	.868
maximum modulation (r)		0.99	0.33	0.31	30.9	88.4	.224
average thickness	μ	54.3	12.0	5.1	9.3	97.7	.064
ellipse modulation (r)		1.68	0.54	0.33	19.4	95.3	.165
ellipse average	μ	54.5	12.5	5.2	9.5	97.7	.424
superior average	μ	56.6	14.9	5.9	10.4	98.0	1.00
inferior average	μ	62.2	16.8	7.1	11.3	97.7	.248
superior integral	mm <sup>2</sup>	0.15	0.039	0.015	10.0	98.0	.021

Legend: as in 3-1.

	between patients (%)	between instruments (%)	within instruments (%)	total (%)
superior maximum	92.9	2.9	4.2	100
inferior maximum	94.2	2.0	3.8	100
symmetry (r)	83.2	5.3	11.5	100
superior ratio (r)	60.4	12.1	27.5	100
inferior ratio (r)	46.2	22.7	31.1	100
superior/nasal (r)	65.3	20.8	13.9	100
the number	84.7	3.7	11.6	100
maximum modulation (r)	68.7	16.1	15.2	100
average thickness	91.9	5.5	2.6	100
ellipse modulation (r)	52.1	29.0	18.9	100
ellipse average	93.1	4.0	2.9	100
superior average	93.1	4.5	2.4	100
inferior average	95.8	0.7	3.5	100
superior integral	87.0	8.1	4.9	100

Analysis of Variance showing the three components that make up the total amount of variance.

**Table 3-3.**  
Variability  
between  
instruments

## References

1. Tjon-Fo-Sang MJ, Lemij HG. The sensitivity and specificity of nerve fiber layer measurements in glaucoma as determined with scanning laser polarimetry. *Am J Ophthalmol* 1997;123:62-9.
2. Weinreb RN, Zangwill L, Berry CC, et al. Detection of glaucoma with scanning laser polarimetry. *Arch Ophthalmol* 1998;116:1583-9.
3. Weinreb RN, Shakiba S, Zangwill L. Scanning laser polarimetry to measure the nerve fiber layer of normal and glaucomatous eyes. *Am J Ophthalmol* 1995;119:627-36.
4. Chi Q, Tomita G, Inazumi K, et al. Evaluation of the effect of aging on the retinal nerve fiber layer thickness using scanning laser polarimetry. *J Glaucoma* 1995;4:406-13.
5. Junghardt A, Schmid MK, Schipper I, et al. Reproducibility of the data determined by scanning laser polarimetry. *Graefes Arch Clin Exp Ophthalmol* 1996;234:628-32.
6. Tjon-Fo-Sang MJ, van Strik R, de Vries J, Lemij HG. Improved reproducibility of measurements with the nerve fiber analyzer. *J Glaucoma* 1997;6:203-11.
7. Waldock A, Potts MJ, Sparrow JM, Karwatowski WS. Clinical evaluation of scanning laser polarimetry: I. Intraoperator reproducibility and design of a blood vessel removal algorithm. *Br J Ophthalmol* 1998;82:252-9.
8. Zangwill L, Berry CA, Garden VS, Weinreb RN. Reproducibility of retardation measurements with the nerve fiber analyzer II. *Journal of Glaucoma* 1997;6:384-9.
9. Holló G, Suveges I, Nagymihaly A, Vargha P. Scanning laser polarimetry of the retinal nerve fibre layer in primary open angle and capsular glaucoma. *Br J Ophthalmol* 1997;81:857-61.
10. Hoh ST, Ishikawa H, Greenfield DS, et al. Peripapillary nerve fiber layer thickness measurement reproducibility using scanning laser polarimetry. *J Glaucoma* 1998;7:12-5.
11. Bland JM, Altman DG. Statistical methods for assessing agreement between two methods of clinical measurement. *Lancet* 1986;307-10.
12. Dreher AW, Reiter K. Retinal laser ellipsometry: a new method for measuring the retinal nerve fiber layer thickness distribution. *Clin Vis Sci* 1992;7:481-8.
13. Tjon-Fo-Sang MJ, de Vries J, Lemij HG. Measurement by nerve fiber analyzer of retinal nerve fiber layer thickness in normal subjects and patients with ocular hypertension. *Am J Ophthalmol* 1996;122:220-7.
14. Weinreb RN, Dreher AW, Coleman A, et al. Histopathologic validation of Fourier-ellipsometry measurements of retinal nerve fiber layer thickness. *Arch Ophthalmol* 1990;108:557-60.



## CHAPTER 4

### *Prevalence of split nerve fiber layer bundles in healthy eyes, imaged with scanning laser polarimetry*

Colen TP and Lemij HG  
Ophthalmology 2001;108(1):151-156

## Abstract

**Purpose** The GDx is a scanning laser polarimeter, designed to assess the peripapillary nerve fiber layer in vivo. On the GDx, a nerve fiber bundle can appear as a single, or as a split bundle. The aim of our study was to determine the prevalence of split nerve fiber layer bundles, and to demonstrate its clinical relevance.

**Design** cross-sectional study.

**Participants** 254 healthy volunteers participated.

**Methods** We imaged 454 eyes of 254 healthy caucasians with the GDx (Laser Diagnostic Technologies, San Diego, CA). All eyes had an intraocular pressure  $\leq 21$  mmHg, normal appearance of the optic nerve head and normal visual fields (Humphrey Field Analyzer 24-2 full threshold program). According to our working definition, a bundle appeared 'split' when the color-coded pixels corresponding to areas of higher retardation were clearly divided into two more or less symmetrical parts, not resembling a wedge defect. The classification was performed by two independent observers who used an identical set of reference examples to standardize the classification.

**Main outcome measures** The presence of a split nerve fiber layer bundle.

**Results** Interobserver agreement was very good ( $\kappa = 0.83$ ) and a consensus was reached in all cases. In 419 eyes (92.3%), there was no split bundle. A split superior bundle was seen in 29 eyes (6.4%). A split inferior bundle was observed in 5 eyes (1.1%) and in 1 eye (0.2%) a split bundle was seen superiorly and inferiorly. When considering subjects, a split superior bundle (either in the right eye, or in the left eye, or in both eyes) occurred in 12.0% of normal subjects. The 'superior maximum' parameter was significantly lower in eyes with a split superior bundle than in eyes with a single superior bundle ( $67.2\mu$  vs  $89.9\mu$ ;  $p < 0.001$ ). The same was observed for the 'symmetry' parameter ( $0.88$  vs  $0.98$ ;  $p < 0.001$ ).

**Conclusions** Split nerve fiber layer bundles are a common finding in healthy eyes when imaged with the GDx. A split superior bundle is the most occurring variation. In these last cases, an abnormal 'superior maximum' or 'symmetry' parameter, otherwise potential indicators of glaucoma, should not readily be interpreted as abnormal.

## Introduction

The GDx (Laser Diagnostic Technologies, San Diego, CA) is a scanning laser polarimeter, that assesses nerve fiber layer (NFL) thickness in the peripapillary retina, and discriminates well between normals and glaucoma patients.<sup>1-3</sup> A detailed description of the GDx has been published elsewhere.<sup>4-6</sup> In short, a beam of polarized laser light is sent through the birefringent retinal NFL. As the light is reflected back into the instru-

ment, the amount of phase shift (retardation) is determined and is thought to linearly reflect NFL thickness, as has been shown in a monkey model.<sup>7</sup> Anterior segment retardation is compensated by the instrument. In about 0.7 seconds the peripapillary retina is scanned at 65536 locations, and a retardation image of 256x256 pixels is constructed. This image is color-coded: a continuous scale from yellow to red to blue represents areas from high to low retardation. As adjacent pixels go from one color to another, the true difference in polarimetric reading may in fact be not as large as it seems.

The grouping of similarly colored, high-retardation pixels, when contrasted with surrounding pixels, gives the appearance of a 'bundle' and we will further refer to this grouping as such. Two such bundles are usually seen, typically superiorly and inferiorly. GDx data is characterized by a large interindividual variability.<sup>3,4</sup> Also the bundles that appear on the GDx vary in shape and thickness. We noticed earlier that some subjects with healthy eyes had an NFL orientation that we first believed indicated NFL defects. Observing this orientation more and more in healthy eyes, we came to believe it is a normal physiological finding. We have started to call this orientation 'split nerve fiber layer bundles', in contrast to single nerve fiber layer bundles that appear in the majority of healthy eyes. Split bundles can easily be distinguished from wedge shaped defects of the NFL, which have a markedly different appearance, as we will show.

The purpose of this study was to propose a definition for these split nerve fiber layer bundles, to investigate their prevalence in a population of healthy eyes, and to demonstrate their effect on some of the GDx parameters.

**Measurement procedures** A measurement session for one eye always consisted of obtaining a minimum of 3 single images of high quality (i.e. well focussed, the optic disc well centered in the image, equal and total illumination in all segments and no motion artifacts). These three images were then aligned and converted by the software into one 'mean image'. During all measurements, we saw to it that patients had their heads as upright as possible. Ambient lights were left on.

## Methods

Areas of blood vessels are a source of noise<sup>8</sup> and are therefore automatically excluded for analysis by the GDx software. The entire image is divided into 4 segments centered on the optic disc: superior 120°, inferior 120°, nasal 50° and temporal 70°. For a quantitative approach, several parameters are available. In this study, the 'superior maximum' and the 'symmetry' parameter were considered. The superior maximum (smax) parameter is the average of the 1500 thickest pixels in the superior segment outside the green peripapillary band. An inferior maximum parameter is defined likewise for the inferior segment. The symmetry parameter is the ratio superior maximum/inferior maximum.

**Subjects** After informed consent was obtained from the volunteers, 454 eyes of 254 healthy caucasians (age range 20-79 years; mean 51.6 years) were imaged with the GDx. Originally, 262 subjects were included for this study, but 8 (3.1%) of them were unsuitable for GDx imaging due to either inability to fixate or extremely large zones of peripapillary atrophy. All subjects were equally distributed across 10-year cohorts

ranging from 20 to 80 years. All subjects were imaged on the same instrument within a time period of 6 months. They had no diabetes or hypertension that required medical treatment, nor any ocular history. All eyes had an intra ocular pressure  $\leq 21$  mm Hg, normal appearance of the optic nerve head and normal visual fields (Humphrey Field Analyzer 24-2 full threshold program).

**The split bundle** Two independent observers, who used the same reference examples, classified the GDx printouts. Some of these reference examples have been presented in fig 4-1. The final classification was established by a consensus, which could be agreed upon in all cases. On the GDx, a nerve fiber bundle can appear as a single bundle (example 1), or as what we call a 'split bundle' (example 2). According to our working definition, a bundle appeared 'split' when the color-coded pixels corresponding to areas of higher retardation were clearly divided into two more or less symmetrical parts, not resembling a wedge defect. We will explain what we mean with 'clearly', 'symmetrical', and a 'wedge defect'.

With 'clearly', we mean that the split has to be 'deep enough'; the blue area separating the two 'legs' of the split bundle has to touch on the green peripapillary band, or extend even further towards the center of the image. In our experience, a single and a split nerve fiber layer bundle are two extremes on a continuous scale. This is partly illustrated in examples 2 and 3, that both meet the criteria of our definition of a split bundle. However, in example 2 the split is 'deeper'; in other words, the blue area separating both legs of the bundle extends further towards the center of the image than in example 3 (also note its effect on the double hump pattern). Descending further down the scale from split to single bundle is example 4, where the split is not 'deep enough' to meet the criteria of our definition. We called this a partially split bundle. This was also how the reference examples worked: any bundle that was split like this, or less, was not a split bundle by our definition.

The next part of our definition relates to symmetry. In examples 2 and 3, the two legs of the split bundle are equally large. Example 5 shows a split that is not symmetrical and has therefore not been classified as a split bundle according to our definition. Clinically, we would refer to this as an asymmetrically split bundle.

The final part of our definition applies to wedge defects that have a distinctly other appearance than split bundles. Example 6 shows the presence of such a wedge defect of the inferior NFL of a 63-year-old glaucoma patient. The wedge defect could be seen with red-free light, there was local cupping of the optic disk and the patient had a superior arcuate scotoma on the visual field test. A wedge defect often appears both on the reflectance image, and on the retardation image. The difference between a split bundle and a wedge defect is that in the latter, the blue area corresponding to the wedge defect is usually sharply demarcated from the adjacent red area. In a split bundle, this transition is more gradual, as seen in examples 2 to 5.

Classifications were performed by two independent observers judging the printouts. An eye had either a split superior or a split inferior bundle, or both, or no split bundle.

**Statistical methods** We evaluated the inter-observer agreement of the classification using kappa statistics. In interpreting the kappa values we followed the guidelines provided by Altman.<sup>9</sup> To investigate the effect of a split superior bundle on two parameters (smax and symmetry), eyes with a split superior bundle were compared with eyes with no split bundle (table 4-2). A Student's t-test was used to test for differences between the two groups. A subgroup of 200 subjects, that had both eyes imaged with the GDx, was separately analyzed to determine an odds-ratio, and to determine occurrence of split superior bundles per subject (instead of per eye).

The prevalence of split bundles, observed by two different investigators, has been presented in table 4-1. The kappa value for inter-observer agreement was 0.83 (SD = 0.05), which is generally considered to be very good. In case of disagreement, a consensus was reached. Out of a total of 454 eyes, 419 eyes (92.3%) were classified as having no split bundle. In 29 eyes (6.4%), a split superior bundle was observed. In 5 eyes (1.1%), a split inferior bundle was seen and 1 eye (0.2%) had both a split superior and a split inferior bundle.

## Results

The mean superior maximum (smax) parameter in subjects with a split superior bundle was statistically significantly lower than the mean smax for the subjects with a single superior bundle (67.2 microns vs 89.9 microns;  $p < 0.001$ ; table 4-2). Also, subjects with a split superior bundle had a mean symmetry parameter that was statistically significantly lower as compared to the group with a single superior bundle (0.88 vs 0.98;  $p < 0.001$ ).

Of all split bundles, a split superior bundle was most frequent (6.4% of all eyes). To determine in what percentage of *subjects* a split superior bundle occurred, only those 200 subjects included in the study with both eyes were considered (table 4-3). Of these, 24 subjects (12.0%) had a split superior bundle (4 in the left eye, 18 in the right eye and 2 in both eyes). A split superior bundle occurred more often in the right eye than in the left eye which was a statistically significant difference ( $p = 0.0043$ ). The odds-ratio of having a split superior bundle in the left eye, relatively to having one in the right eye, was 4.5.

We have shown that the prevalence of so-called split nerve fiber layer bundles as measured with the GDx is approximately 8% in a group of 454 healthy eyes. They occurred in about 12% of normal subjects. A split superior bundle was the more common variation. Given the high prevalence in healthy eyes, we believe that a split bundle is a normal variation of the NFL pattern when imaged with the GDx.

## Discussion

In our clinic, we use a so-called integrated approach to interpreting GDx data: we combine quantitative aspects (the various parameters) and non-quantitative aspects (reflectance image, retardation image, double hump pattern) of the data into an integrated evaluation of the GDx results. Being part of the quantitative data, the superior maximum and symmetry parameter are affected. In addition, also non-quantitative aspects of the data are affected. We have illustrated how a split bundle can alter the usual shape of the double hump pattern. Also, we have shown that it

should not be confused with a pathologic finding such as a wedge defect, which, at the moment, can only poorly be detected quantitatively with the current software. Thus, recognizing a split bundle as a physiological finding is important when interpreting GDx results, and may increase the specificity of the clinician working with the GDx.

We realize that whether there is an anatomical basis for what we call a (split) ‘bundle’, would still need histologic confirmation in our subjects. However, until that question can be adequately addressed, clinicians that use the GDx will continue to be confronted with split bundles, and will need to make sense of them. Our paper does not try to explore the human retinal anatomy, but is only meant to help clinicians towards a better interpretation of GDx results. Interestingly, an expert on red-free fundus photography (Dr. HA Quigley, personal communication) was not surprised by our findings. He told us that arcuate bundles appear split on red-free fundus photography in some cases.

To investigate whether a split bundle is not an early sign of glaucoma, all subjects with split bundles have been included in a long-term follow-up study.

Of all the split bundles, a split superior bundle was the more common variation. We have no explanation for this. Also, we found split bundles to occur more frequently in the right eye than in the left eye. This could be due to measurement artifact or coincidence. Although most split superior bundles occurred unilaterally, having a split bundle in one eye increases the odds of having a split bundle in the fellow eye.

The double hump pattern in patients with a split superior bundle looks similar to the optical coherence tomography graph of normal control subjects as has been presented by Pieroth and coworkers.<sup>10</sup> It is unclear whether this shouldering of the OCT graph is related to the split bundles we have described.

As the GDx has been developed over the last years, parameters have been introduced to quantitatively summarize the data. Since a split bundle does not appear to indicate disease, it would be useful to develop an algorithm that can correct the affected parameters, and that can discriminate between split bundles and wedge defects. Until then, it seems that parameters such as symmetry and superior maximum are less reliable in subjects with a split superior bundle. The clinician is advised to rely heavier on the non-quantitative part of the GDx data in these cases.

**Acknowledgment:** *The authors thank Helen Bakker, MD for participating in this study as the second observer.*

	no split	superior split	inferior split	superior & inferior split	total
number of eyes (observer #1)	421	29	2	2	454
number of eyes (observer #2)	413	37	4	0	454
consensus	419	29	5	1	454
%	92.3%	6.4%	1.1%	0.2%	100%

**Table 4-1.**  
Prevalence of split Nerve Fiber bundles in 454 eyes of 254 subjects.

	Single superior bundle	Split superior bundle	difference	95 % CI	p-value
Smax (m)	89.9	67.2	22.7	20.2 ; 25.1	<0.001
Symmetry	0.98	0.88	0.10	0.055 ; 0.15	<0.001

**Table 4-2.**  
Smax and Symmetry parameters in subjects with a split superior bundle.

The mean superior maximum (smax) and the mean symmetry parameters in subjects with a split superior bundle, as compared to subjects with a single superior bundle. The unit of the smax is  $\mu$ . Also, the difference between these two values, its 95% Confidence Interval (95% CI), as well as the p-value corresponding to the statistical difference of this difference have been given.

SPLIT SUPERIOR OD				
		yes	no	total
split superior OS	yes	2	4	6
	no	18	176	194
	total	20	180	200

**Table 4-3.**  
Prevalence of split superior bundles in subjects who had both eyes imaged (n=200)

In this table only superior split bundles are considered in those 200 subjects where images could be obtained in both eyes. Subjects had either a split superior bundle (in the right eye or in the left eye, or in both eyes) or no split superior bundles.

## References

1. Tjon-Fo-Sang MJ, Lemij HG. The sensitivity and specificity of nerve fiber layer measurements in glaucoma as determined with scanning laser polarimetry. *Am J Ophthalmol* 1997;123:62-9.
2. Weinreb RN, Zangwill L, Berry CC, et al. Detection of glaucoma with scanning laser polarimetry. *Arch Ophthalmol* 1998;116:1583-9.
3. Choplin NT, Lundy DC, Dreher AW. Differentiating patients with glaucoma from glaucoma suspects and normal subjects by nerve fiber layer assessment with scanning laser polarimetry. *Ophthalmology* 1998;105:2068-76.
4. Tjon-Fo-Sang MJ, de Vries J, Lemij HG. Measurement by nerve fiber analyzer of retinal nerve fiber layer thickness in normal subjects and patients with ocular hypertension. *Am J Ophthalmol* 1996;122:220-7.
5. Dreher AW, Reiter K. Retinal laser ellipsometry: a new method for measuring the retinal nerve fiber layer thickness distribution. *Clin Vis Sci* 1992;7:481-8.
6. Nicolela MT, Martinez-Bello C, Morrison CA, et al. Scanning laser polarimetry in a selected group of patients with glaucoma and normal controls. *Am J Ophthalmol* 2001;132:845-54.
7. Weinreb RN, Dreher AW, Coleman A, et al. Histopathologic validation of Fourier-ellipsometry measurements of retinal nerve fiber layer thickness. *Arch Ophthalmol* 1990;108:557-60.
8. Tjon-Fo-Sang MJ, van Strik R, de Vries J, Lemij HG. Improved reproducibility of measurements with the nerve fiber analyzer. *J Glaucoma* 1997;6:203-11.
9. Altman DG. *Practical statistics for medical research*, first ed. London: Chapman and Hall, 1991.
10. Pieroth L, Schuman JS, Hertzmark E, Hee MR. Evaluation of focal defects of the nerve fiber layer using optical coherence tomography. *Ophthalmol* 1999;106:570-9.



## CHAPTER 5

### *Retinal Nerve Fiber Layer thickness in human strabismic amblyopia*

Colen TP, de Faber JT and Lemij HG  
Binocular Vision & Strabismus Quarterly 2000;15(2):141-146

## Abstract

**Purpose** Amblyopia is characterized by histopathological changes in the visual cortex and lateral geniculate nucleus. In the retina, however, no abnormalities have yet been reported. The purpose of this study was to compare the nerve fiber layer (NFL) thickness in the amblyopic eye with that in the sound eye of patients with strabismic amblyopia. As a practical implication, we investigated the validity of comparing Nerve Fiber Analyzer (NFA) measurements obtained in amblyopic eyes to the normative database built into the NFA.

**Methods** NFL thickness was measured with a third generation NFA, the GDx (Laser Diagnostic Technologies, San Diego, CA). This is a scanning laser polarimeter that has been designed for monitoring glaucoma. Twenty patients with strabismic amblyopia were imaged with the NFA. Patients had no nystagmus, neurological disease or glaucoma.

**Results** Nine patients had amblyopia in the right eye, and 11 patients in the left eye. The following NFL thickness parameters (all in microns) were compared: average thickness, superior maximum, inferior maximum, superior average, inferior average, nasal median and temporal median. In general, the sound eyes yielded higher thickness measures than the amblyopic eyes. These differences, however, were small and not statistically significant at the  $\alpha = 0.05$  level.

**Conclusions** Measured with the NFA, there were no statistically significant differences in NFL thickness between the amblyopic and the sound eye in patients with strabismic amblyopia. Thus, when amblyopic eyes are measured with the NFA, the built-in normative database may serve as a reference to amblyopic data.

## Introduction

Amblyopia is characterized by histopathological changes in the visual cortex and lateral geniculate nucleus (LGN).<sup>1</sup> Marked shrinkage of LGN-cells that receive input of the amblyopic eye are well described in human and non-human primates. The decrease in LGN cell size may be caused by retrograde inhibition by the striate cortex in strabismic amblyopia. In the retina of amblyopic eyes, however, no abnormalities have yet been reported.<sup>2,3</sup>

Since the introduction of the Nerve Fiber Analyzer (NFA), it is now possible to assess the thickness of the retinal nerve fiber layer (NFL) in vivo. The aim of this study was to investigate whether the retinal NFL in the amblyopic eye in strabismic amblyopia would differ in thickness as compared to the fellow eye.

Today, the NFA has become a widely used instrument for monitoring glaucoma. The thinner NFL in glaucoma can be quantitatively assessed which discriminates well between normals and glaucoma patients.<sup>4-8</sup> The latest version of the instrument, the NFA/GDx, has a built-in normative database that can be used to compare individual data with. This database consists of data of several hundred normal subjects subdivided into their various ethnic origins. Patients with any ocular disease includ-

ing amblyopia were not included in the database. It is unknown whether the normative database may serve as a valid reference in amblyopic eyes. Our study shows that this comparison is justified.

**The Nerve Fiber Analyzer (NFA)** NFL thickness was assessed with a third generation Nerve Fiber Analyzer, the so-called GDx (Laser Diagnostic Technologies, San Diego, CA). The NFA has been primarily designed for monitoring glaucoma. Changes of the retinal NFL that are characteristic for glaucoma, can be objectively quantified with the NFA.<sup>5</sup> A detailed description of the NFA has been published elsewhere.<sup>9-11</sup> In short, the NFA sends a polarized beam of laserlight into the eye, and analyses the amount of phase shift in the backscattered light. This phase shift, called retardation, is thought to arise from the specific lamellar orientation of the microtubules inside the retinal axons. The retinal NFL thickness value is then obtained by multiplying the degrees of retardation with 7.4, analogous to a monkey model where 7.4  $\mu$  retinal NFL thickness corresponded to 1 deg of retardation.<sup>12</sup>

## Methods

In approximately 0.7 seconds, the peripapillary fundus is scanned with the standard 15 x 15 deg scanning angle and a resolution of 256 x 256 pixels. The data is used to compose a NFL thickness map of the same resolution, that is then color coded, and presented to the operator along with a reflectance fundus image for orientation. Next, the thickness map is automatically divided into 4 segments centered on the optic disc (superior 120 deg, inferior 120 deg, nasal 50 deg and temporal 70 deg). The operator positions a circle on the margin of the optic nerve head. Concentrically, a second circle with 1.75 times the diameter of the first is displayed automatically, excluding all pixels inside this second circle from analysis. Areas of blood vessels are a source of noise<sup>13</sup> and are therefore automatically excluded for analysis by the software.

For a quantitative approach, 14 standard parameters are available to the user. From these, the five absolute thickness parameters were selected, and in addition 2 non-standard parameters were derived by hand from existing standard parameters. The unit of measure of these 7 parameters is microns ( $\mu$ ). **Average thickness** is the average thickness of all pixels in all 4 segments together. **Superior average** and **Inferior average** is the average thickness of all pixels beneath the superior and inferior part of the ellipse respectively. **Superior maximum** and **Inferior maximum** is the average of the 1500 thickest pixels in the superior segment and the inferior segment respectively, reflecting the thickness of the superior and the inferior nerve fiber bundle. **Temporal median**, a non-standard parameter, reflects the mean value of the 1500 median pixels in the temporal segment and is obtained by dividing the superior maximum by the superior ratio. Likewise, **Nasal median**, also a non-standard parameter, reflects the mean value of the 1500 median pixels in the nasal segment and is obtained by dividing the superior maximum by the superior/nasal ratio.

**Patients** Amblyopia was defined as a difference in visual acuity between the two eyes of at least two Snellen lines with optimal correction. Initially, thirty-one patients met the inclusion criteria of strabismic amblyopia, no nystagmus, and no neurological disease. Of these, eleven patients were excluded because no high quality NFA image could be obtained. In these cases the amblyopic eye was unable to fix

when the sound eye was imaged. Our standard image quality criteria were: centered optic disc, sharp focus, equal and total illumination in all segments and no eye movements during image acquisition. Of the remaining 20 patients (mean age 37.7 years; range 15-60) a high quality NFA image could be obtained in both eyes. Strabismic history, visual acuity, and refraction have been presented in table 5-1. Nine patients had amblyopia in the right eye and 11 patients in the left eye. All patients had intraocular pressures <21 mm Hg and normal looking optic discs. Visual acuity ranged from 20/32 to 20/16 in the sound eye, and from counting fingers to 20/25 in the amblyopic eye.

**Scanning procedures** Standard clinical procedures were adopted for this study. During all measurements, we saw to it that patients had their heads as upright as possible. Ambient lights were left on. Multiple scans were obtained in most cases and mean images from three images of high quality were created by the software. All measurements were carried out by the same operator.

**Statistical procedures** All data was entered into an SPSS statistical package. Differences (and 95% confidence interval) between sound eye and the amblyopic eye were calculated per parameter with a paired student's t-test. The level of statistical significance was set at  $\alpha = 0.05$ .

## Results

All parameters except the nasal median showed a thinner retinal nerve fiber layer in the amblyopic eye as compared with the fellow eye (table 5-2). The nasal median parameter was on average  $0.4\mu$  higher in the amblyopic eye than in the sound eye. The differences were small for all parameters, and not statistically significant at the  $\alpha = 0.05$  level.

## Discussion

There was no statistically significant difference in NFL thickness between the two eyes in strabismic amblyopia, as measured with the Nerve Fiber Analyzer. Therefore, strabismic amblyopia does not appear to be associated with structural changes at the level of the retinal nerve fiber layer.

The NFA measures retardation, mainly originating from the structural arrangement of microtubules inside the retinal axons. Therefore, the conclusions of the present study probably apply to structure only, and not to function.

Considering the known changes in the cortex and the LGN, one could hypothesize transsynaptical changes in the retinal ganglion cells and thus in the NFL. Our results do not support this hypothesis. Neither is it supported by results by De Lint,<sup>3</sup> who found no evidence of retinal dysfunction at the level of cone photoreceptors in amblyopic eyes.

## Conclusion

Measured with the Nerve Fiber Analyzer, there are no differences in nerve fiber layer thickness between the amblyopic and the sound eye, in patients with strabismic amblyopia. Therefore, when the NFA is used for monitoring amblyopic eyes, data can be compared with the built-in normative database, that was compiled without amblyopic eyes.

Patient nr.	Age (yrs)	Strabismus History	Treatment	Strab. Actual	VA ODU	Refraction
1	28	ET	none	XT 5 Δ	20/20 20/32	S +0.25 S +4.0
2	52	ET	none	ET 50 Δ	20/50 20/20	S +3.0 S + 0.5
3	48	ET	none	XT 40 Δ	20/200 20/20	n/a
4	26	micro ET	none	ET 5 Δ	20/16 20/200	plano
5	56	ET	Str. surgery	XT 65 Δ	20/20 20/80	S +0.25 C -0.50 x 115° S 0 C -0.25 x 153°
6	30	ET	occlusion	XT 20 Δ RHT 10 Δ	20/40 20/20	S + 4.5 C 0.5 x 5° S + 3.5
7	22	ET	occlusion	XT 30 Δ	20/20 20/125	S + 0.25 S + 0.5
8	21	ET	Str. surgery	XT 20 Δ LHT 16 Δ	20/100 20/16	S + 0.5 C -0.5 x 180° S plano
9	15	ET	Str. surgery	XT 16 Δ	20/50 20/20	S + 1.0 S + 2.0 C -0.5 x 40°
10	41	ET	Str. surgery	XT 25 Δ	20/20 cf	S + 4.5 C -0.75 x 135° S + 5.0 C -0.75 x 180°
11	44	ET	none	XT 40 D	20/20 cf	plano S - 0.50 C +0.5 x 180°
12	23	ET	none	ET 20 D	20/125 20/25	S +5.0 C -1.5 x 90° S +4.25 C -2.0 x 90°
13	45	ET	Str. surgery	15 Δ RHT 8 Δ	20/32 20/20	S +1.5 C -1.0 x 90° S -1.0 C -0.5 x 80°
14	60	ET	none	ET 10 Δ RHT 5 Δ	20/200 20/20	S + 1.5 S + 2.75 C - 0.5 x 180°
15	28	n/a	none	n/a	20/32 20/20	n/a
16	55	ET	n/a	n/a	20/20 20/200	S plano C -0.5 x 68° S + 0.75 C -0.75 x 81°
17	34	ET	Str. surgery	n/a	20/20 20/200	S + 2.0 C -0.5 x 152° S + 3.75 C -1.0 x 10°
18	51	n/a	n/a	n/a	20/16 20/25	n/a
19	30	ET	Str. surgery	10 Δ	20/200 20/20	S plano C + 1.0 x 90° S -1.5 C + 2.5 x 90°
20	44	ET	n/a	n/a	20/32 20/20	n/a

**Table 5-1.**  
Patient characteristics and strabismic history

For every patient, age at NFA measurement and strabismic history are given where available. N/A stands for not available clinical data. In addition, visual acuity (VA; cf stands for counting fingers) and refraction are presented.

**Table 5-2.**  
NFL thickness  
parameters in  
the amblyopic  
and the sound  
eye.

parameter	sound eye ( $\mu$ )	amblyopic eye ( $\mu$ )	difference in thickness ( $\mu$ )	95% CIN for difference ( $\mu$ )	p-value
<b>average thickness</b>	67.4 (11.4)	66.4 (9.9)	1.0	-3.2 ; 5.2	0.627
<b>superior average</b>	82.6 (13.4)	82.6 (12.3)	0.0	-4.5 ; 4.5	1.000
<b>inferior average</b>	81.5 (10.7)	78.7 (12.0)	2.8	-2.6 ; 8.2	0.290
<b>temporal median</b>	43.5 (13.7)	41.6 (10.3)	1.9	-3.7 ; 7.4	0.492
<b>nasal median</b>	48.0 (12.6)	48.4 (9.2)	-0.4	-5.7 ; 5.0	0.883
<b>superior maximum</b>	100.2 (14.8)	99.4 (17.0)	0.8	-5.7 ; 7.3	0.799
<b>inferior maximum</b>	95.2 (11.7)	90.6 (13.7)	4.6	-0.9 ; 10.1	0.096

NFL thickness parameters are all in microns ( $\mu$ ). Presented is the average thickness in the sound eye and in the amblyopic eye, together with its standard deviation (in parentheses). Next, the mean differences in thickness between the sound eye and the amblyopic eye, as well as its 95% confidence interval (CIN) and p-values are given.

1. Von Noorden G, Crawford M. The lateral geniculate nucleus in human strabismic amblyopia. *Investigative Ophthalmology & Visual Science* 1992;33:2729-32.
2. Romano PE, Bird JJ. Fluorescein Retinal Angiographic Studies of Functional Amblyopia. *Journal of Pediatric Ophthalmology and Strabismus* 1980;17:318-9.
3. Delint P, Weissenbruch C, Berendschot T, Norren D. Photoreceptor function in unilateral amblyopia. *Vision Research* 1998;38:613-7.
4. Weinreb RN, Shakiba S, Sample PA, et al. Association between quantitative nerve fiber layer measurement and visual field loss in glaucoma. *Am J Ophthalmol* 1995;120:732-8.
5. Tjon-Fo-Sang MJ, Lemij HG. The sensitivity and specificity of nerve fiber layer measurements in glaucoma as determined with scanning laser polarimetry. *Am J Ophthalmol* 1997;123:62-9.
6. Xu L, Chen PP, Chen YY, et al. Quantitative nerve fiber layer measurements using scanning laser polarimetry and modulation parameters in the detection of glaucoma. *J Glaucoma* 1998;7:270-7.
7. Weinreb RN, Zangwill L, Berry CC, et al. Detection of glaucoma with scanning laser polarimetry. *Arch Ophthalmol* 1998;116:1583-9.
8. Choplin NT, Lundy DC, Dreher AW. Differentiating patients with glaucoma from glaucoma suspects and normal subjects by nerve fiber layer assessment with scanning laser polarimetry. *Ophthalmology* 1998;105:2068-76.
9. Tjon-Fo-Sang MJ, de Vries J, Lemij HG. Measurement by nerve fiber analyzer of retinal nerve fiber layer thickness in normal subjects and patients with ocular hypertension. *Am J Ophthalmol* 1996;122:220-7.
10. Dreher AW, Reiter K. Retinal laser ellipsometry: a new method for measuring the retinal nerve fiber layer thickness distribution. *Clin Vis Sci* 1992;7:481-8.
11. Weinreb RN, Shakiba S, Zangwill L. Scanning laser polarimetry to measure the nerve fiber layer of normal and glaucomatous eyes. *Am J Ophthalmol* 1995;119:627-36.
12. Weinreb RN, Dreher AW, Coleman A, et al. Histopathologic validation of Fourier-ellipsometry measurements of retinal nerve fiber layer thickness. *Arch Ophthalmol* 1990;108:557-60.
13. Tjon-Fo-Sang MJ, van Strik R, de Vries J, Lemij HG. Improved reproducibility of measurements with the nerve fiber analyzer. *J Glaucoma* 1997;6:203-11.

## References





## CHAPTER 6

### ***Axonal loss in a patient with anterior ischemic optic neuropathy as measured with scanning laser polarimetry***

Colen TP, Van Everdingen JAM and Lemij HG  
American Journal of Ophthalmology 2000;130(6):847-850

## Abstract

**Case report** A 58-year old man with acute AION had repeated NFA/GDx scans of the nerve fiber layer adjacent to the optic nerve head of the involved eye, as well as repeated HFA 30-2 (Humphrey Field Analyzer) visual field examinations. At presentation (day 0), he had a normal superior nerve fiber bundle on the NFA/GDx, with a deep inferior hemifield scotoma. By day 21 and day 36, the superior nerve fiber bundle thinned on the NFA/GDx, whereas the scotoma remained practically unchanged. These findings suggest that after the onset of an AION, there is acute loss of axonal function resulting in scotoma, presumably due to ischaemia. This is followed by a gradual disappearance of nerve fiber tissue, as measured with the NFA/GDx, within several weeks.

---

Anterior ischemic optic neuropathy (AION) is thought to result from insufficiency in perfusion of the short posterior ciliary arteries<sup>1</sup> and leads to infarction of axons in the retinal nerve fiber layer (NFL).

The Nerve Fiber Analyzer (NFA; Laser Diagnostic Technologies, San Diego, CA) is a scanning laser polarimeter, designed for the detection and follow-up of glaucoma. It uses a polarized laserbeam to assess NFL thickness in the peripapillary retina, and discriminates well between normals and glaucoma patients.<sup>2,3</sup> The current standard in scanning laser polarimetry is the GDx, a third generation NFA.

A 58-year old white man presented with blurred vision in the inferior visual field of his right eye (day 0). His symptoms had gradually worsened in the previous 10 days. He did not have any headaches, scalp tenderness or jaw claudication. He had no ocular history.

His visual acuity was RE: 20/40 and LE: 20/15. His signs were a swollen optic disc in the right eye. Erythrocyte sedimentation rate (ESR, Westegren) was 4 mm and the C reactive protein (CRP) was less than 1 (normal less than 8). The right eye showed a deep scotoma in the inferior visual field (HFA 30-2, Humphrey Field Analyzer, Humphrey Systems, San Leandro, CA) and a normal superior nerve fiber bundle on the NFA/GDx (Fig 6-1). The left eye was unremarkable.

A diagnosis of non-arteritic AION was made. The patient was treated with aspirin (ASA) 100mg daily, and re-imaged with the NFA/GDx on day 15, 21 and 36. On these days, a visual field test was also performed (Fig 6-2).

A NFA/GDx scan consists of a reflectance image (Fig 6-1, left), a retardation images (Fig 6-1, middle) and a double hump pattern (Fig 6-1, right). The retardation image with a resolution of 65536 pixels relates to NFL thickness. All pixels are color-coded: from yellow to red to blue, the colors represent a gradually thinner NFL. In addition, 14 parameters are on the NFA/GDx printout. One parameter, the superior maximum parameter (smax), has been presented in fig 6-1. The smax is defined as the mean of the 1500 thickest pixels in the superior segment and represents the thickness of the superior nerve fiber bundle.

On day 0, a normal superior nerve fiber bundle was seen with a scotoma in the inferior visual field. On consecutive visits, the visual fields showed no improvement,

apart from some restoration of vision around the blind spot. The superior nerve fiber bundle, however, disappeared on the retardation image within the course of about 3 weeks. The  $s_{max}$  parameter decreased from  $89\mu$  on day 0 to  $62\mu$  (day 15),  $49\mu$  (day 21) and  $51\mu$  (day 36). After 9 months, the  $s_{max}$  was still stable at  $48\mu$ .

The case demonstrates that an AION can result in progressive loss of NFL tissue, stabilizing in about 3 weeks.

**References**

1. Hayreh SS. Acute ischemic disorders of the optic nerve: pathogenesis, clinical manifestations, and management. *Ophthalmol Clin North Am* 1996;9:407-442.
2. Tjon-Fo-Sang MJ, Lemij HG. The sensitivity and specificity of nerve fiber layer measurements in glaucoma as determined with scanning laser polarimetry. *Am J Ophthalmol* 1997;123:62-69.
3. Weinreb RN, Zangwill L, Berry CC, Bathija R, Sample PA. Detection of glaucoma with scanning laser polarimetry. *Arch Ophthalmol* 1998;116:1583-1589.

## CHAPTER 7

### *Sensitivity and specificity of new GDx parameters*

Colen TP, Tang NEML, Mulder PGH and Lemij HG  
Submitted for publication

## Abstract

**Purpose** The GDx is a scanning laser polarimeter that assesses peripapillary nerve fiber layer thickness. In addition to the 14 existing outcome parameters, 4 new parameters have been described recently: the Ellipse Standard Deviation (ESD), the Normalized Superior Area (NSA), the Normalized Inferior Area (NIA), and the Discriminant Analysis (DA). The aim of this study was to investigate the sensitivity and specificity of these 4 new parameters.

**Methods** Only one randomly selected eye of 263 healthy volunteers and 241 glaucoma patients was considered. The healthy group was randomly divided into a reference set (n=132) to calculate the 10th percentile of the normal distribution and a test set (n=131) to calculate the specificity against these newly established cut-off points. Sensitivity was calculated for all glaucoma patients (n=241) and again for three separate subgroups: early glaucoma (n=90), moderate glaucoma (n=93) and advanced glaucoma (n=58).

**Results** When the 10th percentile of the normal distribution was used as a cut-off point, the sensitivity and specificity pairs of the new parameters were 61.8 & 87.6%, 61.8 & 89.1%, 50.2 & 92.2% and 72.6 & 95.3 % for the ESD, NSA, NIA and the DA, respectively. The area under the ROC curve was 0.86, 0.86, 0.87 and 0.90, respectively. Among the existing parameters, the Number discriminated best (sensitivity and specificity: 76.8 & 89.1%, respectively; area under the ROC curve: 0.90). When compared to the Number, the DA was equally good, whereas the other three new parameters performed statistically significantly worse. In general, the area under the ROC curve increased from early to moderate to advanced glaucoma.

**Conclusions** The new GDx parameters discriminated well between normal subjects and glaucoma patients. None of the new parameters discriminated better than the Number.

Key words: scanning laser polarimetry, GDx, sensitivity, specificity, parameters.

## Introduction

The GDx (Laser Diagnostic Technologies, San Diego, CA) is a scanning laser polarimeter that assesses nerve fiber layer (NFL) thickness in the peripapillary retina. The technology discriminates well between normal subjects and glaucoma patients.<sup>1-3</sup> A detailed description of the GDx has been published elsewhere.<sup>4-6</sup> In short, a beam of polarized laser light is sent through the retinal NFL. As the light passes through the form-birefringent NFL, a phase shift called retardation occurs, which is thought to be linearly correlated with NFL thickness, as has been shown in a monkey model.<sup>7</sup> The instrument compensates for retardation arising from the cornea on the assumption that the corneal polarization axis (CPA) is oriented 15 degrees nasally downward. In patients who have a different CPA, this compensation may be inadequate.<sup>8</sup> The peripapillary retina is scanned, and a retardation image of 256x256 pixels is constructed. An operator centers a circle or an ellipse on the optic nerve head, and a 10-pixel wide band with an inner margin of 1.75 times the diameter of the cir-

cle or ellipse is added automatically. The NFL thickness under the band is displayed separately in a so-called double-hump graph. Both the retardation image and the double-hump graph allow a quantitative assessment of the retinal NFL.

For a quantitative approach to the retardation image, several automated parameters are available to the user. For example, the superior maximum parameter averages the 1500 thickest pixels in the 120 deg superior sector, and reflects the thickness of the superior nerve fiber bundle. Since the introduction of the GDx, 14 standard parameters have been available. These include a parameter called 'the Number', which is a summary parameter calculated by a proprietary algorithm, that has been developed with the help of a neural network.

Over the past few years, several authors have developed new parameters, to better discriminate between normal subjects and glaucoma patients. Four of these have been examined in this paper. The Ellipse Standard Deviation (ESD), developed by Choplin *et al.*,<sup>3</sup> is the standard deviation around the mean of the values contained in the measuring ellipse. The Normalized Superior Area (NSA, in mm<sup>2</sup>) developed by Xu *et al.*,<sup>9</sup> is the area under a 90 deg sector of the double hump graph with the highest retardation in the superior region. The Normalized Inferior Area (NIA, in mm<sup>2</sup>) is defined likewise, only for the inferior region. The fourth parameter is called the Discriminant Analysis (DA), which is identical to the Linear Discriminant Function developed by Weinreb *et al.*<sup>2</sup> It is calculated by an algorithm that uses three existing parameters: average thickness, ellipse modulation and ellipse average. The exact definitions of the four new parameters, as provided by the manufacturer, are presented in the appendix.

To date, these four parameters have not been formally tested on a large group of patients by others than their inventors. We have calculated the sensitivity and specificity of these parameters using data of 241 glaucoma patients and 263 control subjects. For comparison, the sensitivity and specificity values of the 14 existing parameters have been added. To facilitate comparison with other reports, we have included the area under the ROC curve (AUROC) for every parameter. We have also stratified our data for patients with early, moderate and advanced glaucoma.

**Measurement procedures** A GDx measurement trial for one eye consisted of taking as many images as needed that yielded 3 high quality ones. High quality was defined as good focus, centered optic disc, equal image illumination in all sectors and the absence of motion artifacts. The 3 images were then aligned and converted by the software into one 'mean image'. For this study we used software version 2.0.09. During all measurements, we saw to it that patients had their heads as upright as possible. Pupils were undilated and ambient lights were left on. Three different experienced operators imaged all subjects on the same instrument within a time period of 2 years. The glaucoma patients were all examined twice within a six-week period; only the data from the second visit was considered.

## Methods

The following GDx settings were used for our study: the entire image was automatically divided into 4 sectors centered on the optic disc (superior 120°, inferior 120°, nasal 50° and temporal 70°). Our operators then positioned a circle on the margin

of the optic nerve head: the optic disc circle. The circle diameter equaled the largest disc diameter. Instead of using a circle, others prefer to fit an ellipse to the optic disc. We used a circle to obtain measurements that were, in principle, at the same distance from the optic disc center in all sectors. We think this is important, notably to compare ratio and ellipse parameters across subjects. Using a circle rather than an ellipse is not a prerequisite for obtaining the new parameters. After the circle was positioned, the software automatically displayed a green measurement band. This band was 10 pixels wide with an inner circle of 1.75 times the diameter of the optic disc circle. The 14 standard parameters relate either to the pixels under the measurement band, or to those peripheral to it. The data was subsequently exported into a statistical software package (SPSS version 9.0, SPSS Inc., Chicago, IL). A special version of the software that also calculates and exports the 4 new parameters was kindly provided to us by the manufacturer.

**Subjects** Originally, 272 healthy volunteers were recruited mainly from the hospital staff, their friends and relatives, and spouses of patients. They met the inclusion criteria of: Caucasian ethnic origin, age between 20-80 years, best corrected visual acuity of 20/25 or better, intraocular pressure (IOP)  $\leq 21$  mm Hg, a normal appearance of the optic nerve head and normal visual fields (Humphrey Field Analyzer 24-2 full threshold program). Exclusion criteria were: diabetes, systemic hypertension requiring medical treatment, any ocular history, a vertical cup/disc ratio of 0.6 or higher, and asymmetry of greater than 0.2 cup/disc ratios between the two eyes. Refractive error was not a selection criterion as long as an image was of high quality. Nine of the recruited volunteers (3.3%) were unsuitable for GDx imaging due to either a very large zone of peripapillary atrophy under or outside the measurement band, or a tilted disc yielding an unreliable GDx scan. In the end, reliable images of high quality could be obtained in 263 subjects (96.7%).

We recruited 255 consecutive glaucoma patients from our glaucoma clinic. The gold standard that separated the normal subjects from the glaucoma patients was the clinical diagnosis of glaucoma. This diagnosis was established by one of our three glaucoma specialists on the basis of a reliable and repeated abnormal visual field (Humphrey Field Analyzer 24-2 full threshold program) that matched the glaucomatous appearance of the optic disc. A visual field exam was classified as reliable when it met the criteria described by Anderson,<sup>10</sup> and as abnormal when the glaucoma hemifield test was outside normal limits. Other inclusion criteria were Caucasian ethnic origin and age between 20-80 years. Exclusion criteria were diabetes, systemic hypertension requiring medical treatment, any ocular history other than glaucoma or any ocular surgery. IOP was not among the selection criteria for the glaucoma patients. Of all recruited patients, 14 (5.5%) were unsuitable for GDx imaging due to a very large zone of peripapillary atrophy outside the measurement band (13 patients), or due to an inability to fixate (1 patient). In the end, reliable images of high quality could be obtained in 241 (94.5%) glaucoma patients.

IRB/ Ethics Committee approval was obtained for this study. Written informed consent was required from all participants after the nature of all procedures had been fully explained. Normal subjects were selected so that six 10-year cohorts ranging



from 20 to 80 years would be represented. We recruited extra control subjects in the 50-60 and 60-70 cohort to better match the expected age distribution in our glaucoma patients. Demographic data of the normal subjects and of the glaucoma patients has been summarized in table 7-1.

**Statistical methods** From all normal subjects, only one randomly selected eye per subject was used for analysis. If a glaucoma patient had unilateral glaucoma, that eye was selected for analysis. In case of bilateral disease, one eye was selected at random. Next, the group of normal subjects (n=263) was randomly divided into a reference set (n=132) to establish normative values for all parameters, and a test set (n=131) for calculating the specificity. To obtain approximately 90% specificity, we set the following criteria. An abnormal 'the Number' parameter was defined as a value above the 90th percentile of the reference set. An abnormal symmetry parameter was defined as a value above the 95th percentile or below the 5th percentile of the reference set. All other parameters, including the four new parameters, were defined as abnormal when their value was below the 10th percentile. With these criteria, we determined the specificity per parameter in the test set. With the same criteria, we determined the sensitivity per parameter in the glaucoma group. In addition, we calculated the sensitivity for separate glaucoma subgroups. Three groups were defined based on the values of their mean deviation (MD) on visual field testing: the early glaucoma group (MD>-6 dB), the moderate glaucoma group (MD<-6 dB but >-15 dB) and the advanced glaucoma group (MD <-15 dB). The specificities in the various subgroups were identical to the specificity in the 'all patients' group, since the same group of control subjects was used.

In addition to the sensitivity and specificity values, ROC curves were constructed for every parameter. In an ROC curve, sensitivity is plotted on the y-axis against 1-specificity on the x-axis. We also calculated the area under the ROC curve (AUROC) for every parameter and for the three glaucoma subgroups separately.

In the 'all patients' group, we tested the AUROC values of the four new parameters against the best two existing parameters for statistical significance. To that end, we used a paired test described by DeLong *et al.*,<sup>11</sup> with the level of statistical significance set at  $\alpha = 0.05$ . To assess whether the AUROC values of all parameters increased statistically significantly from early to moderate to advanced glaucoma, a Jonckheere-Terpstra non-parametric test was used with the level of statistical significance set at  $\alpha = 0.05$ .

All four new parameters discriminated well between normal subjects and glaucoma patients. When all glaucoma patients were considered together, the AUROC values for the ESD, NSA, NIA and the DA were 0.86, 0.86, 0.87 and 0.90, respectively. This data has been summarized in table 7-2, together with AUROC values of the existing parameters. All AUROC values are given again for the three glaucoma subgroups. In general, the AUROC values increased with the severity of glaucoma ( $p < 0.001$ ). Sensitivity and specificity values have also been given. The specificity values related to the same group of normal subjects and have thus been presented only once.

## Results

In the 'all patients' group, the AUROC value of the DA was higher than that of the maximum modulation ( $p=0.0059$ ) but not higher than that of The Number ( $p=0.91$ ; Table 7-3). In the same group, the AUROC values of the ESD, NSA and NIA were not statistically significantly higher than the AUROC value of the maximum modulation. They were statistically significantly lower than the AUROC value of the Number.

## Discussion

We have calculated the sensitivity, specificity, and AUROC values for four newly proposed GDx parameters. Their high AUROC values (0.86-0.90) confirmed that they discriminate well between normal and glaucomatous eyes. When compared to the best existing single parameter (maximum modulation), the DA performed better whereas the other 3 new parameters were equally good. When compared to The Number, the DA was equally good, whereas the other 3 new parameters performed worse.

We speculate that feeding the ESD, NSA and the NIA into another neural network to generate a new algorithm for an updated the Number will further increase its ability to distinguish normal from glaucomatous eyes. The DA is perhaps less likely to contribute to such a new algorithm because it is computed from three existing parameters that are already used by the current algorithm of the Number.

The AUROC value for the DA was 0.90 in our study population. This was in agreement with the value of 0.89 found by Weinreb *et al.*,<sup>2</sup> who evaluated only patients with early to moderate glaucoma. Subsequent studies from the same group report values of 0.85 and 0.79, respectively.<sup>12,13</sup> In our study population, the DA discriminated as well as the Number.

The AUROC value for the NSA and NIA was 0.86 and 0.87, respectively, in our population. The group that developed the NSA and NIA tested these parameters on a separate, screening population and found slightly higher values (0.92 and 0.91, respectively) than we did.<sup>14</sup>

We have excluded patients with systemic hypertension from our study because we assumed that (subclinical) retinal ischaemia might occur in those patients, potentially leading to secondary degeneration of the retinal nerve fiber layer, thereby introducing bias. The exclusion of patients with hypertension may limit the validity of our results to a normotensive population. By excluding one kind of bias, a new kind of selection bias may have been introduced because relatively more patients might have been excluded from the glaucoma group. It would be of interest to investigate whether patients with hypertension have different nerve fiber layer characteristics as measured with the GDx than patient with normal blood pressure. Also among the selection criteria was a glaucomatous appearance of the optic disc for inclusion in the glaucoma group. It is possible that this requirement introduced a bias towards increased sensitivity in our analysis.

Age may confound trials that compare NFL thickness between normal and glaucomatous eyes, because NFL thickness is inversely correlated with age.<sup>4,6,15,16</sup> Although our normal population was, on average, somewhat younger than the glaucoma population, age is unlikely to have introduced any bias in our study: we determined age dependent nor-

mal values in a large group of subjects, ranging widely in age. The age range of our glaucoma population sat well within the age range of our normal subjects.

The instrument compensates for retardation arising from the cornea assuming a corneal polarization axis (CPA) of 60 nanometer at an orientation of 15 degrees nasally downward. In eyes with a different CPA, this compensation may be inadequate.<sup>8</sup> A better compensation will probably affect the retardation values and all derived parameters, but the extent of this effect remains to be investigated.

Our study has confirmed previous studies that the GDx allows better discrimination between normal subjects and glaucoma patients with more advanced disease. The clinical significance of this intuitive result has yet to be determined in various settings, such as screening programs and general ophthalmic clinics, where the adopted criteria may be tailored to specific clinical needs.

**The Ellipse standard deviation (ESD)** Originally called Intra Ellipse Sector Variability.<sup>3</sup> It is the standard deviation around the mean of the values contained in the measuring ellipse. The unit of measure is microns. It is a measure of the variability of the measurements contained in the ellipse and an indirect measure of the “peak to trough” difference and thus another modulation parameter. The mean thickness is determined from the measurement points along the ellipse. That value is subtracted from each point along the ellipse giving the standard deviation for each point. The deviations are totaled giving the ellipse standard deviation. Normal eyes, having higher superior and inferior peaks than glaucoma patients, show the greatest variability and hence the highest ellipse standard deviation values.

## **Appendix Definition of new GDx Parameters**

**The Normalized Superior Area (NSA) and the Normalized Inferior Area (NIA).** Based on the ReModS and ReModI parameters by Xu et al.<sup>9</sup> The software evaluates the temporal 90° of the ellipse to find the lowest temporal thickness value. The software then evaluates the remaining 270° to find the lowest nasal thickness value. These two values are then averaged to determine a baseline value. Next, a best-fit algorithm is applied to determine which 90° along the ellipse (between the previously described temporal/nasal points) contain the thickest superior and inferior RNFL to calculate the Normalized Superior Area and Normalized Inferior Area. The positions for these superior and inferior 90° sectors are not fixed. The baseline value is then subtracted from the values contained in the 90° superior and inferior ellipse sectors. These integral (area) values are expressed in mm<sup>2</sup> and are calculated by measuring the thickness of the nerve fiber layer (above the baseline) at each point of the ellipse along the entire 90° sector. These values are totaled. A high value represents high modulation of the double-hump TSNIT pattern as seen in normal patients.

**Discriminant Analysis (DA)** Originally called Linear Discriminant Function (LDF).<sup>2</sup> It is calculated by the following algorithm:  $-4.442655 - (0.156 \times \text{Average Thickness}) + (0.935 \times \text{Ellipse Modulation}) + (0.183 \times \text{Ellipse Average})$ . The DA has no unit of measure. Positive values are within normal limits and negative values are outside normal limits.

**Table 7-1.**  
Demographic  
data of all  
participants

		n	Mean Age (SD)	OD:OS	MD (SD)
Normal subjects	Reference set	132	51.5 (16.7)	60:72	
	Test set	131	49.8 (16.1)	73:58	
Glaucoma subjects	All patients	241	62.4 (10.2)	121:120	-10.4 (7.3)
	Early	90	63.3 (9.0)	45:45	-3.5 (1.8)
	Moderate	93	62.0 (11.1)	43:50	-10.4 (2.7)
	Advanced	58	61.7 (10.3)	33:25	-20.9 (4.8)

Demographic data for all 263 normal subjects (for the reference set and the test set separately), and for all 241 glaucoma subjects (for early, moderate and advanced glaucoma separately). Presented are: number of subjects per group (n), their mean age in years with the standard deviation in parentheses, the ratio of right versus left eyes (OD:OS), and the average of the mean deviation on visual field testing (MD) in decibels (dB) with its standard deviation (SD) in parentheses.

PARAMETER	unit	ALL PATIENTS				EARLY		MODERATE		ADVANCED	
		Spec	Sens	AUROC		Sens	AUROC	Sens	AUROC	Sens	AUROC
ESD	μ	87.6	61.8	.86		40.0	.80	68.8	.88	84.5	.94
NSA	mm <sup>2</sup>	89.1	61.8	.86		48.9	.80	61.3	.87	82.8	.94
NIA	mm <sup>2</sup>	92.2	50.2	.87		28.9	.81	53.8	.89	77.6	.95
DA		95.3	72.6	.90		56.7	.84	77.4	.92	89.7	.98
The Number											
Max Modulation		89.1	76.8	.90		65.6	.84	77.4	.92	93.1	.98
Inferior Ratio		90.7	61.4	.85		47.8	.78	64.5	.85	77.6	.92
Ellipse Mod		91.5	55.6	.82		40.0	.75	60.2	.84	72.4	.90
Superior/Nasal		90.7	58.5	.82		44.4	.76	59.1	.82	79.3	.91
Superior Ratio		95.3	36.9	.82		23.3	.77	35.5	.83	60.3	.89
Inf. Maximum	μ	90.7	45.6	.79		31.1	.72	44.1	.80	70.7	.90
		87.6	43.2	.75		31.1	.68	39.8	.76	67.2	.85
Inferior Average	μ	89.9	44.0	.74		28.9	.65	46.2	.77	63.8	.83
Superior Average	μ	83.7	49.0	.74		41.1	.80	49.5	.75	60.3	.82
Sup Maximum	μ	87.6	37.3	.74		26.7	.67	33.3	.74	60.3	.83
Ellipse Average	μ	87.6	45.6	.71		33.3	.64	49.5	.72	58.6	.79
Superior Integral	mm <sup>2</sup>	87.6	36.1	.69		28.9	.62	30.1	.70	56.9	.76
Average	μ	88.4	27.8	.65		18.9	.59	29.0	.65	39.7	.72
Symmetry		89.9	21.6	.53		22.2	.54	20.4	.49	22.4	.55

All investigated parameters are listed: the top 4 parameters are: the Ellipse Standard Deviation (ESD), the Normalized Superior Area (NSA), the Normalized Inferior Area (NIA) and the Discriminant Analysis (DA). All 14 existing parameters are given below, ranked by their AUROC values in the 'all patients' group. The unit of measure is given where applicable. Both sensitivity and specificity values are given in percentages. The sensitivity and specificity for every parameter is first presented for the group of 'all patients' together. To the right, the sensitivity is given again for patients with 'early', 'moderate' and 'advanced' glaucoma separately. The specificity values for these three subgroups are by definition the same as for the entire glaucoma group, and are omitted to save space. In addition, the AUROC values are given for every parameter.

**Table 7-2.**  
Sensitivity, specificity and area under the ROC curve (AUROC) values for all GDx parameters

**Table 7-3.**  
Differences in  
AUROC values  
between vari-  
ous parameters  
in the 'all  
patients' group.

	DIFFERENCE IN AUROC VALUE AS COMPARED TO:	
	Maximum Modulation	The Number
<b>Ellipse Standard Deviation (ESD)</b>	0.018 (0.54)	-0.038 (0.0035)
<b>Normalized Superior Area (NSA)</b>	0.011 (0.65)	-0.043 (0.0016)
<b>Normalized Inferior Area (NIA)</b>	0.024 (0.35)	-0.030 (0.037)
<b>Discriminant Analysis (DA)</b>	0.055 (0.0059)	0.001 (0.91)

Presented are the AUROC values of the new parameters minus those of the maximum modulation (with p-values in parentheses) and the Number respectively. A positive sign indicates a better performance of the new parameters. With a negative sign, the existing parameters discriminated better. All data relate to the 'all patients' group.

1. Tjon-Fo-Sang MJ, Lemij HG. The sensitivity and specificity of nerve fiber layer measurements in glaucoma as determined with scanning laser polarimetry. *Am J Ophthalmol* 1997;123:62-9.
2. Weinreb RN, Zangwill L, Berry CC, et al. Detection of glaucoma with scanning laser polarimetry. *Arch Ophthalmol* 1998;116:1583-9.
3. Choplin NT, Lundy DC, Dreher AW. Differentiating patients with glaucoma from glaucoma suspects and normal subjects by nerve fiber layer assessment with scanning laser polarimetry. *Ophthalmology* 1998;105:2068-76.
4. Tjon-Fo-Sang MJ, de Vries J, Lemij HG. Measurement by nerve fiber analyzer of retinal nerve fiber layer thickness in normal subjects and patients with ocular hypertension. *Am J Ophthalmol* 1996;122:220-7.
5. Dreher AW, Reiter K. Retinal laser ellipsometry: a new method for measuring the retinal nerve fiber layer thickness distribution. *Clin Vis Sci* 1992;7:481-8.
6. Weinreb RN, Shakiba S, Zangwill L. Scanning laser polarimetry to measure the nerve fiber layer of normal and glaucomatous eyes. *Am J Ophthalmol* 1995;119:627-36.
7. Weinreb RN, Dreher AW, Coleman A, et al. Histopathologic validation of Fourier-ellipsometry measurements of retinal nerve fiber layer thickness. *Arch Ophthalmol* 1990;108:557-60.
8. Greenfield DS, Knighton RW, Huang XR. Effect of corneal polarization axis on assessment of retinal nerve fiber layer thickness by scanning laser polarimetry. *Am J Ophthalmol* 2000;129:715-22.
9. Xu L, Chen PP, Chen YY, et al. Quantitative nerve fiber layer measurements using scanning laser polarimetry and modulation parameters in the detection of glaucoma. *J Glaucoma* 1998;7:270-7.
10. Anderson DR, Patella VM. *Automated Static Perimetry*. 2nd ed. St. Louis: Mosby; 1999:104.
11. DeLong ER, DeLong DM, Clarke-Pearson DL. Comparing the areas under two or more correlated receiver operating characteristics curves: A nonparametric Approach. *Biometrics* 1988;44:837-45.
12. Zangwill LM, Bowd C, Berry CC, et al. Discriminating between normal and glaucomatous eyes using the Heidelberg Retina Tomograph, GDx Nerve Fiber Analyzer, and Optical Coherence Tomograph. *Arch Ophthalmol* 2001;119:985-93.
13. Bowd C, Zangwill LM, Berry CC, et al. Detecting early glaucoma by assessment of retinal nerve fiber layer thickness and visual function. *Invest Ophthalmol Vis Sci* 2001;42:1993-2003.
14. Yamada N, Chen PP, Mills RP, et al. Glaucoma screening using the scanning laser polarimeter. *J Glaucoma* 2000;9:254-61.
15. Chi Q, Tomita G, Inazumi K, et al. Evaluation of the effect of aging on the retinal nerve fiber layer thickness using scanning laser polarimetry. *J Glaucoma* 1995;4:406-13.
16. Poinosawmy D, Fontana L, Wu JX, et al. Variation of nerve fibre layer thickness measurements with age and ethnicity by scanning laser polarimetry. *Br J Ophthalmol* 1997;81:350-4.





## CHAPTER 8

### *Sensitivity and specificity of the GDx; clinical judgement of standard print-outs vs the Number*

Colen TP and Lemij HG  
J Glaucoma, in press

## Abstract

**Purpose** The Number is a standard parameter of the GDx that reportedly separates well between normal and glaucomatous eyes. We evaluated the sensitivity and specificity of the Number and examined whether expert clinical judgement of GDx printouts might lead to a better separation.

**Methods** Two experienced observers judged 800 GDx scans on 400 randomly presented printouts from 200 glaucoma patients and 200 age-matched normal subjects. Their sensitivity was assessed for all glaucoma patients together, and also for mild, moderate and severe glaucoma separately. Their specificity was determined in the normal subjects. The same was also done for the Number, at various critical values.

**Results** Both observers discriminated better than the Number. At a critical value of 23, the specificity of the Number was 81.5%, which matched the lowest specificity of the 2 observers: 82.5% and 92.0% for observers #1 and #2, respectively. At these specificities, the sensitivity of the two observers and of the Number were 92.0%, 89.5% and 85.5%, respectively. The sensitivity increased with the severity of glaucoma. The Kappa values for intra observer agreement were 0.80 and 1.0.

**Conclusions** The Number yielded acceptable sensitivity and specificity values at a critical value of 23 in our test population. However, the clinical judgements of the printouts by both expert observers resulted in a better separation between normal and glaucomatous eyes.

## Introduction

The GDx (Laser Diagnostic Technologies, San Diego, CA) is a scanning laser polarimeter<sup>1</sup> that assesses nerve fiber layer (NFL) thickness in the peripapillary retina. The working principle of the GDx is based on the phase shift of polarized laser light as it passes through a birefringent medium such as the retinal NFL. This phase shift is called retardation and is thought to be linearly correlated with NFL thickness, as has been shown in a monkey model.<sup>2</sup> The GDx has been shown to discriminate well between normal and glaucomatous eyes.<sup>3-18</sup>

Today, there are no standard procedures for interpreting GDx data. The software compares 13 parameters to a normative database and flags those that are outside normal limits. A 14th parameter is called the Number, which is a probability score ranging from 1 (low probability of glaucoma) to 100 (high probability of glaucoma). The Number is derived from other parameters by a proprietary algorithm that has been established by a neural network. The sensitivity and specificity of each individual parameter, as well as of fixed combinations in an advanced statistical model, have been examined.<sup>7,12,13,16-19</sup> Of these, the Number is generally the single best parameter, at cut-off levels ranging between 17 and 39.<sup>7,12,16,17</sup>

Another way of assessing GDx data would be by examining the so-called symmetry analysis printout. In such a printout, each of both eyes is represented by a reflectance

image, a color-coded retardation map, the 14 parameters and a so-called TSNIT graph. This graph represents the circumferential cross-sectional retardation at a specified distance around the optic disc. We would argue that an expert clinical judgement and weighing of all available information on the printouts might yield a better discrimination between normal and glaucomatous cases than any single parameter would. This approach was tentatively explored by Choplin and Lundy.<sup>18</sup> The expert observer might readily recognize artifacts, e.g. caused by motion or large areas of peripapillary atrophy,<sup>20-22</sup> and therefore judge the printouts differently from a fairly simple software algorithm. In addition, experience with the large variation across normal eyes, both in general NFL thickness, and in typical distributions such as split bundles,<sup>23</sup> might also add to the separating power of expert subjective judgement. The same would apply to localized, wedge-shaped NFL defects that are, in our experience, typically missed by the standard parameters. Finally, examining both eyes on a single printout would allow appreciating any marked asymmetries between the two eyes, and might further improve the detection of glaucoma.

In this study, we assessed the sensitivity and specificity of expert clinical judgement of 'symmetry analysis' printouts of 200 glaucoma patients and 200 age-matched normal subjects. Their scores were compared to the sensitivity and specificity of the Number at various cut-off values.

**Subjects** We used the so-called symmetry analysis printout that provides information of both eyes simultaneously, because this resembled a clinical setting. The tenet of our approach was that we looked at paired eyes per person, instead of at individual eyes.

## Methods

We recruited 255 consecutive glaucoma patients from our glaucoma clinic. Inclusion criteria were: Caucasian ethnic origin, age between 20-80 years and a diagnosis of glaucoma (on the basis of reliable and repeated glaucomatous visual field abnormalities with matching optic disc abnormalities as established by one of our three glaucoma specialists). A visual field exam was classified as reliable when it met the reliability criteria described by Anderson and Patella.<sup>24</sup> Exclusion criteria were diabetes, hypertension requiring medical treatment, any history or ocular disease or surgery. Of these, 14 patients (5.5 %) were unsuitable for GDx imaging due to a very large zone of peripapillary atrophy (13 patients) or inability to fix (1 patient). In the end, reliable, high quality images could be obtained in 241 (94.5 %) glaucoma patients.

As control subjects, 272 healthy volunteers were recruited from the hospital staff, their friends and relatives, and spouses of patients. They met the inclusion criteria of: Caucasian ethnic origin, age between 20-80 years, intra ocular pressure  $\leq 21$  mm Hg, a normal appearance of the optic nerve head and both normal and reliable visual fields (Humphrey Field Analyzer, 24-2 full threshold program, Dublin, CA). Exclusion criteria were: diabetes, hypertension requiring medical treatment, any history of eye disease or surgery, a vertical cup/disc ratio of 0.6 or more, and an asymmetry in cup/disc ratio greater than 0.2 between the two eyes. Nine of them (3.3 %) were unsuitable for GDx imaging due to either a very large zone of peripapillary atrophy, or a tilted disc yielding an unreliable GDx scan. In the end, reliable, high quality images could be obtained in 263 subjects (96.7%).

IRB/ Ethics Committee approval was obtained for this study and written informed consent was obtained from all participants after all procedures had been fully explained.

After all participants were imaged, we found that the glaucoma group was, on average, older than the normal group. Since age is shown on the GDx printout, this could potentially bias the results. Therefore, we used a computer algorithm to select 200 normal subjects and 200 glaucoma subjects so that the mean age for both groups was comparable (57.8 years versus 59.7 years;  $p=0.061$ ). Demographic data of the normal subjects and glaucoma patients have been summarized in table 8-1.

**Measurement procedures** All subjects were imaged with the GDx (Laser Diagnostic Technologies, San Diego, CA, software version 2.0.09) by two experienced operators. An imaging session for one eye consisted of obtaining 3 single images of high quality (i.e. good focus, centered optic disc, equal image illumination throughout the image and no motion artifacts). These 3 images were then aligned and converted by the software into one 'mean image'. The results for both eyes were printed on a single sheet of paper (the so-called symmetry analysis printout). During all measurements, we saw to it that patients had their heads as upright as possible. Pupils were undilated and ambient lights were left on.

**Interpreting the printouts** A total of 400 GDx printouts were presented in random order to the two authors. This was done in two separate sessions on two separate days. The optic nerve head on the reflectance image was masked by a third person with the use of a non-transparent marker. The observers were also masked to the name of the patient and operator initials. The observers had to identify a scan either as glaucomatous (when one or both eyes were glaucomatous) or as normal (when both eyes were normal).

Judging the printouts consisted of these steps: assessing image quality, assessment of the retardation image (overall impression, symmetry between superior and inferior bundle, presence of split bundles, presence of wedge-shaped defects), assessment of the TSNIT plot (position of the plot relative to the normal distribution, symmetry between superior and inferior bundle, shape and maximum height of superior and inferior humps relative to the nasal area), assessment of symmetry between the two TSNIT plots, and finally, evaluation of the Number. The observers were also allowed to look at the other parameters.

**Statistical Methods** In addition to determining the sensitivity for the entire glaucoma group ( $n=200$ ), we also calculated the sensitivity separately for patients with mild glaucoma (mean deviation  $>-6$  dB), moderate glaucoma (mean deviation  $<-6$  dB but  $>-15$  dB) and severe glaucoma (mean deviation  $<-15$  dB). The specificity was the percentage of the normal subjects that were scored as normal.

Of all 400 scans, 20 were randomly selected and presented again to both observers, in order to calculate the kappa value for intra-observer reproducibility.

The sensitivity and specificity of the Number was first calculated at a critical value of 30, since this value is suggested by the manufacturer and used by many clinicians. We repeated the calculations at a critical value of 23. We selected this value because it lowered the specificity to a level that best matched the lowest specificity of the 2 observers, to facilitate the comparison of sensitivities.

Observer #1 achieved an overall sensitivity and specificity of 92.0% and 82.5%, respectively (table 8-2). For observer #2, these values were 89.5% and 92.0%, respectively. The sensitivities and specificities of the Number have also been given in the table at critical values of 30 and 23. Both observers performed better than the Number at a cut-off value of 23, especially in the group with mild glaucoma.

## Results

The sensitivity increased with the severity of glaucoma. Intra-observer reproducibility was very good for observer #1 (Kappa = 1.0) and good for observer #2 (Kappa = 0.80).

In this study, we explored the sensitivity and specificity of both the Number, and of two expert observers, in a large group of glaucoma patients and age-matched controls. We found that both observers discriminated better than the Number which confirms a similar study by Sanchez-Galeana *et al.*<sup>25</sup> The difference between expert judgement and the Number in our study was most marked in the group of early glaucoma. In another study (Colen *et al.*, unpublished data) we found that none of the standard parameters discriminated better than the Number.

## Discussion

Choplin and Lundy<sup>18</sup> first explored the power of expert clinical judgement of GDx printouts for detecting glaucoma. This resulted in an average sensitivity and specificity of 80% and 91%, respectively. Nicolela *et al.*,<sup>26</sup> also compared the performance of expert clinical judgement of printouts with the performance of parameters. They concluded that clinical judgement of printouts was inferior to the performance of automatically generated parameters (both the Number and a newly devised logistic regression model), which contrasts with our findings and those of Sanchez-Galeana *et al.*<sup>25</sup> Differences in study design may account for this contrast: the glaucoma patients in our study had been consecutively recruited from the glaucoma clinic, whereas Nicolela *et al.*,<sup>26</sup> selected their patients on the basis of typical visual field defects. Moreover, they judged images of only one eye per patient. In our study, the observers judged images of both eyes of each patient, allowing them to look for any asymmetries. Sanchez-Galeana *et al.*,<sup>25</sup> also used the single eye printouts and their reported sensitivity and specificity values were slightly lower than in our study.

It is often unclear how subjective assessments are made. To our knowledge, we are the first to present a systematic description of this process. Our methods have recently become available as an interactive CD-ROM tutorial on the interpretation of GDx data.<sup>27</sup> We have also described four image quality criteria. The maximum diagnostic power of the GDx may be limited by a poor quality of the images. Especially motion artifacts have a substantial effect on retardation values, as we have recently described.<sup>22</sup> This was also illustrated in the study by Nicolela *et al.*,<sup>26</sup> where

the sensitivity of two observers increased after 6 images with motion artifacts were excluded from the study group.

Sensitivity and specificity values in the lower eighties to lower nineties, as found in our study, suggest that the GDx may be useful in an ophthalmic clinic. Its role for follow-up for glaucoma may be more important, but still needs to be assessed. Some investigators state that the GDx may not be suited for a screening setting,<sup>25</sup> because the sensitivity and specificity values will be lower in a population with less advanced glaucoma. Indeed, we found that the sensitivity increased from early to moderate to advanced glaucoma, both for the observers and for the Number. This was also reported by others.<sup>7,12,26</sup> However, we argue that the GDx may also play a role in a screening setting. Those who are diagnosed as having glaucoma in a screening project are not exclusively patients with early glaucoma. In fact, in a recent, publicly advertised glaucoma screening program, 22 of 197 screened subjects were found to have glaucoma.<sup>10</sup> Their average mean defect (MD) was  $-8.2$  dB, which may be classified as worse than early glaucoma. In general, the earlier glaucoma is detected, the better, as long as the specificity maintains an acceptable level. To keep the specificity acceptable, one may have to accept that one misses the early glaucoma cases. One has to assess whether the benefits of screening, i.e. detecting the (more advanced) cases of glaucoma, outweigh the costs, which include the missed (earlier) cases. These missed cases may perhaps be detected later with more advanced disease.

The sensitivity and specificity values of the Number (at a critical value of 23) were 86% and 82%, respectively. Sensitivity and specificity values reported by other investigators vary widely.<sup>7,10,12,13,16,17,25,26,28-30</sup> Several factors may have contributed to these differences of which the most important probably are: differences in population and sample size, the severity of glaucoma, differences in image quality, and the cut-off point of the Number. Therefore, a direct comparison of the various reports probably has only limited meaning.

The GDx compensates for retardation arising from the cornea assuming corneal birefringence of 60 nanometer with a slow axis of 15 degrees nasally downward. In eyes with a different axis, this compensation may be inadequate.<sup>31</sup> With the aid of a macular scan and a hardware modification of the instrument, the corneal retardation can now more effectively be removed.<sup>32</sup> Preliminary data from our own group has shown that such a better corneal compensation increases the sensitivity and specificity further, although the exact extent of this effect remains to be investigated (Reus *et al.*, unpublished data).

Bias in the current study was reduced by masking the observers to everything on the printout that contained information regarding the diagnosis of the patient except for polarization data. They were, however, allowed to evaluate the reflectance image outside the optic disc to check the location of the blood vessels. Any information about the optic disc on the reflectance image was removed with a black marker, to keep polarimetry data as pure as possible. In addition, because nerve fiber layer thickness decreases with age, the groups of normal subjects and glaucoma patients were age-matched. As it stands, scanning laser polarimetry yields reasonable sensitivity and specificity values when only the Number is considered. Better values are achieved when clini-

cians judge the printouts, but this requires experience. A more detailed description of how the authors interpret GDx data is now available on CD-ROM. Future research will focus on how to translate the way the observers interpret a printout into a mathematical model that can be used by the software, thus facilitating an automated diagnostic procedure.

	n	Age (years)	Mean deviation (dB)
<b>Normal subjects</b>	200	57.8 (11.6)	-0.13 (0.91)
<b>All glaucoma patients</b>	200	59.7 (9.1)	-10.5 (7.5)
• Mild	74	60.6 (8.1)	-3.5 (1.8)
• Moderate	78	59.3 (10.1)	-10.3 (2.7)
• Severe	48	58.9 (9.1)	-21.2 (4.8)

**Table 8-1.**  
Demographic  
data of the  
study  
population

Presented are the number of subjects (n), their mean age and their mean deviation (MD) in dB on visual field testing. Standard deviations are presented in parentheses. For the glaucoma patients, the data is given again for the three subgroups separately.

	Observer #1		Observer #2		The Number @ 30		The Number @ 23	
	sens	spec	sens	spec	sens	spec	sens	spec
<b>All</b>	92.0	82.5	89.5	92.0	75.0	90.5	85.5	81.5
Mild	85.1		82.4		63.5		75.7	
Moderate	94.8		92.2		73.1		85.9	
Severe	98.0		95.9		95.8		100	

**Table 8-2.**  
Sensitivity and  
Specificity as  
obtained by two  
different  
observers, and  
The Number

Sensitivity (sens) and specificity (spec) values are given in percentages (%) for observer #1, for observer #2, for the Number at a cut-off value of 30 and at a value of 23. The values are given for the glaucoma group as a whole, as well as for the three subgroups.

## References

1. Dreher AW, Reiter K. Retinal laser ellipsometry: a new method for measuring the retinal nerve fiber layer thickness distribution. *Clin Vis Sci* 1992;7:481-8.
2. Weinreb RN, Dreher AW, Coleman A, et al. Histopathologic validation of Fourier-ellipsometry measurements of retinal nerve fiber layer thickness. *Arch Ophthalmol* 1990;108:557-60.
3. Weinreb RN, Shakiba S, Zangwill L. Scanning laser polarimetry to measure the nerve fiber layer of normal and glaucomatous eyes. *Am J Ophthalmol* 1995;119:627-36.
4. Holló G, Suveges I, Nagymihaly A, Vargha P. Scanning laser polarimetry of the retinal nerve fibre layer in primary open angle and capsular glaucoma. *Br J Ophthalmol* 1997;81:857-61.
5. Xu L, Chen PP, Chen YY, et al. Quantitative nerve fiber layer measurements using scanning laser polarimetry and modulation parameters in the detection of glaucoma. *J Glaucoma* 1998;7:270-7.
6. Waldock A, Potts MJ, Sparrow JM, Karwatowski WS. Clinical evaluation of scanning laser polarimetry: II. Polar profile shape analysis. *Br J Ophthalmol* 1998;82:260-6.
7. Weinreb RN, Zangwill L, Berry CC, et al. Detection of glaucoma with scanning laser polarimetry. *Arch Ophthalmol* 1998;116:1583-9.
8. Choplin NT, Lundy DC, Dreher AW. Differentiating patients with glaucoma from glaucoma suspects and normal subjects by nerve fiber layer assessment with scanning laser polarimetry. *Ophthalmology* 1998;105:2068-76.
9. Reyes RD, Tomita G, Kitazawa Y. Retinal nerve fiber layer thickness within the area of apparently normal visual field in normal-tension glaucoma with hemifield defect. *J Glaucoma* 1998;7:329-35.
10. Yamada N, Chen PP, Mills RP, et al. Glaucoma screening using the scanning laser polarimeter. *J Glaucoma* 2000;9:254-61.
11. Lee VW, Mok KH. Retinal nerve fiber layer measurement by nerve fiber analyzer in normal subjects and patients with glaucoma. *Ophthalmology* 1999;106:1006-8.
12. Tribble JR, Schultz RO, Robinson JC, Rothe TL. Accuracy of scanning laser polarimetry in the diagnosis of glaucoma. *Arch Ophthalmol* 1999;117:1298-304.
13. Vitale S, Smith TD, Quigley T, et al. Screening performance of functional and structural measurements of neural damage in open-angle glaucoma: a case-control study from the Baltimore Eye Survey. *J Glaucoma* 2000;9:346-56.
14. Kamal DS, Bunce C, Hitchings RA. Use of the GDx to detect differences in retinal nerve fibre layer thickness between normal, ocular hypertensive and early glaucomatous eyes. *Eye* 2000;14:367-70.
15. Essock EA, Sinai MJ, Fechtner RD, et al. Fourier analysis of nerve fiber layer measurements from scanning laser polarimetry in glaucoma: emphasizing shape characteristics of the 'double-hump' pattern. *J Glaucoma* 2000;9:444-52.
16. Lauande-Pimentel R, Carvalho RA, Oliveira HC, et al. Discrimination between normal and glaucomatous eyes with visual field and scanning laser polarimetry measurements. *Br J Ophthalmol* 2001;85:586-91.
17. Poinosawmy D, Tan JC, Bunce C, Hitchings RA. The ability of the GDx nerve fibre analyser neural network to diagnose glaucoma. *Graefes Arch Clin Exp Ophthalmol* 2001;239:122-7.
18. Choplin NT, Lundy DC. The sensitivity and specificity of scanning laser polarimetry in the detection of glaucoma in a clinical setting. *Ophthalmology* 2001;108:899-904.
19. Tjon-Fo-Sang MJ, Lemij HG. The sensitivity and specificity of nerve fiber layer measurements in glaucoma as determined with scanning laser polarimetry. *Am J Ophthalmol* 1997;123:62-9.
20. Kogure S, Chiba T, Kinoshita T, et al. Effects of artefacts on scanning laser polarimetry of retinal nerve fibre layer thickness measurement. *Br J Ophthalmol* 2000;84:1013-7.



21. Hoh ST, Greenfield DS, Liebmann JM, et al. Factors affecting image acquisition during scanning laser polarimetry. *Ophthalmic Surg Lasers* 1998;29:545-51.
22. Colen TP, Lemij HG. Motion artifacts in scanning laser polarimetry. *Ophthalmology* 2002;109(8):1568-72.
23. Colen TP, Lemij HG. Prevalence of split nerve fiber layer bundles in healthy eyes imaged with scanning laser polarimetry. *Ophthalmology* 2001;108:151-6.
24. Anderson DR, Patella VM. *Automated Static Perimetry*. 2nd ed. St. Louis: Mosby; 1999:104.
25. Sanchez-Galeana C, Bowd C, Blumenthal EZ, et al. Using optical imaging summary data to detect glaucoma. *Ophthalmology* 2001;108:1812-8.
26. Nicolela MT, Martinez-Bello C, Morrison CA, et al. Scanning laser polarimetry in a selected group of patients with glaucoma and normal controls. *Am J Ophthalmol* 2001;132:845-54.
27. Colen TP, Lemij HG. The Rotterdam GDx Course [Computer program/ CD-ROM]. Rotterdam, The Netherlands: The Rotterdam Eye Hospital. 2002.
28. Greaney MJ, Hoffman DC, Garway-Heath DF, et al. Comparison of optic nerve imaging methods to distinguish normal eyes from those with glaucoma. *Invest Ophthalmol Vis Sci* 2002;43:140-5.
29. Bowd C, Zangwill LM, Berry CC, et al. Detecting early glaucoma by assessment of retinal nerve fiber layer thickness and visual function. *Invest Ophthalmol Vis Sci* 2001;42:1993-2003.
30. Zangwill LM, Bowd C, Berry CC, et al. Discriminating between normal and glaucomatous eyes using the Heidelberg Retina Tomograph, GDx Nerve Fiber Analyzer, and Optical Coherence Tomograph. *Arch Ophthalmol* 2001;119:985-93.
31. Greenfield DS, Knighton RW, Huang XR. Effect of corneal polarization axis on assessment of retinal nerve fiber layer thickness by scanning laser polarimetry. *Am J Ophthalmol* 2000;129:715-22.
32. Zhou Q, Weinreb RN. Individualized compensation of anterior segment birefringence during scanning laser polarimetry. *Invest Ophthalmol Vis Sci* 2002;43:2221-8.



## CHAPTER 9

### *General discussion*

In this thesis, Scanning Laser Polarimetry (SLP) has been investigated. The clinical studies here have led to the development of image quality criteria and limits for statistically significant change. We have also found that the standard database of the GDx can be used for evaluating amblyopic eyes for glaucoma. Also, the GDx can measure damage to the NFL in non-glaucomatous diseases such as an AION. Further, we have developed a systematic approach for the clinical interpretation of GDx scans. We have found that split bundles (a specific pattern of NFL orientation) are a common finding in healthy eyes. We have shown that the Number is the best single standard parameter for discriminating between glaucomatous and normal eyes. The 4 recently developed GDx parameters did not seem to add to the Number in this respect. Still, the sensitivity and specificity of the Number could be further increased by subjective judgement of all available data on the printout. With this method, the sensitivity and specificity for two different observers was 92.0% and 82.5%, and 89.5% and 92.0% respectively.

Glaucoma remains a disease of which we do not know the precise origin. Many ophthalmologists may have little trouble recognizing the disease when they see its signs in most of their patients. Unfortunately, the inter-observer agreement of optic disc assessment is generally moderate.<sup>1,3</sup> We still cannot exactly define glaucoma because there is no consensus on the criteria for the signs on which we base our diagnosis.<sup>4</sup> The aim of this thesis was to find out whether scanning laser polarimetry provided better criteria for the definition and detection of glaucoma. The answers to this question have not been equivocal.

The GDx has been used on thousands of normal subjects,<sup>5-11</sup> people with ocular hypertension<sup>12-14</sup> and glaucoma patients<sup>15-41</sup> and its advantages are clear. The applicability is high.<sup>38</sup> We found that in a group of 527 subjects, high quality images could be obtained in even 94.5% of glaucoma patients and 96.7% of normal subjects (chapter 7). Perimetry is considerably less applicable. In one study, only 68.5% of subjects managed to produce a reliable<sup>42</sup> visual field test result.<sup>43</sup> Image acquisition with the GDx is fast and objective. The GDx has a high reproducibility of measurements.<sup>44-46</sup> It has a normative database that is stratified for ethnicity and different age groups. The sensitivity and specificity found by us are comparable to those of visual field testing, which is currently used as a gold standard by many clinicians. Other topics, however, are still unclear.

First, sensitivity and specificity results for SLP differ greatly in the literature. Results roughly fall into two categories: sensitivity and specificity of automated analysis (e.g. the performance of the Number) and of subjective assessment of the printouts. We have investigated both of them (chapter 7 and 8). In our study, sensitivity and specificity values for the Number (at a critical value of 23) were 86% and 82%, respectively. The results from other studies vary greatly, and they are usually not as favorable as ours.<sup>30-40</sup> This may be for several reasons. One reason may be that the maximum diagnostic power of the GDx could be limited by a poor quality of the images. We were the first to demonstrate that motion artifacts have a substantial effect on retardation values (chapter 2). This led to the development of 4 image quality criteria that we applied routinely to all our images. Almost none of the other reports mentioned image quality. Only one study group recalculated their data after

exclusion of images with motion artifacts and found that sensitivity increased.<sup>34</sup> Another reason for the differences may be that our results were based on the largest sample of test subjects (527 subjects) ever reported. Other sample sizes were smaller, with typically fewer than 50 glaucoma patients. Glaucoma may present as different types of damage in different severities. We therefore believe that a large database of test subjects is needed. Finally, other factors that may have contributed to the differences in findings include differences in population and recruitment methods, the severity of glaucoma and the cut-off point for the Number.

Apart from the sensitivity and specificity of the automated parameters, we investigated the performance of subjective expert judgement of the printouts (chapter 8). Choplin and Lundy<sup>47</sup> first explored the power of expert clinical judgement of GDx printouts for detecting glaucoma. This resulted in an average sensitivity and specificity of 80% and 91%, respectively. Choplin and Lundy did not compare their data to the sensitivity and specificity of the Number in their group. We found that two expert observers better discriminated between normal eyes and glaucomatous eyes than the Number did. This was in agreement with the findings of Sanchez-Galeana *et al.*,<sup>32</sup> However, Nicolela *et al.*<sup>34</sup> concluded that clinical judgement of printouts was inferior to the performance of automatically generated parameters (both the Number and a newly devised logistic regression model). Differences in study design may account for this contrast: the glaucoma patients in our study had been consecutively recruited from the glaucoma clinic, whereas Nicolela *et al.*<sup>34</sup> selected their patients on the basis of typical visual field defects. Moreover, they judged images of only one eye per patient. We think that by comparing the 2 eyes one may obtain more useful clinical information, notably with interocular asymmetries, as was done in our study. The manufacturer now also recognizes that information on asymmetry between the 2 eyes may be valuable and in the latest versions of the GDx software all parameters are now compared between eyes with the differences presented on the printout. Whether this leads to a better separation between normal and glaucomatous eyes remains to be investigated.

There is a second topic that lacks clarity. At present it may still be unclear how to interpret clinical GDx data and there is no consensus on how to define an abnormal GDx scan. In most studies, the Number is the best separating parameter between normal and glaucomatous eyes. We showed that the four newly devised parameters add little in that respect. There is some agreement on what cut-off point for the Number should be used. We found a value of 23 to yield the best trade-off between sensitivity and specificity. This agrees with the values between 17 and 35 found in the literature.<sup>34,38-40</sup> In contrast, there is almost no information on how the GDx printouts are best subjectively assessed. We were the first to describe how we interpreted the printouts. Later, this was more extensively covered in the GDx course we developed. Some clinicians have copied this approach but it remains to be investigated what sensitivity and specificity values these clinicians reach with this method of interpretation.

Also, SLP has not been histologically validated in humans. Retardation values were correlated to the histological thickness of the NFL in two monkey eyes with their corneas removed,<sup>48</sup> and in one monkey eye with an intact cornea.<sup>5</sup> No human data

is presently available. One might argue that this is not a problem as long as the measurements discriminate well between normal subjects and glaucoma patients as well as reliably detect change over time. Yet, before a claim can be made that SLP measures NFL thickness, this needs to be validated first. A human validation study has recently been initiated by our group.

There is insufficient data on whether the GDx can detect glaucomatous progression. Thus far, we have evaluated parameters only for case finding. Parameters with a high sensitivity and specificity are not necessarily also the best parameters for follow up. Although we found some evidence that the GDx can detect glaucomatous change, we do not presently know what parameters are most suited to monitor this. A good parameter would need to be valid, and have a high reproducibility of measurements.<sup>49</sup> Validity (also called accuracy) means that the measurement (e.g. NFL thickness) is correct for the patient being studied and relevant for the disease being studied. This means that the parameter will change as the state of the disease changes. Reproducibility of measurements (also called reliability or precision) is the extent to which repeated measurements of a relatively stable phenomenon fall closely to each other. In case of glaucoma, this means that the parameter will not change when the state of the disease remains stable. With the GDx, reproducibility of measurements is high.<sup>44-46,50-52</sup> Our study was the first to express reproducibility of measurements in terms of limits of agreement.<sup>53</sup> These limits indicate how much a GDx parameter from two consecutive measurements is allowed to change before becoming statistically significant. Our study identified those parameters that had, on average, the best limits of agreement. It is, however, unlikely that the same limits apply to every subject. Ideally, one would like to obtain limits of agreement per parameter *per subject*, but this would be very elaborate. Even though the parameters with the best limits of agreement have been identified in chapter 3, a large follow-up study would be needed to establish whether these parameters hold sufficient validity to detect glaucomatous change. Such a study has already been launched by our group.

The output parameters merit additional research. Although there are different parameters that relate to different locations of the retardation image, they do not take into account the patients individual pattern of NFL orientation. We identified one such pattern and named it a split bundle (chapter 4). We showed that the outcome of some parameters could depend on the pattern of NFL orientation.<sup>54</sup> Specificity of those parameters may increase when, in the future, parameters would be normalized for different patterns of the imaged NFL. Whereas a split bundle reflected a normal NFL variation, a wedge shaped defect is recognized as an early sign of glaucoma.<sup>15,55</sup> In our experience, wedge shaped defects are easily and regularly observed in the retardation image. However, there is no algorithm available that can detect them. Such an algorithm may greatly improve the sensitivity of the automated analysis of GDx images. Another parameter that may be worth developing would focus on the temporal part of the arcuate bundles instead of the entire bundle. Glaucomatous damage tends to be more prominent over the temporal part than over the nasal part of the NFL, notably in the earlier stages of the disease. Over the past few years, there have been attempts to create new parameters.<sup>25,56 40</sup> Four of these have been tested in chapter 7. It was found that they discriminated well

between normal eyes and glaucomatous eyes, but none of the 4 new parameters, on their own, discriminated better than the Number. The high sensitivity and specificity of the new parameters, however, does suggest that they may add to a new algorithm of the Number. Such a contribution is less likely for the Discriminant Analysis (DA), since it is calculated from 3 already existing parameters. It is unclear what the performance of such a discriminant analysis would be with 4 (or more) input variables. Anyhow, the high performance of the DA was already a surprising finding; being calculated from only 3 existing parameters (average thickness, ellipse modulation and ellipse average) the area under the ROC curve was the same as for the Number. In contrast, the algorithm for the Number consists of a combination of 28 parameters, of which only 13 are included on the printout. This suggests that all the information the Number needed up to now, was already contained in those three parameters. This also suggests that some of the parameters that have a low area under the ROC curve might better be left off the printout. On today's version of the GDx Access (a portable version of the GDx, but with comparable hardware) printout, 5 parameters that performed poorly in chapter 7 have been omitted in the printout.

We know little about the NFL thickness in subjects who have other diseases than glaucoma. In chapter 5 we reported measurements in amblyopia and found no differences in NFL thickness between amblyopic eyes and normal eyes.<sup>57</sup> This was later confirmed by a second report.<sup>58</sup> We also documented SLP measurements in an AION patient (chapter 6).<sup>59</sup> Others have documented GDx measurements in patients with intracranial and intracranial lesions to the optic nerve,<sup>60</sup> traumatic optic neuropathy,<sup>61</sup> demyelinating optic neuritis,<sup>62</sup> myelinated retinal nerve fibers,<sup>63</sup> and Alzheimer's dementia.<sup>64</sup> Of even more clinical interest, would be to know whether and how more common disorders such as diabetes or systemic hypertension would affect the SLP measurements. Only one study reports on changes found in diabetic patients, but the studied group was small (12 patients).<sup>65</sup>

Despite the promising results that are presently obtained with the GDx, the clinician is still faced with over 10% of inaccurate test results. Part of these misclassifications can probably be explained by the cornea. The GDx compensates for retardation arising from the cornea and crystalline lens on the assumption that a corneal birefringence of 60 nanometer with a slow axis of 15 degrees nasally downward exists in all patients. Greenfield *et al.* showed that the corneal birefringence varies considerably between subjects.<sup>66</sup> It was estimated later that in eyes with a corneal polarization axis (CPA) that differed substantially from average, the compensation was inadequate.<sup>67,68</sup> Garway-Heath *et al.* showed that a software correction of the retardation images, based on retardation data of the macular region, could narrow the variability of retardation readings in normals and glaucoma patients.<sup>69</sup> Also, the sensitivity for discriminating between normal subjects and glaucoma patients increased. Greenfield *et al.* measured the CPA in a group of patients using a slit lamp mounted device that incorporated two crossed linear polarizers and an optical retarder.<sup>70</sup> They found that the incorporation of the CPA in their logistic regression model increased the power to discriminate between normal and glaucomatous eyes. Later, Zhou and Weinreb reported results using a modified GDx that accommodated a variable corneal compensator.<sup>71</sup> A polarimetry image of the Henle fiber layer was

used to set the variable compensator before acquiring peripapillary data. Using a macular scan to verify the effectiveness of compensation, they showed that individualized anterior segment compensation was feasible. A new generation GDx that features this variable corneal compensation is called GDx VCC and has recently become commercially available. We expect that the sensitivity and specificity for detecting glaucoma will increase further with the GDx VCC, although this is still under investigation.

SLP has evolved at a high pace over the past decade. This has added to the need for practical instruction to those who are new to or inexperienced with the technology and has prompted us to develop The Rotterdam GDx Course. This course has been presented to about 800 ophthalmologists and ophthalmic technicians worldwide. From feedback of the course participants we know that hands-on imaging training and instruction for interpretation of clinical data were highly appreciated. This might be a signal to the manufacturer that new techniques may not reach their full potential until they are accompanied by clinically relevant instructions and training. Now that the Rotterdam GDx Course has been translated onto an electronic platform, it will hopefully be available to a wider audience. We speculate that the need for systematic training also applies to other imaging techniques in glaucoma.

In summary, the GDx provides fast, objective and quantitative data on NFL thickness. The applicability and reproducibility of measurements are high, and measurements are user and patient friendly. The GDx yields useful sensitivity and specificity values for the detection of glaucoma, whereas its role in follow-up remains to be investigated. As it stands, the GDx holds insufficient validity to serve as a single test for glaucoma. It does, however, provide a very useful addition to the existing tests we run in patients to make the correct diagnosis.



1. Varma R, Steinmann WC, Scott IU. Expert agreement in evaluating the optic disc for glaucoma. *Ophthalmology* 1992;99:215-21.
2. Gaasterland DE, Blackwell B, Dally LG, et al. The Advanced Glaucoma Intervention Study (AGIS): 10. Variability among academic glaucoma subspecialists in assessing optic disc notching. *Trans Am Ophthalmol Soc* 2001;99:177-84; discussion 184-5.: Notes: CORPORATE NAME: Advanced Glaucoma Intervention Study Investigators.
3. Nicoletta MT, Drance SM, Broadway DC, et al. Agreement among clinicians in the recognition of patterns of optic disk damage in glaucoma. *Am J Ophthalmol* 2001;132:836-44.
4. Sommer A. Doyné Lecture. Glaucoma: facts and fancies. *Eye* 1996;10:295-301.
5. Morgan JE, Waldock A. Scanning laser polarimetry of the normal human retinal nerve fiber layer: a quantitative analysis. *Am J Ophthalmol* 2000;129:76-82.
6. Toprak AB, Yilmaz OF. Relation of optic disc topography and age to thickness of retinal nerve fibre layer as measured using scanning laser polarimetry, in normal subjects. *Br J Ophthalmol* 2000;84:473-8.
7. Kurimoto Y, Matsuno K, Kaneko Y, et al. Asymmetries of the retinal nerve fibre layer thickness in normal eyes. *Br J Ophthalmol* 2000;84:469-72.
8. Poinsoosawmy D, Fontana L, Wu JX, et al. Variation of nerve fibre layer thickness measurements with age and ethnicity by scanning laser polarimetry. *Br J Ophthalmol* 1997;81:350-4.
9. Ozdek SC, Onol M, Gurelik G, Hasanreisoglu B. Scanning laser polarimetry in normal subjects and patients with myopia. *Br J Ophthalmol* 2000;84:264-7.
10. Essock EA, Sinai MJ, Fechtner RD. Interocular symmetry in nerve fiber layer thickness of normal eyes as determined by polarimetry. *J Glaucoma* 1999;8:90-8.
11. Funaki S, Shirakashi M, Abe H. Relation between size of optic disc and thickness of retinal nerve fibre layer in normal subjects. *Br J Ophthalmol* 1998;82:1242-5.
12. Tjon-Fo-Sang MJ, de Vries J, Lemij HG. Measurement by nerve fiber analyzer of retinal nerve fiber layer thickness in normal subjects and patients with ocular hypertension. *Am J Ophthalmol* 1996;122:220-7.
13. Anton A, Zangwill L, Emdadi A, Weinreb RN. Nerve fiber layer measurements with scanning laser polarimetry in ocular hypertension. *Arch Ophthalmol* 1997;115:331-4.
14. Mistlberger A, Liebmann JM, Greenfield DS, et al. Assessment of optic disc anatomy and nerve fiber layer thickness in ocular hypertensive subjects with normal short-wavelength automated perimetry. *Ophthalmology* 2002;109:1362-6.
15. Weinreb RN. Evaluating the retinal nerve fiber layer in glaucoma with scanning laser polarimetry. *Arch Ophthalmol* 1999;117:1403-6.
16. Kremmer S, Ayerley HD, Selbach JM, Steuhl KP. Scanning laser polarimetry, retinal nerve fiber layer photography, and perimetry in the diagnosis of glaucomatous nerve fiber defects. *Graefes Arch Clin Exp Ophthalmol* 2000;238:922-6.
17. Tjon-Fo-Sang MJ, Lemij HG. The sensitivity and specificity of nerve fiber layer measurements in glaucoma as determined with scanning laser polarimetry. *Am J Ophthalmol* 1997;123:62-9.
18. Kamal DS, Bunce C, Hitchings RA. Use of the GDx to detect differences in retinal nerve fibre layer thickness between normal, ocular hypertensive and early glaucomatous eyes. *Eye* 2000;14:367-70.
19. Weinreb RN, Shakiba S, Sample PA, et al. Association between quantitative nerve fiber layer measurement and visual field loss in glaucoma. *Am J Ophthalmol* 1995;120:732-8.
20. Weinreb RN, Shakiba S, Zangwill L. Scanning laser polarimetry to measure the nerve fiber layer of normal and glaucomatous eyes. *Am J Ophthalmol* 1995;119:627-36.

21. Kwon YH, Hong S, Honkanen RA, Alward WL. Correlation of automated visual field parameters and peripapillary nerve fiber layer thickness as measured by scanning laser polarimetry. *J Glaucoma* 2000;9:281-8.
22. Lee VW, Mok KH. Retinal nerve fiber layer measurement by nerve fiber analyzer in normal subjects and patients with glaucoma. *Ophthalmology* 1999;106:1006-8.
23. Reyes RD, Tomita G, Kitazawa Y. Retinal nerve fiber layer thickness within the area of apparently normal visual field in normal-tension glaucoma with hemifield defect. *J Glaucoma* 1998;7:329-35.
24. Chen Y, Chen P, Xu L, et al. Correlation of peripapillary nerve fiber layer thickness by scanning laser polarimetry with visual field defects in patients with glaucoma. *J Glaucoma* 1998;7:312-6.
25. Choplin NT, Lundy DC, Dreher AW. Differentiating patients with glaucoma from glaucoma suspects and normal subjects by nerve fiber layer assessment with scanning laser polarimetry. *Ophthalmology* 1998;105:2068-76.
26. Holló G, Suveges I, Nagymihaly A, Vargha P. Scanning laser polarimetry of the retinal nerve fibre layer in primary open angle and capsular glaucoma. *Br J Ophthalmol* 1997;81:857-61.
27. Gluck R, Rohrschneider K, Kruse FE, Volcker HE. Detection of glaucomatous nerve fiber damage. Laser polarimetry in comparison with equivalent visual field loss. *Ophthalmologie* 1997;94:815-20.
28. Sturmer J, Bernasconi P, Caubergh MJ, et al. Value of scanning laser ophthalmoscopy and polarimetry compared with perimetry in evaluating glaucomatous changes in the optic papilla and nerve fiber layer. *Ophthalmologie* 1996;93:520-6.
29. Kook MS, Sung K, Kim S, et al. Study of retinal nerve fibre layer thickness in eyes with high tension glaucoma and hemifield defect. *Br J Ophthalmol* 2001;85:1167-70.
30. Greaney MJ, Hoffman DC, Garway-Heath DE, et al. Comparison of optic nerve imaging methods to distinguish normal eyes from those with glaucoma. *Invest Ophthalmol Vis Sci* 2002;43:140-5.
31. Bowd C, Zangwill LM, Berry CC, et al. Detecting early glaucoma by assessment of retinal nerve fiber layer thickness and visual function. *Invest Ophthalmol Vis Sci* 2001;42:1993-2003.
32. Sanchez-Galeana C, Bowd C, Blumenthal EZ, et al. Using optical imaging summary data to detect glaucoma. *Ophthalmology* 2001;108:1812-8.
33. Zangwill LM, Bowd C, Berry CC, et al. Discriminating between normal and glaucomatous eyes using the Heidelberg Retina Tomograph, GDx Nerve Fiber Analyzer, and Optical Coherence Tomograph. *Arch Ophthalmol* 2001;119:985-93.
34. Nicoleta MT, Martinez-Bello C, Morrison CA, et al. Scanning laser polarimetry in a selected group of patients with glaucoma and normal controls. *Am J Ophthalmol* 2001;132:845-54.
35. Poinosawmy D, Tan JC, Bunce C, Hitchings RA. The ability of the GDx nerve fibre analyser neural network to diagnose glaucoma. *Graefes Arch Clin Exp Ophthalmol* 2001;239:122-7.
36. Lauande-Pimentel R, Carvalho RA, Oliveira HC, et al. Discrimination between normal and glaucomatous eyes with visual field and scanning laser polarimetry measurements. *Br J Ophthalmol* 2001;85:586-91.
37. Yamada N, Chen PP, Mills RP, et al. Glaucoma screening using the scanning laser polarimeter. *J Glaucoma* 2000;9:254-61.
38. Vitale S, Smith TD, Quigley T, et al. Screening performance of functional and structural measurements of neural damage in open-angle glaucoma: a case-control study from the Baltimore Eye Survey. *J Glaucoma* 2000;9:346-56.
39. Tribble JR, Schultz RO, Robinson JC, Rothe TL. Accuracy of scanning laser polarimetry in the diagnosis of glaucoma. *Arch Ophthalmol* 1999;117:1298-304.
40. Weinreb RN, Zangwill L, Berry CC, et al. Detection of glaucoma with scanning laser polarimetry. *Arch Ophthalmol* 1998;116:1583-9.

41. Tannenbaum DP, Zangwill LM, Bowd C, et al. Relationship between visual field testing and scanning laser polarimetry in patients with a large cup-to-disk ratio. *Am J Ophthalmol* 2001;132:501-6.
42. Anderson DR, Patella VM. *Automated Static Perimetry*. 2nd ed. St. Louis: Mosby; 1999:104.
43. Katz J, Sommer A, Gaasterland DE, Anderson DR. Comparison of analytic algorithms for detecting glaucomatous visual field loss. *Arch Ophthalmol* 1991;109:1684-9.
44. Colen TP, Tjon-Fo-sang MJ, Mulder PG, Lemij HG. Reproducibility of measurements with the nerve fiber analyzer (NFA/GDx). *J Glaucoma* 2000;9:363-70.
45. Kook MS, Sung K, Park RH, et al. Reproducibility of scanning laser polarimetry (GDx) of peripapillary retinal nerve fiber layer thickness in normal subjects. *Graefes Arch Clin Exp Ophthalmol* 2001;239:118-21.
46. Rhee DJ, Greenfield DS, Chen PP, Schiffman J. Reproducibility of retinal nerve fiber layer thickness measurements using scanning laser polarimetry in pseudophakic eyes. *Ophthalmic Surg Lasers* 2002;33:117-22.
47. Choplin NT, Lundy DC. The sensitivity and specificity of scanning laser polarimetry in the detection of glaucoma in a clinical setting. *Ophthalmology* 2001;108:899-904.
48. Weinreb RN, Dreher AW, Coleman A, et al. Histopathologic validation of Fourier-ellipsometry measurements of retinal nerve fiber layer thickness. *Arch Ophthalmol* 1990;108:557-60.
49. Fletcher RH, Fletcher SW, Wagner EH. *Clinical Epidemiology*. 2nd ed. Baltimore: Williams and Wilkins; 1988:23.
50. Waldock A, Potts MJ, Sparrow JM, Karwatowski WS. Clinical evaluation of scanning laser polarimetry: I. Intraoperator reproducibility and design of a blood vessel removal algorithm. *Br J Ophthalmol* 1998;82:252-9.
51. Hoh ST, Ishikawa H, Greenfield DS, et al. Peripapillary nerve fiber layer thickness measurement reproducibility using scanning laser polarimetry. *J Glaucoma* 1998;7:12-5.
52. Klemm M, Rumberger E, Walter A, Richard G. Reproducibility of measuring retinal nerve fiber density. Comparison of optical coherence tomography with the nerve fiber analyzer and the Heidelberg retinal tomography device. *Ophthalmologie* 2002;99:345-51.
53. Bland JM, Altman DG. Statistical methods for assessing agreement between two methods of clinical measurement. *Lancet* 1986;307-10.
54. Colen TP, Lemij HG. Prevalence of split nerve fiber layer bundles in healthy eyes imaged with scanning laser polarimetry. *Ophthalmology* 2001;108:151-6.
55. Tuulonen A, Airaksinen PJ. Initial glaucomatous optic disk and retinal nerve fiber layer abnormalities and their progression. *Am J Ophthalmol* 1991;111:485-90.
56. Xu L, Chen PP, Chen YY, et al. Quantitative nerve fiber layer measurements using scanning laser polarimetry and modulation parameters in the detection of glaucoma. *J Glaucoma* 1998;7:270-7.
57. Colen TP, de Faber JT, Lemij HG. Retinal nerve fiber layer thickness in human strabismic amblyopia. *Binocul Vis Strabismus Q* 2000;15:141-6.
58. Baddini-Caramelli C, Hatanaka M, Polati M, et al. Thickness of the retinal nerve fiber layer in amblyopic and normal eyes: a scanning laser polarimetry study. *J AAPOS* 2001;5:82-4.
59. Colen TP, van Everdingen JA, Lemij HG. Axonal loss in a patient with anterior ischemic optic neuropathy as measured with scanning laser polarimetry. *Am J Ophthalmol* 2000;130:847-50.
60. Meier FM, Bernasconi P, Sturmer J, et al. Axonal loss from acute optic neuropathy documented by scanning laser polarimetry. *Br J Ophthalmol* 2002;86:285-7.
61. Medeiros FA, Susanna R Jr. Retinal nerve fiber layer loss after traumatic optic neuropathy detected by scanning laser polarimetry. *Arch Ophthalmol* 2001;119:920-1.

62. Steel DH, Waldock A. Measurement of the retinal nerve fibre layer with scanning laser polarimetry in patients with previous demyelinating optic neuritis. *Journal of Neurology, Neurosurgery & Psychiatry* 1998;64:505-9.
63. Tatlipinar S, Gedik S, Mocan MC, et al. Polarimetric nerve fiber analysis in patients with peripapillary myelinated retinal nerve fibers. *Acta Ophthalmol Scand* 2001;79:399-402.
64. Kergoat H, Kergoat MJ, Justino L, et al. An evaluation of the retinal nerve fiber layer thickness by scanning laser polarimetry in individuals with dementia of the Alzheimer type. *Acta Ophthalmol Scand* 2001;79:187-91.
65. Lopes de Faria JM, Russ H, Costa VP. Retinal nerve fibre layer loss in patients with type 1 diabetes mellitus without retinopathy. *Br J Ophthalmol* 2002;86:725-8.
66. Greenfield DS, Knighton RW, Huang XR. Effect of corneal polarization axis on assessment of retinal nerve fiber layer thickness by scanning laser polarimetry. *Am J Ophthalmol* 2000;129:715-22.
67. Knighton RW, Huang XR. Linear birefringence of the central human cornea. *Invest Ophthalmol Vis Sci* 2002;43:82-6.
68. Weinreb RN, Bowd C, Greenfield DS, Zangwill LM. Measurement of the magnitude and axis of corneal polarization with scanning laser polarimetry. *Arch Ophthalmol* 2002;120:901-6.
69. Garway-Heath DE, Greaney MJ, Caprioli J. Correction for the erroneous compensation of anterior segment birefringence with the scanning laser polarimeter for glaucoma diagnosis. *Invest Ophthalmol Vis Sci* 2002;43:1465-74.
70. Greenfield DS, Knighton RW, Feuer WJ, et al. Correction for corneal polarization axis improves the discriminating power of scanning laser polarimetry. *Am J Ophthalmol* 2002;134:27-33.
71. Zhou Q, Weinreb RN. Individualized compensation of anterior segment birefringence during scanning laser polarimetry. *Invest Ophthalmol Vis Sci* 2002;43:2221-8.

## CHAPTER 10

### *Summary & Samenvatting*

## Summary

The number of people with glaucoma has been estimated at 66.8 million, with 6.7 million suffering from bilateral blindness. This makes glaucoma the second leading cause of irreversible blindness worldwide. When left untreated, glaucoma results in visual field loss and eventually in blindness. In considering the diagnosis of glaucoma, the physician will evaluate the intraocular pressure, the optic nerve head and the visual field. This seems to be a straightforward diagnostic process, but, surprisingly, there is still no consensus on the criteria for the signs on which the diagnosis is based.

Glaucoma is a progressive optic neuropathy characterized by death of retinal ganglion cells (RGC). The course of events that eventually leads to death of these cells is not exactly known. As the RGCs die, the retinal nerve fiber layer (NFL), which is made up of the axons of the RGCs, thins. Scanning laser polarimetry (SLP) is an imaging technique that can detect glaucoma by assessing the thickness of the retinal NFL.

SLP came onto the market in 1993. The working principle is based on the NFL being form-birefringent. As a polarized beam of laser light is sent through the NFL, a shift in polarization occurs. This phase shift is called retardation and is thought to be linearly correlated with NFL thickness, as has been shown in a monkey model. In the past, SLP has shown to discriminate well between normal and glaucomatous eyes. The first scanning laser polarimeter that came onto the market was called the Nerve Fiber Analyzer (NFA). When the research described in this thesis began, the instrument had recently undergone extensive hard- and software revisions and was henceforward called the GDx. The goal of this thesis was to investigate the clinical performance of the GDx (mainly its ability to discriminate between healthy and glaucomatous eyes) and to explore ways of how to improve this.

We found that some images in some patients reproduced poorly. This turned out to be caused by eye movements during image acquisition, resulting in what we called “motion artifacts”. These motion artifacts went undetected by the system’s built-in image quality check. In *chapter 2*, we demonstrated that motion artifacts led to an increase in retardation values. In glaucomatous eyes, motion artifacts might lead to overlooking the disease. In following normal eyes, a baseline image with motion artifacts followed by an image without motion artifacts may mimic progression.

In *chapter 3*, the reproducibility of measurements was studied. It was found that the reproducibility of measurements was high, and that it hardly differed between single images and mean images. It also varied across different parameters. We therefore calculated limits of agreement separately for every parameter. These limits may later serve as critical values for progression. For example, limits of agreement for the superior maximum parameter in normal subjects were 7.2 microns. This meant that any measured change in this parameter would not be statistically significant until it exceeded these 7.2 microns.

The normal population, when measured with the GDx, is characterized by a large variation in NFL thickness and orientation. A typical pattern, coined ‘split bundles’ by us, was described and illustrated in *chapter 4*. We found that it was a common

finding in healthy individuals with a prevalence of almost 8%. We also examined the effect of superior split bundles on the parameters and found that the superior maximum parameter was lower in cases with a split bundle. We argued that, in patients with a split bundle, an abnormal 'superior maximum' parameter, otherwise a potential indicator of glaucoma, should not readily be interpreted as abnormal.

The GDx has a built-in normative database against which all calculated parameters are tested. For subjects of different age or race, a separate database exists, because both factors are known to affect the thickness of the nerve fiber layer. In *Chapter 5* we described that human strabismic amblyopia was not correlated with a difference in NFL thickness. This meant that for amblyopic eyes the standard database could be used, and that there was no need to construct a separate database for these patients.

*Chapter 6* is a case report of a patient that was followed after the onset of an anterior ischemic optic neuropathy (AION). A part of the optic nerve is damaged by a perfusion insufficiency. This usually results in a decrease in visual acuity and visual field damage. The case report shows a progressive decrease in NFL thickness over the course of 4 weeks, as measured with the GDx.

To increase the power of the GDx to discriminate between normal eyes and glaucomatous eyes, several authors have developed new GDx parameters. In *chapter 7*, we determined the sensitivity and specificity of 4 such new parameters, and compared the values with those of the 14 standard parameters. We found that the Number had a sensitivity and specificity for detecting glaucoma of 77% and 89%, respectively. None of the other parameters, including the new ones, discriminated better than the Number. Some of the existing parameters performed poorly, suggesting that those might better be left out of the printout altogether.

In *chapter 8*, an experiment is described where we tested our clinical impression that an expert clinical judgement of the entire printouts would yield a better discrimination between normal and glaucomatous eyes than a mere interpretation of the parameters. Both observers performed better than the Number at a cut-off value of 23, especially in the group with mild glaucoma. In this chapter, we have also described how we interpreted the clinical GDx data. A more detailed explanation has been translated into the Rotterdam GDx Course, and over the past few years it was presented to ophthalmologists and technicians worldwide. Recently, an interactive CD-ROM version of the Rotterdam GDx Course has become available. The CD can be found in the appendix.

In summary, the GDx provides fast, objective and quantitative data on NFL thickness. The applicability and reproducibility of measurements are high and the image acquisition is user and patient friendly. The GDx yields useful sensitivity and specificity values for the detection of glaucoma, whereas its role in follow-up remains to be investigated. As it stands, the GDx holds insufficient validity to serve as a single test for glaucoma. It does, however, provide a very useful addition to the existing tests we run in patients to make the correct diagnosis.

## Samenvatting

Het aantal glaucoompatiënten wereldwijd wordt geschat op 66.8 miljoen. Hiervan zijn ongeveer 10% blind aan beide ogen. Dit zet glaucoom wereldwijd op de tweede plaats van meest voorkomende oorzaken van irreversibele blindheid. Onbehandeld leidt glaucoom tot gezichtsvelduitval en uiteindelijk blindheid. Als de diagnose glaucoom wordt overwogen, zal de oogarts met name letten op de oogdruk, het aspect van de oogzenuw en het gezichtsveldonderzoek van de patiënt. Dit lijkt gemakkelijk, maar onder experts is er nog steeds geen overeenstemming over de exacte definitie van glaucoom.

Glaucoom is een progressieve aandoening van de oogzenuw, veroorzaakt door verlies van ganglion cellen in het netvlies. Het is niet precies bekend waarom deze cellen afsterven. Normaal wordt de zenuwvezellaag in het netvlies gevormd door uitlopers van deze ganglion cellen, zogeheten axonen. Doordat de axonen ook afsterven, wordt de zenuwvezellaag dunner bij glaucoompatiënten. Scanning laser polarimetry (SLP) is een imaging techniek waarbij de dikte van de zenuwvezellaag in het netvlies gemeten kan worden.

SLP kwam op de markt in 1993. De eerste SLP machine heette de Nerve Fiber Analyzer. Toen de research waarover dit proefschrift gaat begon, had de NFA net een ingrijpende software and hardware revisie ondergaan, en ging verder onder de naam GDx (van glaucoma diagnostics). Het werkingsprincipe van de GDx is gebaseerd op de dubbelbrekende eigenschap van de zenuwvezellaag. Als er gepolariseerd licht doorheen valt, verandert de richting van polarisatie. Bij SLP wordt een gepolariseerde laser bundel op het netvlies gericht. Hoe dikker de zenuwvezellaag, hoe groter de verandering van polarisatie. Deze verandering heet retardatie, en wordt gemeten nadat de laserbundel is teruggekaatst uit het oog, en in het apparaat is opgevangen. Het doel van dit promotie onderzoek was om te onderzoeken hoe goed de GDx voldeed in het opsporen van glaucoom, en of er manieren waren om dit te verbeteren.

We ontdekten dat sommige GDx images slecht reproduceerbaar waren. Dit bleek te komen door artefacten (verstoringen in de meting) veroorzaakt doordat het oog van de patiënt bewogen had tijdens de meting. We noemden deze artefacten ‘motion artifacts’, en het bleek dat deze nauwelijks bekend waren bij andere GDx gebruikers. Het effect van deze motion artifacts was dat de retardatie waarden te hoog uitvielen. In *hoofdstuk 2* hebben we laten zien dat enkele parameters duidelijk toenamen in images met motion artifacts. Een scan van een oog met glaucoom zou er op die manier ‘normaler’ uit kunnen gaan zien. Op deze manier zou een gebruiker die niet bekend is met het bestaan van motion artifacts glaucoom over het hoofd kunnen zien. Omgekeerd zouden motion artifacts kunnen leiden tot ‘valse verslechtering’. Een baseline scan met motion artifacts gevolgd door een scan zonder motion artifacts zou onterecht de impressie kunnen geven van verslechtering. Iemand zou op die manier onterecht voor glaucoom behandeld kunnen worden. Ons advies is om scans met motion artifacts niet te accepteren.

In *hoofdstuk 3* hebben we de reproduceerbaarheid van GDx metingen onderzocht. Deze bleek goed en verschilde niet voor ‘single’ images en ‘mean’ images. Wel verschilden deze reproduceerbaarheid per parameter. Om later progressie te kunnen



beoordelen, hebben we grenzen uitgerekend waarbinnen parameters van opeenvolgende metingen mogen vallen, voordat dat statistisch significant is.

We hebben meer dan 300 gezonde vrijwilligers gemeten met de GDx. Het bleek dat zelfs in zo een grote groep de zenuwvezellaag er bij iedereen anders uitzag. Het ging hierbij om een verschil in dikte, maar ook in patroon. Eén bepaald patroon, dat aanvankelijk leek op een beschadiging van de zenuwvezellaag, bleek vaak voor te komen in onze groep gezonde ogen. Dit patroon noemden we een ‘split bundle’ en wordt in *hoofdstuk 4* besproken. Het bleek in 8% van de gezonde ogen voor te komen. Ook bleek dat in een oog met een split bundle de superior maximum parameter lager uitviel dan gemiddeld. Normaal gesproken is dit een aanwijzing voor glaucoom, maar dit gaat dus niet op voor ogen met een ‘split bundle’.

De GDx heeft een ingebouwde normatieve database. Alle parameters die berekend worden bij het scannen van een oog, worden met deze normaal waarden vergeleken. Voor verschillende rassen en leeftijden bestaan aparte databases, want deze factoren beïnvloeden de normale zenuwvezellaagdikte. In *hoofdstuk 5* onderzochten we amblyope (luie) ogen op basis van strabisme (scheelzien). Het bleek dat de zenuwvezellaagdikte in deze amblyope ogen niet verschilde vergeleken met het gezonde oog van de onderzochte patiënten. Dit bevestigde de huidige opvatting over amblyopie, namelijk dat de afwijking niet in het amblyope oog zelf gelegen is, maar elders (namelijk de hersenen). Verder betekende dit dat wanneer amblyope ogen met de GDx worden gemeten, deze met de standaard database vergeleken kunnen worden en we dus geen aparte database voor amblyope ogen nodig hebben.

*Hoofdstuk 6* is een case report over een patiënt die enkele malen gemeten is met de GDx nadat er een anterieure ischemische opticus neuropathie optrad. Bij deze aandoening is er een plotseling tekort in bloeddoorstroming van de oogzenuw. De oogzenuw (en de zenuwvezellaag) lopen hierdoor ernstige schade op. In de GDx scans is te zien hoe de zenuwvezellaag in de loop van 4 weken fors afneemt in dikte.

Om het vermogen van de GDx om te onderscheiden tussen normale en glaucomateuze ogen te vergroten, hebben enkele onderzoekers nieuwe parameters bedacht. In *hoofdstuk 7* hebben we de sensitiviteit en specificiteit van deze 4 nieuwe parameters bepaald, en vergeleken met die van de 14 bestaande parameters. Het bleek dat the Number een sensitiviteit en specificiteit had van 77% en 89%. Geen van de bestaande, noch van de nieuwe parameters onderscheidde beter dan the Number. Een aantal van de bestaande parameters onderscheidde dermate slecht, zodat er reden is om deze van de standaard printout te schrappen.

Geruime tijd bestond er het vermoeden dat de GDx printout meer informatie bevatte dan tot uiting kwam in de geautomatiseerde analyse middels de parameters. Met andere woorden, een zogenaamde ‘expert clinical judgement’ van de printout zou wel eens een betere sensitiviteit en specificiteit kunnen hebben dan de best beschikbare parameter. *Hoofdstuk 8* beschrijft een experiment waaruit bleek dat de twee artsen een hogere sensitiviteit en specificiteit haalden dan the Number, met name in de groep van vroeg glaucoom. In dit hoofdstuk wordt ook beschreven hoe die interpretatie in zijn werk gaat. Deze manier van interpreteren vormde ook het onder-

werp van The Rotterdam GDx Course, die door de auteur van dit proefschrift ontworpen is. Deze cursus werd in de loop van de laatste jaren aan honderden oogartsen, assistenten en paramedisch personeel gegeven. Onlangs is deze cursus ook als CD-ROM uitgekomen. De CD is opgenomen in de appendix van dit proefschrift.

Samengevat levert de GDx snelle objectieve data over de dikte van de zenuwvezellaag in het netvlies. De toepasbaarheid en de reproduceerbaarheid van de metingen is groot. De metingen zijn gebruikers- en patiëntvriendelijk. Met de GDx worden bruikbare sensitiviteit en specificiteit waarden verkregen voor het detecteren van glaucoom. Over de rol van de GDx bij de follow-up van glaucoom is nog weinig bekend. Als enige test voor glaucoom is de GDx nog ongeschikt. Wel is gebleken dat de GDx een zeer waardevolle aanvulling is voor de glaucoomdiagnostiek.

Al met al is het in elkaar draaien van een proefschrift voor mij een erg leuke klus geweest. Dit is met name het geval omdat ik heb mogen samenwerken met een hoop leuke mensen. Jullie hulp, hoe groot of klein ook, is essentieel geweest voor de wording van dit boekje. Ik bedank iedereen van harte voor alle hulp die ik van jullie gekregen heb. Een aantal mensen verdienen echter een speciale vermelding.

Prof van Rij; bedankt voor de uiterst efficiënte wijze waarop u het laatste deel van mijn promotie hebt vormgegeven. Ik heb altijd gedacht dat de universitaire ambtelijke molen log en traag was. Echter, de middag dat we hadden besloten dat de research afgerond was en we een boekje zouden gaan maken, vlogen mij direct de standaardbrieven al om de oren. Ook verbluffend was de snelheid waarmee de officiële documenten door u langs de diverse instanties werden gehamerd; dit was precies wat ik nodig had.

Ik bedank de commissieleden voor het lezen van mijn proefschrift, hun opmerkingen daarover en het voeren van de oppositie.

Dr. Lemij, beste Hans. Als begeleider ben jij de stuwende kracht geweest die mij in staat heeft gesteld dit werk te voltooien. Ik was nog maar net met dit project begonnen of ik werd direct in een baan om de aarde gelanceerd en meegesleept naar allerlei internationale congressen en meetings. Hierdoor was onderzoek doen vanaf het begin ontzettend spannend en leuk. Ik bewonder je vermogen om mensen de vrijheid te geven hun eigen weg te zoeken. Ik ben blij dat je me met alles hebt laten kennis maken wat voor een jonge onderzoeker belangrijk is: scherp denken, efficiënt werken en helder formuleren. Dat wat ik ervan opgestoken heb ligt nu voor je en ik hoop dat ik de kans krijg om deze eigenschappen in de toekomst te blijven ontwikkelen.

Als je zoveel leert van iemand gaat je relatie een beetje lijken op die van een vader en zoon. Blijkbaar zien anderen dat ook, zoals op gegeven moment bleek aan het einde van één van mijn presentaties. Na een hoop complimenten werd opgemerkt dat je toch wel kon zien dat ik er “één van Hans was.” Ik weet nog hoe ontzettend trots ik daar toen op was. En dat is daarna niet meer overgegaan.

Beste mensen van LDT en Laser Vision, met name Ulrich, June, Leo, Jos en Erik: met jullie apparatuur begon dit avontuur allemaal. Bedankt voor jullie inzet om steeds weer te komen helpen als er iets kapot was of als er apparatuur aangepast moest worden aan onze specifieke wensen (ook al was dat soms vlak na de release van een nieuwe versie...). Uiteindelijk kwam de GDx toch steeds weer op een hoger niveau uit.

Ik wil iedereen in Het Oogziekenhuis bedanken voor de hulp die ik gekregen heb bij mijn werk. De heren Hiddema en Sol voor hun aanhoudende interesse en support. Martha die mij de beginselen met de NFA heeft bijgebracht en op wiens schouders dit werk is gebouwd. Mei Lie die, met haar beslissing om in Leiden te gaan werken, mij de kans bood haar onderzoek voort te zetten. Samen als onderzoeker starten in het OZR en onze eeuwige discussies over ‘the O-word’ hebben de basis gelegd voor onze vriendschap. Christine van Roekel, hoofd afdeling gezelligheid in de bieb, zorgde ervoor dat iedereen van tijd tot tijd even stopte met werken voor koffie (en daarna ook weer aan het werk ging). Houdijn Beekhuis: jij hebt mijn eerste stappen als keuze-co in het OZR begeleid. Jouw enthousiasme voor onderzoek en charisma-

tische levenshouding hebben mij veel inspiratie bezorgd. Ook de mannen van de fotografie stonden altijd klaar om mijn presentaties van dia's te voorzien, ook al waren het lange series die 'morgen' klaar moesten zijn. Alle dames van de perimetrie (met name Marjo, Els, Anita, Tineke, Eleen, Marianne, Annemiek en Geeske) bedankt dat jullie een deel van jullie wachtkamer hebben afgestaan voor mijn speelgoed en van de peri een gezellige plek maakten om te werken. (Zo gezellig dat soms gewoon de deur dicht moest). Mieke en Sophie: bedankt dat jullie je jarenlang uit de naad hebben gewerkt om de grootste perimetrische en polarimetrische database ter wereld te maken. Als AGNIO/AGIO heb ik het voorrecht in een hechte en gezellige assistentengroep te werken zodat ook de laatste loodjes van mijn proefschrift een beetje gezellig bleven. Verder bedank ik iedereen die ervoor zorgt dat het OZR een geweldig leuke plek is om te werken!

Ook alle vrijwilligers die aan mijn onderzoek hebben meegedaan verdienen een speciale vermelding. Inmiddels is hun aantal opgelopen tot ongeveer 1500. Als zij niet bereid waren geweest om een deel van hun tijd te schenken aan wetenschappelijk onderzoek, was er van dit hele proefschrift niks geworden.

Paul Mulder, bedankt voor alle statistische hulp die ik van je gekregen heb. Altijd stond je klaar om me met mijn rekenwerk te helpen en me met advies ter zijde te staan.

Ik ben blij dat Eelco, Oscar, Rick, Brigitte en Bart tegelijk met mij aan het promoveren waren: het was fijn om mijn onderzoekstijd met jullie te delen. Verder bedank ik mijn vrienden voor hun begrip en geduld als ik weer eens druk bezig was of de verjaardag van Walter miste. Ik verheug me al op de tijd die ik nu ga overhouden.

Klaas-Jan, bedankt voor de leuke tijd die we samen op de perimetrie en congressen beleefden. Samen met Axel zijn jullie de perfecte paranimfen. Bedankt voor alle tijd die daar in ging zitten en de steun die ik van jullie heb gekregen.

Esther, ik ben ontzettend blij dat jij in de eindfase de leiding over de lay-out hebt overgenomen. Je hebt er een prachtig boekje van gemaakt (en me voor die lelijke poster behoed...).

Lieve ouders, ik draag dit werk aan jullie op. Ik bedank jullie voor de vrijheid die ik altijd heb gekregen om mijn eigen ding te doen. Dit is volgens mij het grootste geschenk dat je in je leven kunt krijgen. Het resultaat hiervan ligt nu voor jullie, maar mijn dankbaarheid daarvoor past niet in dit boekje.

Tot slot, lieve Evelyne, jij hebt me waarschijnlijk in het meest ongunstige deel van het traject leren kennen, namelijk de eindfase. Bedankt voor al je geduld, support en liefde die ik van je heb gekregen, met name in tijden van tegenwind en wanneer ik weer eens het gevoel had twee banen tegelijkertijd te hebben. Maar vooral ben ik blij dat je zag dat ik het zelf allemaal heel graag wilde en dat dat er mocht zijn.

Rotterdam, 16 februari 2003.

**Colen TP** and Lemij HG. Motion artifacts in scanning laser polarimetry. **Publications** Ophthalmology 2002;109(8):1568-1572.

**Colen TP**, Tjon-Fo-Sang MJ, Mulder PG and Lemij HG. Reproducibility of measurements with the nerve fiber analyzer (NFA/GDx). J Glaucoma 2000;9(5):363-370.

**Colen TP** and Lemij HG. Prevalence of split nerve fiber layer bundles in healthy eyes imaged with scanning laser polarimetry. Ophthalmology 2001;108(1):151-156.

**Colen TP**, de Faber JT and Lemij HG. Retinal nerve fiber layer thickness in human strabismic amblyopia. Binocul Vis Strabismus Q 2000;15(2):141-146.

**Colen TP**, van Everdingen JA and Lemij HG. Axonal loss in a patient with anterior ischemic optic neuropathy as measured with scanning laser polarimetry. Am J Ophthalmol 2000;130(6):847-850.

**Colen TP**, Tang NEML, Mulder PGH and Lemij HG. Sensitivity and specificity of new GDx parameters. Submitted for publication.

**Colen TP** and Lemij HG. Sensitivity and specificity of the GDx; Clinical judgement of standard print-outs vs the Number. J Glaucoma. In press.

Nicolela MT, Martinez-Bello C, Morrison CA, LeBlanc RP, Lemij HG, **Colen TP** and Chauhan BC. Scanning laser polarimetry in a selected group of patients with glaucoma and normal controls. Am J Ophthalmol 2001;132(6):845-854.

**Colen TP**, Paridaens DA, Lemij HG, Mourits MP and van Den Bosch WA. Comparison of artificial eye amplitudes with acrylic and hydroxyapatite spherical enucleation implants. Ophthalmology 2000;107(10):1889-1894.

Van Goudoever JB, **Colen T**, Wattimena JL, Huijmans JG, Carnielli VP and Sauer PJ. Immediate commencement of amino acid supplementation in preterm infants: effect on serum amino acid concentrations and protein kinetics on the first day of life. J Pediatr 1995;127(3):458-65.

Lemij HG, **Colen TP**, Tjon-Fo-Sang MJH. From NFA to GDx. Evolution of the Nerve Fiber Analyzer. In: The Shape of Glaucoma; Quantitative Neural Imaging Techniques. Edited by Lemij HG and Schuman JS. Kugler Publications, The Hague, The Netherlands 2000. p105-27. **Book chapters**

**Colen TP**, Tjon-Fo-Sang, Mulder PGH and Lemij HG. Understanding your clinical NFA/GDx data. In: The Shape of Glaucoma; Quantitative Neural Imaging Techniques. Edited by Lemij HG and Schuman JS. Kugler Publications, The Hague, The Netherlands 2000. p307-319.

**Colen TP** and Lemij HG. Image Quality with the GDx and the importance of avoiding motion artifacts. In: Analise de camada de fibras nervosas da retina. Edited by R. Lauande-Pimentel and Vital P Costa. Cultura Medica Publishers, Rio de Janeiro, Brasil 2001. p53-64.

**Colen TP** and Lemij HG. The Rotterdam GDx course; an interactive training session on the interpretation of clinical GDx data. Published by The Rotterdam Eye Hospital, Rotterdam, The Netherlands. 2002. **CD-ROM**

FIGURES

Fig 1-1. (legend on p. 105)

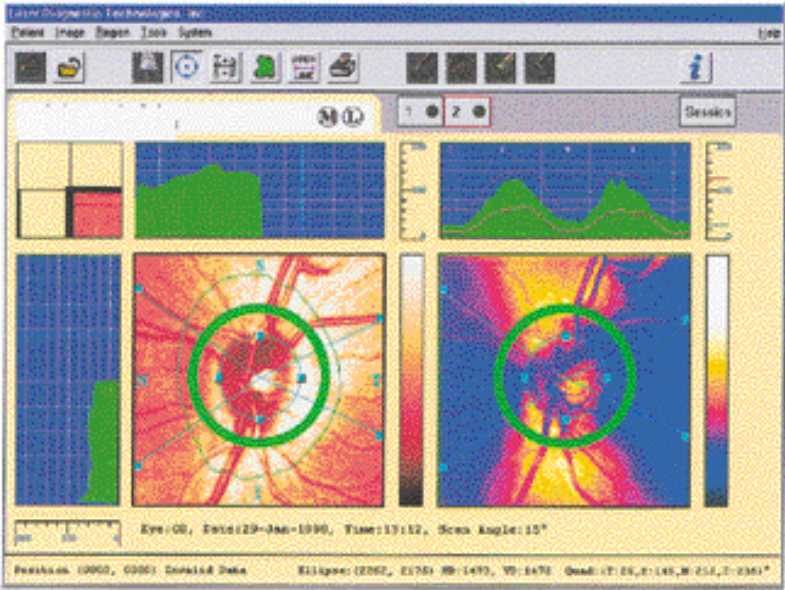
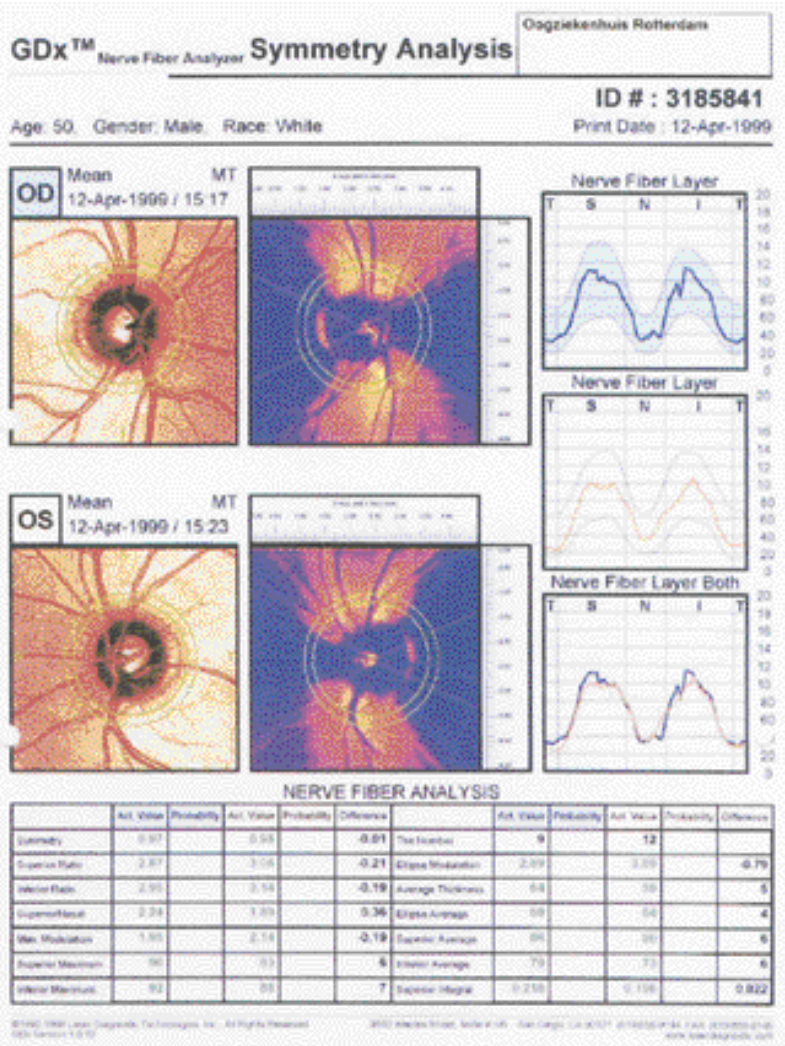


Fig 1-2. (legend on p. 105)



**Fig 2-1.** (legend on p. 105)

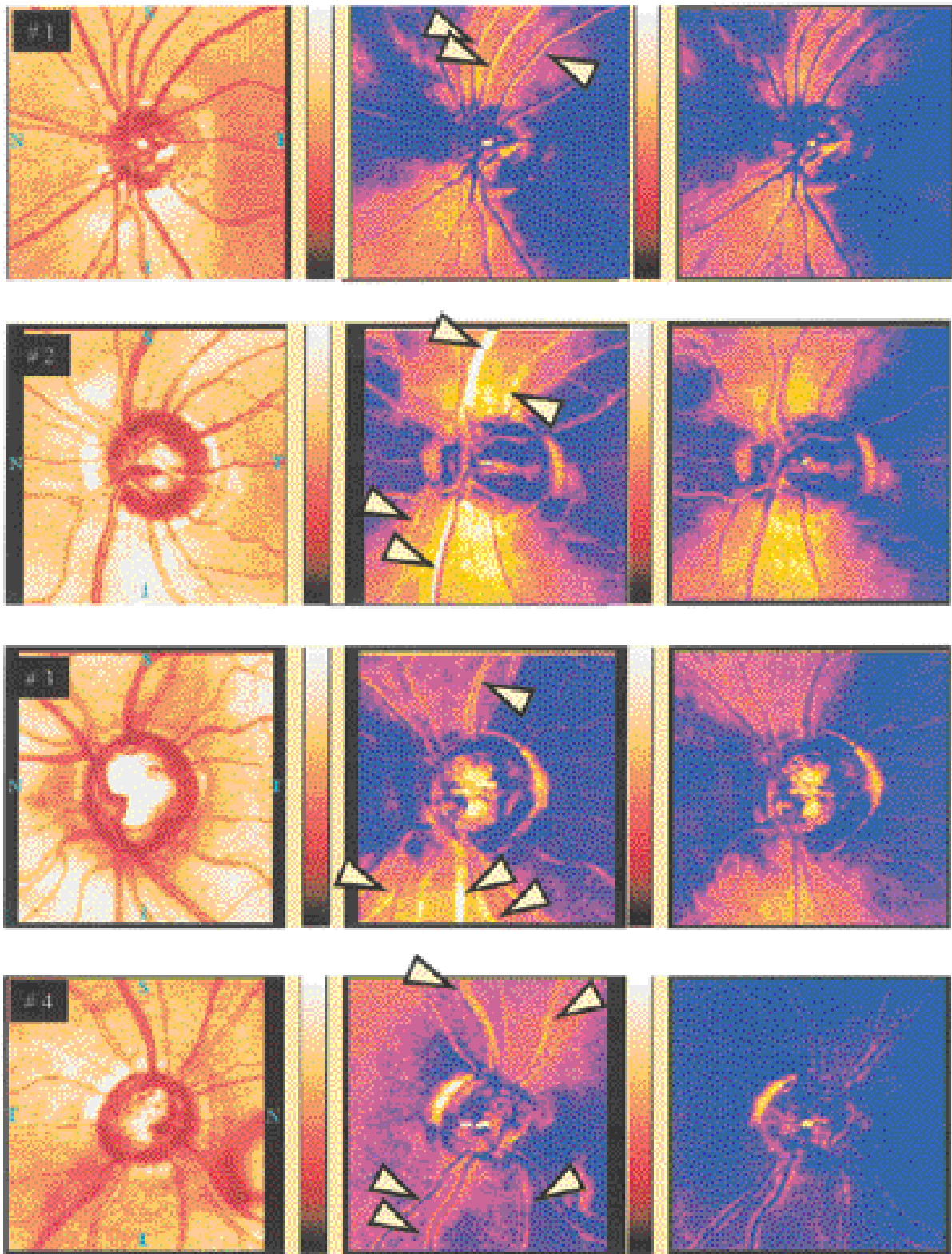
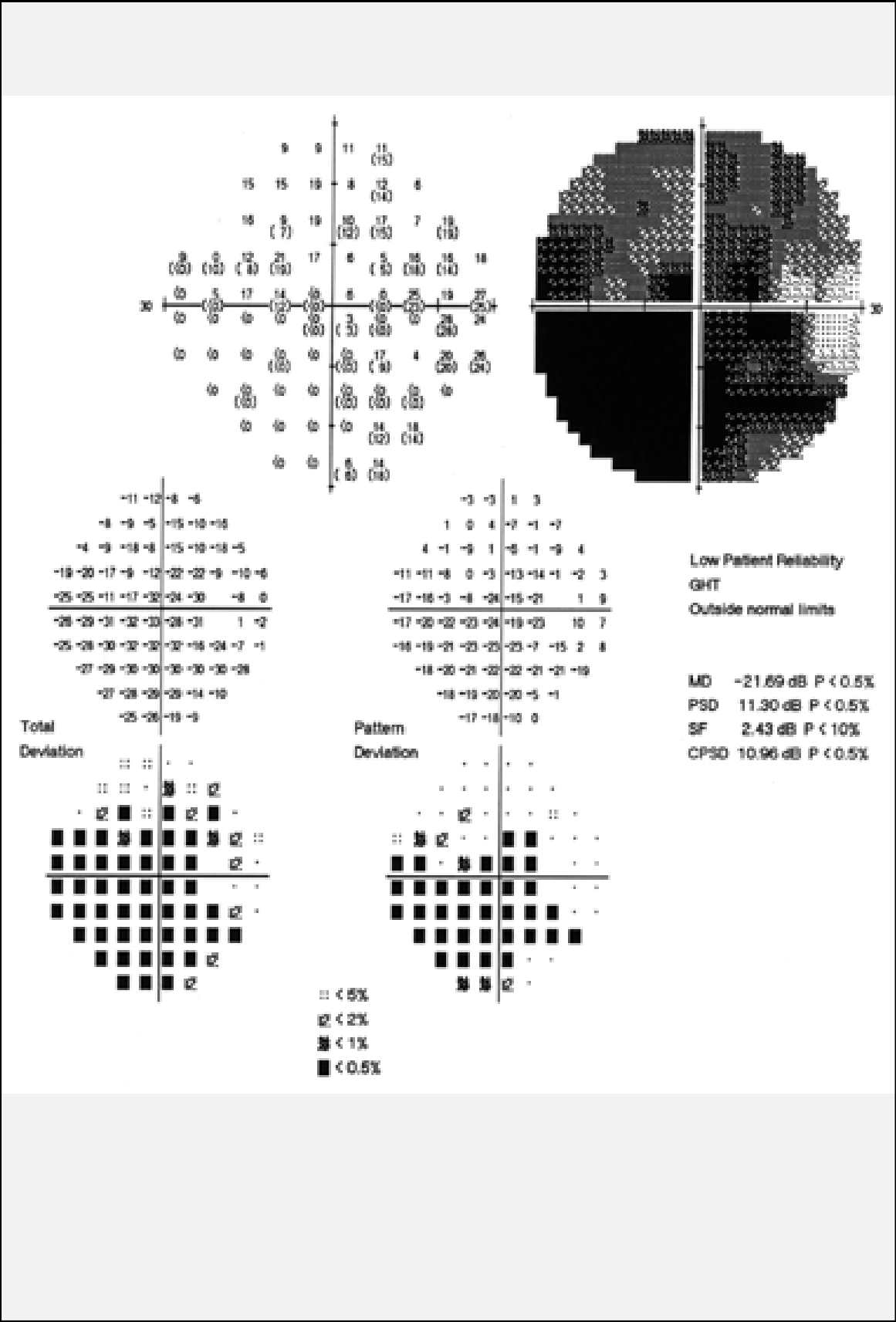


Fig. 2-2. (legend on p. 105)





<< **Fig 1-1.** GDx scan of a normal eye.

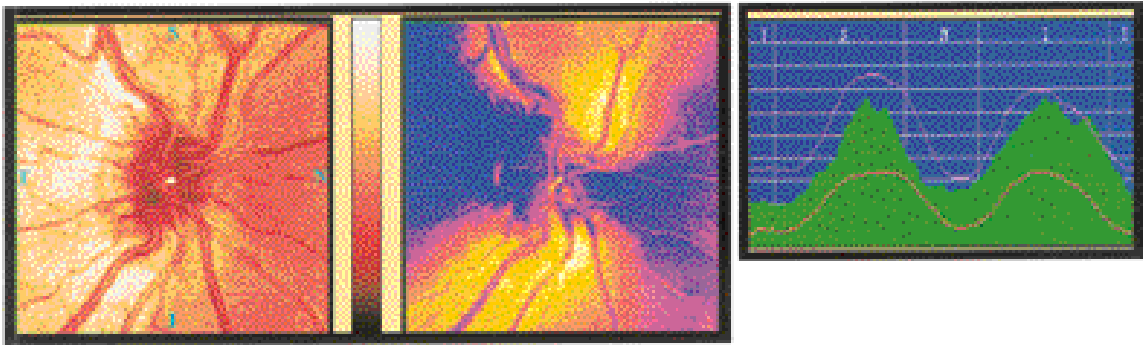
**Legend**

<< **Fig 1-2.** The GDx printout contains a retardation image and a reflection image of each eye, a double hump graph for each eye, a symmetry graph, and 14 parameters for each eye.

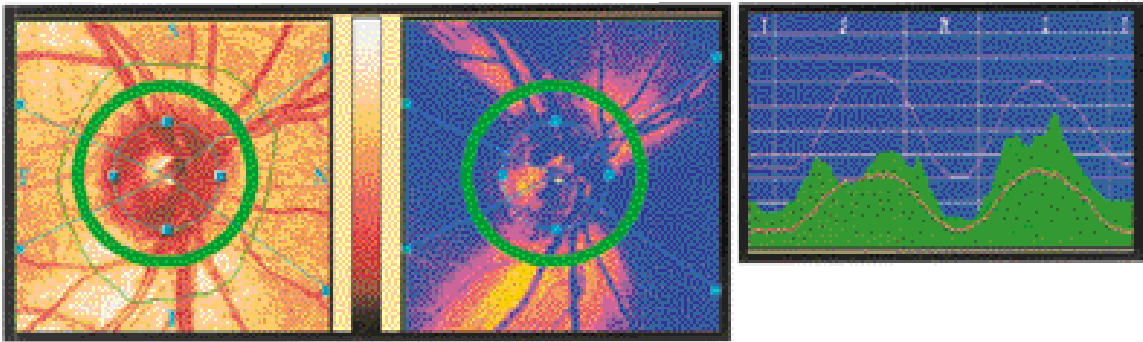
<< **Fig 2-1.** Examples of motion artifacts in four different subjects (#1-4). Of every subject, the reflectance image is shown (left), the retardation image (middle) with the motion artifacts (indicated with an arrow), and the retardation image without motion artifacts (right). How to recognize the motion artifacts is explained in the methods section.

<< **Fig. 2-2.** Visual Field examination (HFA 30-2) of the glaucoma patient in example #4.

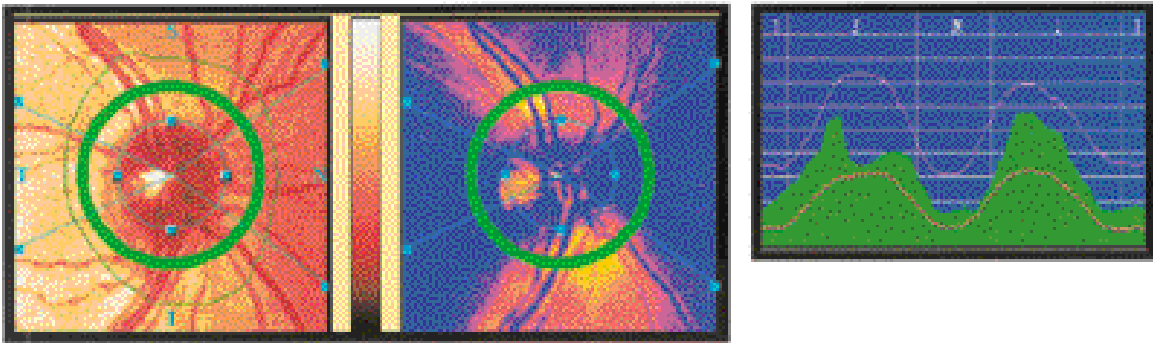
**Fig 4-1. examples #1-3** (legend on p. 108)



example # 1; normal NFL

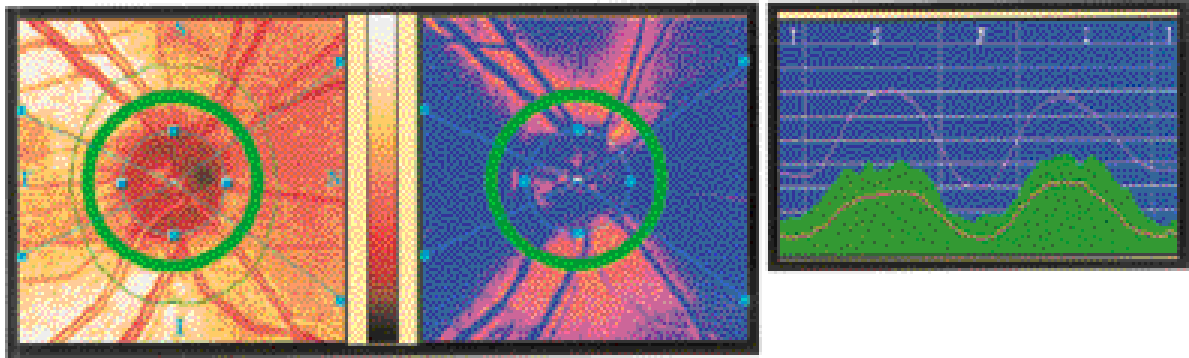


example # 2; split superior bundle

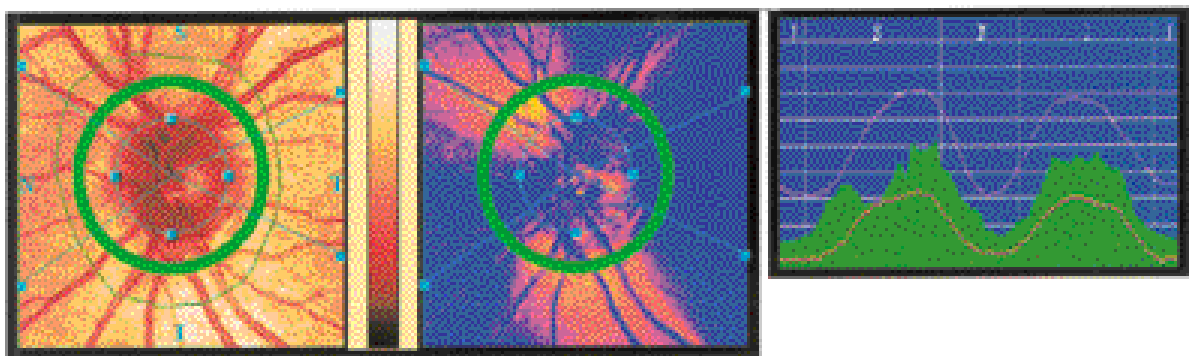


example # 3; split superior bundle

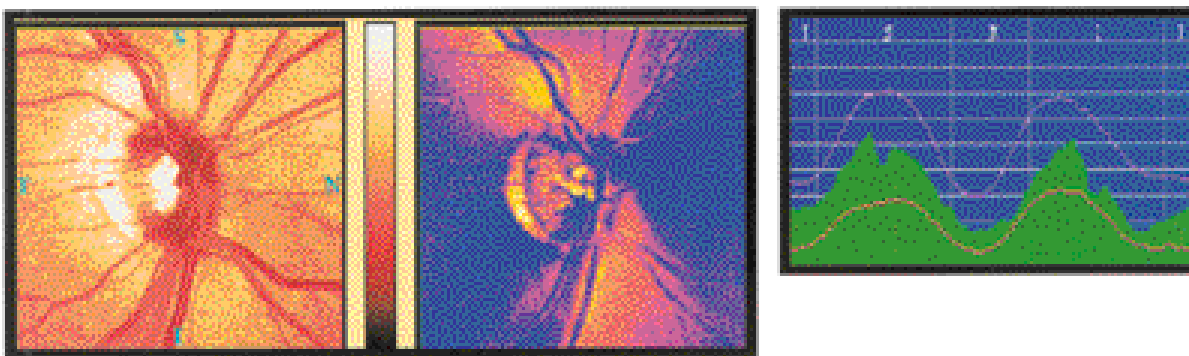
**Fig 4-1. continued examples #4-6** (legend on p. 108)



example # 4; partially split superior bundle



example # 5; partially split superior bundle



example # 6; wedge defect

## Legend

### << Fig 4-1.

Some of the reference examples used for the classifications in this study. Every example consists of a fundus reflectance image (left), a retardation image (middle) and a double hump graph (right). All examples have been obtained in individuals with healthy eyes, except example no. 6, that was obtained in a glaucoma patient. Example 1 shows single nerve fiber layer bundles superiorly and inferiorly. Example 2 and 3 show split superior nerve fiber layer bundles. Examples 4 and 5 show cases that did not meet the criteria of our definition of a split bundle; example 4 is referred to as a partially split bundle, and example 5 is called an asymmetrically split bundle. Example 6 shows a wedge defect in the inferior nerve fiber layer bundle of a glaucoma patient.

**Fig 6-1. >>**

Consecutive NFA/GDx scans on day 0, 15, 21 and 36. A scan includes a reflectance image (left), retardation image (middle) and a double hump pattern (right). The outer green circle is 1.75 times the diameter of the (estimated) diameter of the optic nerve head. The inner green circle is at a 10-pixel distance of the outer circle. In addition, the smax (superior maximum) parameter has been presented. >>

**Legend****Figure 6-2. >>**

Consecutive HFA 30-2 visual fields on day 0, 15, 21 and 36. Displayed are actual threshold values in dB (left) and the gray scale pattern (right). >>

**Fig 6-1. GDx scans on four consecutive visits** (legend on p. 109)

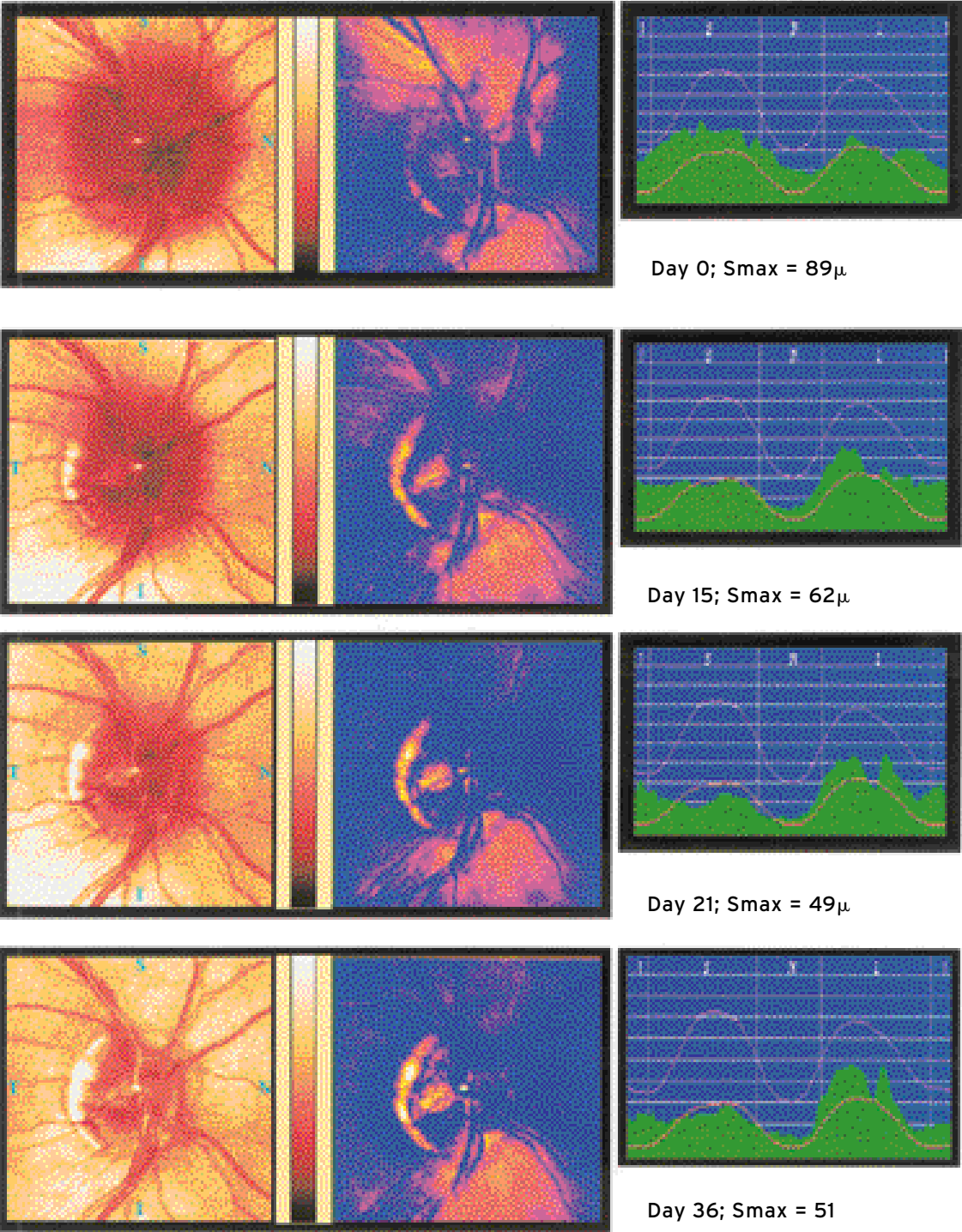
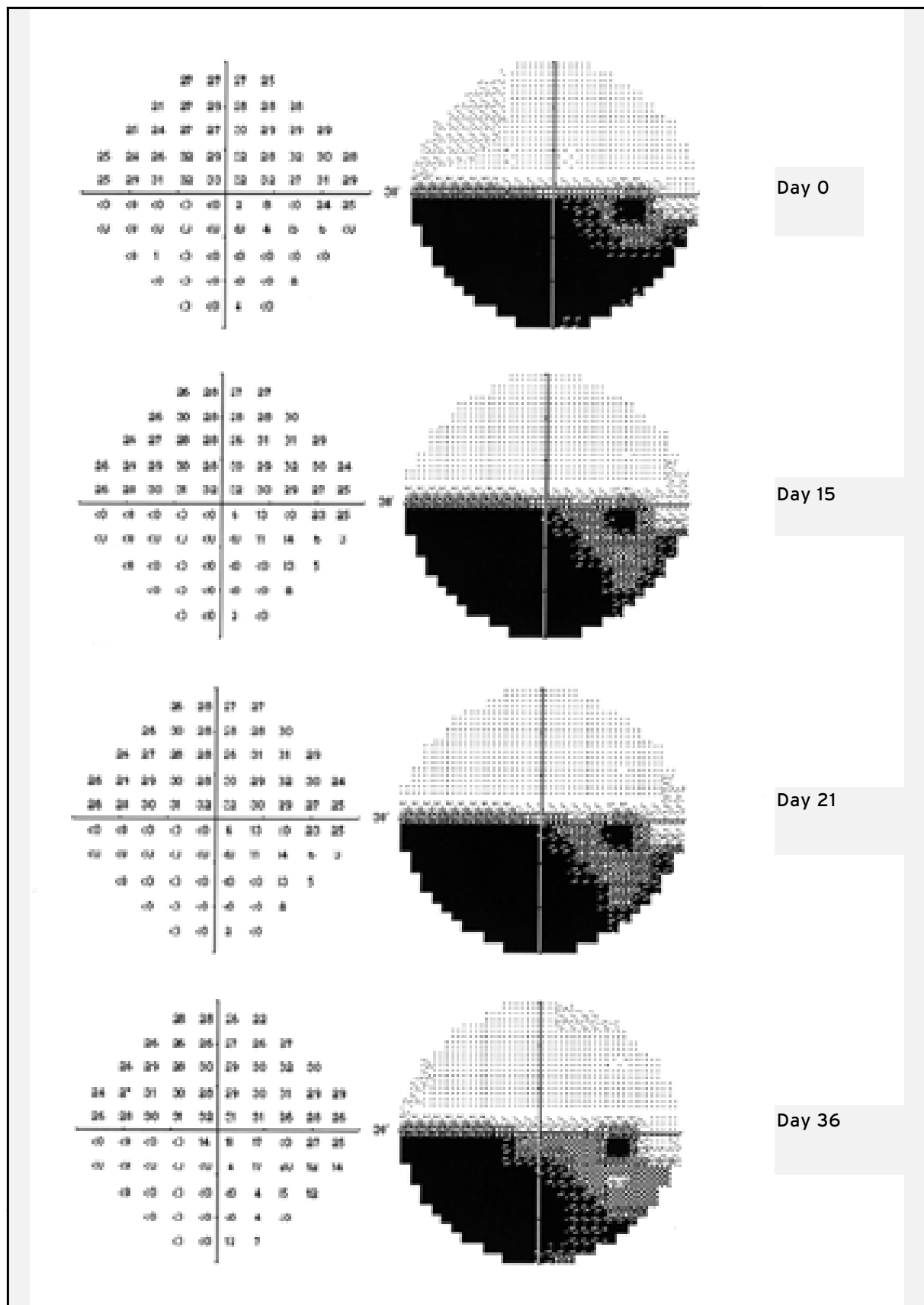


**Figure 6-2. Visual Fields on four consecutive visits** (legend on p. 109)



## **Curriculum vitae**

Thomas Peter Colen werd geboren op 31 augustus 1970 te Halle-Westfalen (Duitsland). Na zijn eindexamen VWO aan het Westland College te Naaldwijk, begon hij in 1988 aan zijn studie geneeskunde aan de Erasmus Universiteit Rotterdam. In 1995 behaalde hij zijn artsexamen en was vervolgens gedurende 1 jaar werkzaam als AGNIO chirurgie in het Merwede Ziekenhuis te Dordrecht. Zijn belangstelling voor de oogheelkunde en de medische research voerde hem vervolgens naar het Oogziekenhuis, alwaar hij in 1996 als onderzoeker een project begon over oog- en ooglid motoriek. In 1997 startte hij, onder leiding van Dr. HG Lemij, zijn onderzoek naar scanning laser polarimetrie, waarvan dit proefschrift het resultaat is. In 2000 werd hij AGNIO in Het Oogziekenhuis Rotterdam, waar hij vanaf 2001 in opleiding is tot oogarts (opleider Drs. GS Baarsma).

## **Appendix**

The CD ROM version of the Rotterdam GDx Course is included in this thesis. If it cannot be found here, you may request your copy from the author.

If you need help installing the CD, please visit [www.oogziekenhuis.nl/zorg/opleiding/GDX.htm](http://www.oogziekenhuis.nl/zorg/opleiding/GDX.htm) for frequently asked questions.

